U.S. DEPARTMENT OF THE INTERIOR
GEOLOGICAL SURVEY

Special Earthquake Report for the September 1, 1981, Samoa Islands Region Earthquake

by

R.E. Needham
R.P. Buland
G.L. Choy
J.W. Dewey
E.R. Engdahl
S.A. Sipkin
W. Spence
M.D. Zirbes

Open-File Report 82-781
1982

This report is preliminary and has not been reviewed
for conformity with U.S. Geological Survey editorial standards.

Index

ABSTRACT

The September 1, 1981, Samoa Islands Region earthquake occurred at the extreme northern end of the Tonga arc in a region where the Pacific plate may be disjointed along a hinge fault. In the last 50 years, magnitude 7 or greater earthquakes have occurred in this region on the average of once every six years, but four 7+ events have now occurred within the last six years. The mainshock was preceded about two hours earlier by a foreshock that was used as a calibration event for the Joint Epicenter Determination relocation of the mainshock and nearby seismicity occurring within a period seven months prior to and one week after the mainshock. The foreshock, better-located events of the prior seismicity, and most aftershocks are concentrated in a group near the mainshock epicenter, but several more distant aftershocks suggest that the aftershock zone may have been as large as 125 km in length and trended about S35°E. Identification of depth phases from a full suite of broadband records gives source depths of 25±3km for the mainshock and 29.5±3 km for the foreshock using a JB earth model.

Source parameters were determined for the mainshock utilizing WWSSN analog and GDSN digital data. The preferred fault plane solution based on P-wave first motion data is a south by southwesterly steeply dipping normal fault, remarkably similar to the mechanism reported by Johnson and Molnar (1972) for the nearby earthquake of April 20, 1968. A waveform inversion technique described by Sipkin (1982), when applied to long-period P waveforms, gives an "average" point source solution for a purely deviatoric moment rate tensor at a preferred source depth of 22 km. Very similar results were obtained from long-period GDSN body-wave and mantle-wave data using a centroid-moment tensor inversion technique described in Dziewonski, and others (1981). Both techniques provide solutions very close to a double couple source with a south by southwesterly shallow-dipping normal fault mechanism.

To obtain the scalar mantle wave moment, GDSN vertical and transverse records 20,000 sec in length were processed as described by Buland and Taggart (1981). Averaging all the data from Rayleigh and Love waves yields an estimate of 3.8×10^{27} dyne-cm (as compared to about 1.9×10^{27} from body-wave moment tensor inversions) or a moment magnitude (M_w) of 7.6.

For the portion of the waveform analysed (50-58 sec), the body-wave inversion performed by Sipkin gives a source time function of duration approximately 28 sec with two peaks in activity. Simultaneous analysis of short-period records, and broadband ground displacements and velocities, using a method described by Harvey and Choy (1982) and Choy and Boatwright (1981) revealed a complex rupture consisting of two subevents, of about the same moment, separated in time by about 25 sec, and with durations of about 25 sec each. The two peaks in activity resolved by the body-wave moment tensor inversion correspond to the first of these subevents.

Introduction

This report on the September 1, 1981 Samoa Islands Region earthquake is the first Special Earthquake Report to be assembled by a staff of the USGS Seismologists, utilizing the expertise of these scientists to elucidate the seismological and tectonic characteristics of this earthquake.

The goal of this report is to present information on the tectonic setting of the focal area, historical seismicity, location and source parameters for the September 1, 1981 Samoa Islands Region earthquake.

Data from the National Earthquake Information Service (NEIS) Preliminary Determination of Epicenter (PDE) reports as well as digital data from the Global Digital Seismograph Network (GDSN) are the basis for this report. The Samoa Islands Region earthquake hypocenter solution as well as the list of stations used in this report are presented in Appendix I.

Tectonic Setting - Spence

The earthquake of September 1, 1981, occurred at the extreme northern end of the Tonga arc (Figure 1). Here the trend of the arc swings 90° (counterclockwise) from N20°E to N70°W. East and north of the Tonga arc the Pacific plate moves westward with respect to the complicated eastern end of the Australia-India plate, with a relative E-W motion of about 9 cm/year (Minster and Jordan, 1978).

Four large earthquakes were found by Isacks and others (1969) to have similar focal mechanisms, in that the steeply dipping nodal planes for these earthquakes strike parallel to the relative plate motion vector (Figure 2) and have slip vectors mostly vertical, down on the south side (Tonga ridge) and up on the north side. The locations of these earthquakes near the northeast corner of the Tonga arc and their preferred nodal planes suggest that the Pacific plate here is becoming disjointed along a hinge fault. North of the hinge fault, the Pacific plate continues its westward motion, whereas south of this hinge fault the Pacific plate is being subducted beneath the Tonga arc. This portion of the Pacific plate is about 100 million years old (Schlater and others, 1981) with an estimated lithospheric thickness of about 75 km (Leeds, 1975).

Historical Seismicity - Needham

A search was made of the Hypocenter Data File (HDF) for all earthquakes with a magnitude of 6 or greater, occurring within ±2.0° of the September 1, 1981, hypocenter. The 89 earthquakes that met the search criteria are listed in Appendix II. The average number of earthquakes of magnitude 6 or greater that occurred per year, from 1930 to 1981, is 1.78. The two longest gaps that appear in the chronological distribution (Table 1) took place between June 16, 1936, to June 8, 1939, (36 months) and October 11, 1944, to June 29, 1948, (44 months). There is no evidence for an increase in the occurrence rate of earthquakes following these quiet periods nor do these periods precede a large magnitude earthquake.

The magnitude distribution for these events is shown in Table 2. The large numbers reported for magnitudes of 6.0, 6.3 6.5 and 6.8 are because early reports using 1/4 magnitude intervals were rounded off.

Ten earthquakes with magnitudes of 7 or greater were found. Eight are south of the September 1 hypocenter and one appears in approximately the same location. On the average, an earthquake with a magnitude of 7 or greater occurred once every 6.25 years, in the last 50 years. Four, including the event under study, have occurred within the last 6 years, indicating a possible increase in the occurrence rate.

TABLE 1

HISTORICAL SEISMICITY CHRONOLOGICAL DISTRIBUTION OF EARTHQUAKES WITHIN ±2° DISTANCE FROM SEPTEMBER 1, 1981 HYPOCENTER MAGNITUDE ≧6.0 (1930 THROUGH SEPTEMBER 1, 1981)

YEAR	NO.	YEAR	NO.	YEAR	NO.	YEAR	NO.
1930	0	1943	2	1956	5	1969	2
1931	2	1944	1	*1957	3	1970	0
1932	0	1945	0	1958	4	1971	0
1933	3	1946	0	1959	2	1972	5
1934	2	1947	0	1960	2	1973	2
1935	1	*1948	1	1961	1	1974	2
1936	2	*1949	2	1962	2	*1975	2
1937	0	1950	3	1963	0	1976	1
1938	0	1951	3	1964	0	*1977	3
*1939	2	1953	2	1966	0	*1978	3
1940	4	1953	2	1966	0	1979	0
1941	1	1954	0	1967	1	1980	3
1942	1	1955	2	1968	1	*1981	1

* MAGNITUDE ≧7 OCCURRED

TABLE 2

HISTORICAL SEISMICITY MAGNITUDE DISTRIBUTION OF EARTHQUAKES WITHIN ±2° DISTANCE FROM SEPTEMBER 1, 1981 HYPOCENTER MAGNITUDE ≧6.0 (1913 THROUGH SEPTEMBER 1, 1981)

MAG.	NO.	MAG.	NO.	MAG.	NO.	MAG.	NO.
6.0	17	6.7	2	7.4	1	8.1	0
6.1	6	6.8	13	7.5	1	8.2	0
6.2	6	6.9	3	7.6	1	8.3	0
6.3	11	7.0	3	7.7	1	8.4	0
6.4	5	7.1	0	7.8	0	8.5	0
6.5	14	7.2	2	7.9	0	8.6	0
6.6	2	7.3	0	8.0	0	8.7	1

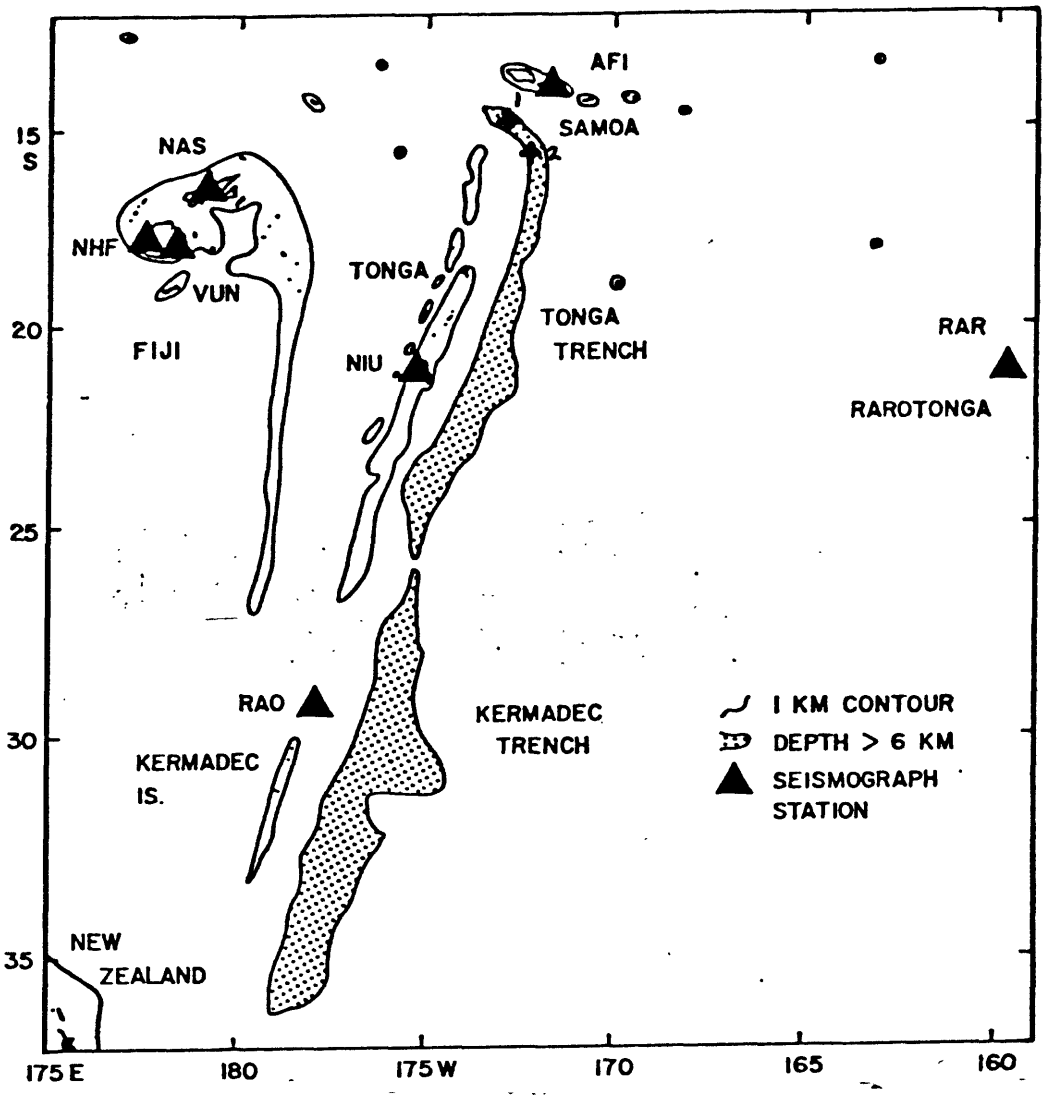

Figure 1. Samoa Islands Region, Mitronovas, Isacks, and Seeber, 1969; showing locations (+'s) of (1) 1 September earthquake and (2) the 20 April 1968 earthquake, Johnson and Molnar, 1972.

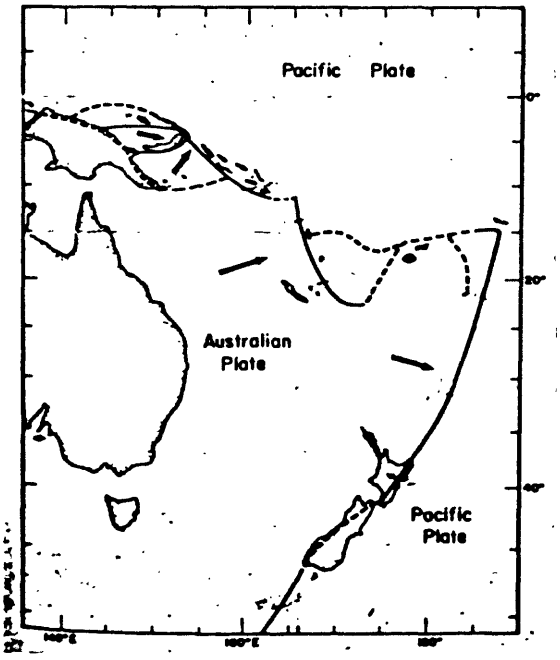

Figure 2. Inferred plate motion in the southwest Pacific region. Broad arrows show direction and magnitude of motion with respect to the Pacific Plate (from Johnson and Molnar, 1972).

Global Digital Seismograph Network - Needham and Zirbes

Since digital data from the Global Digital Seismograph Network (GDSN) were utilized in each of the source orientation solutions of this report, a brief description of the GDSN is presented.

The GDSN comprises three types of digital station observatories: the Seismic Research Observatory (SRO), the Abbreviated Seismic Research Observatory, (ASRO), and the Digital Worldwide Standardized Seismograph Network (DWWSSN). Digital tapes from these networks are collected by the USGS and compiled into network-day tapes. These tapes are made available to research organizations throughout the world.

Seismic Research Observatory (SRO)

Since 1975, 12 SRO stations have been installed throughout the world as shown in Table 3. These stations use a borehole seismometer, located approximately 100 meters beneath the surface of the earth, which virtually eliminates wind generated noise at frequecies of interest. Normal digital operation of the SRO system consists of three long-period components recorded on a continuous basis, and one short-period vertical component recording automatically detected signals only.

Abbreviated Seismic Research Observatory (ASRO)

The 5 ASRO stations have exactly the same digital format as the SRO stations. The difference is that they do not have borehole seismometers. The sensors are long-period seismometers (HGLP, High Gain Long-Period) which are located in sealed metal tanks bolted to concrete floors at the observatory and a conventional short-period seismometer.

Digital Worldwide Standardized Seismograph Network (DWWSSN)

Installation of the DWWSSN stations began in the spring of 1980 (Table 3). The format for the DWWSSN stations consists of three long-period components recorded on a continuous basis, three intermediate-period components and one short-period vertical component, both recorded on an event-only basis.

The GDSN stations available for this study are listed in Table 4 along with usage of and comments about the data, and their distribution is shown on an equi-distant-azimuthal map projection in Figure 3.

TABLE 3

GLOBAL DIGITAL SEISMIC NETWORK (GDSN)

JANUARY 1, 1982

STATION	TYPE	DATE INSTALLED	COMMENTS
ANMO	SRO	09/01/74	
ANTO	SRO	08/01/78	
BCAO	SRO	06/12/79	STATION DOWN 01/01/82
BOCO	SRO	03/13/78	
CHTO	SRO	07/01/77	STATION DOWN 01/01/82
GRFO	SRO	10/01/78	
GUMO	SRO	12/01/75	
MAIO	SRO	12/01/75	STATION NOT OPERATING
NWAO	SRO	04/01/76	
SHIO	SRO	07/01/78	STATION DOWN 01/01/82
SNZO	SRO	03/15/76	
TATO	SRO	05/13/76	
CTAO	ASRO	10/09/76	
KAAO	ASRO	05/10/77	DATA INTERMITTENT
KONO	ASRO	09/01/78	
MAJO	ASRO	06/15/77	
ZOBO	ASRO	09/10/76	
AFI	DWWSSN	05/15/81	
ALQ	DWWSSN	04/02/81	
BER	DWWSSN	08/10/81	
JAS	DWWSSN	10/01/80	NEW SEISMOMETER INSTALLED
KEV	DWWSSN	10/14/81	
LON	DWWSSN	10/01/80	
SCP	DWWSSN	01/29/81	MINOR PROBLEMS
SLR	DWWSSN	10/24/81	
TAU	DWWSSN	06/10/81	
TOL	DWWSSN	11/03/81	
COL	DWWSSN		INSTALLATION IN PROGRESS
BDF	DWWSSN		FUTURE INSTALLATION
FVM	DWWSSN		FUTURE INSTALLATION
GDH	DWWSSN		FUTURE INSTALLATION
KIP	DWWSSN		FUTURE INSTALLATION
LEM	DWWSSN		FUTURE INSTALLATION
QUE	DWWSSN		FUTURE INSTALLATION
SBA	DWWSSN		FUTURE INSTALLATION

TABLE 4

GDSN DIGITAL DATA
(AVAILABLE FOR THE SEPTEMBER 1, 1981 SAMOA ISLANDS EARTHQUAKE)

STA.	LAT.	LON.	GEOGRAPHIC NAME	TYPE	USAGE				COMMENTS
					FPS	WFI	MWM	BBA	
ANMO	34.95N	106.46W	ALBUQUERQUE, NEW MEXICO	SRO	X	X	X		SP-C
CHTO	18.79N	98.98E	CHIANG MAI, THAILAND	SRO	X	X			
GUMO	13.59N	144.87E	GUAM, MARIANAS ISLANDS	SRO	X	X	X		SP-PC LP-PC
NWAO	32.93S	117.24E	NARROGIN, AUSTRALIA	SRO	X	X	X		LP-C
GRFO	49.69N	11.22E	GRAFENBERG, GERMANY	SRO	X		X		LP-PC
TATO	24.98N	121.49E	TAIPEI, TAIWAN	SRO	X	X	X	X	LP-PC
SNZO	41.31S	174.70E	SOUTH KARORI, NEW ZEALAND	SRO	X	X	X	X	
CTAO	20.09S	146.25E	CHARTERS TOWERS, AUSTRALIA	ASRO	X	X	X		
KAAO	34.54N	69.04E	KABUL, AFGHANISTAN	ASRO			X		
MAJO	36.54N	138.21E	MATSUSHIRO, JAPAN	ASRO	X	X	X	X	
KONO	54.65N	9.60E	KONGSBERG, NORWAY	ASRO	X		X	X	
SCP	40.79N	77.87W	STATE COLLEGE, PENNSYLVANIA	DWWSSN	X		X	X	
LON	46.75N	121.81W	LONGMIRE, WASHINGTON	DWWSSN	X		X	X	SP-C
AFI	13.91S	171.78W	AFIAMALU, WESTERN SAMOA	DWWSSN	X				SP-C LP-C
TAU	42.91S	147.32E	HOBART, TASMANIA	DWWSSN	X		X	X	

ABBREVIATIONS:

FPS FAULT PLANE SOLUTION
WFI WAVE-FORM INVERSION
MWM MANTLE-WAVE MOMENT
BBA BROADBAND ANALYSIS

SP-C SHORT-PERIOD DATA CLIPPED
LP-C LONG-PERIOD DATA CLIPPED
SP-PC SHORT-PERIOD DATA POSSIBLY CLIPPED
LP-PC LONG-PERIOD DATA POSSIBLY CLIPPED

Samoa Islands Region

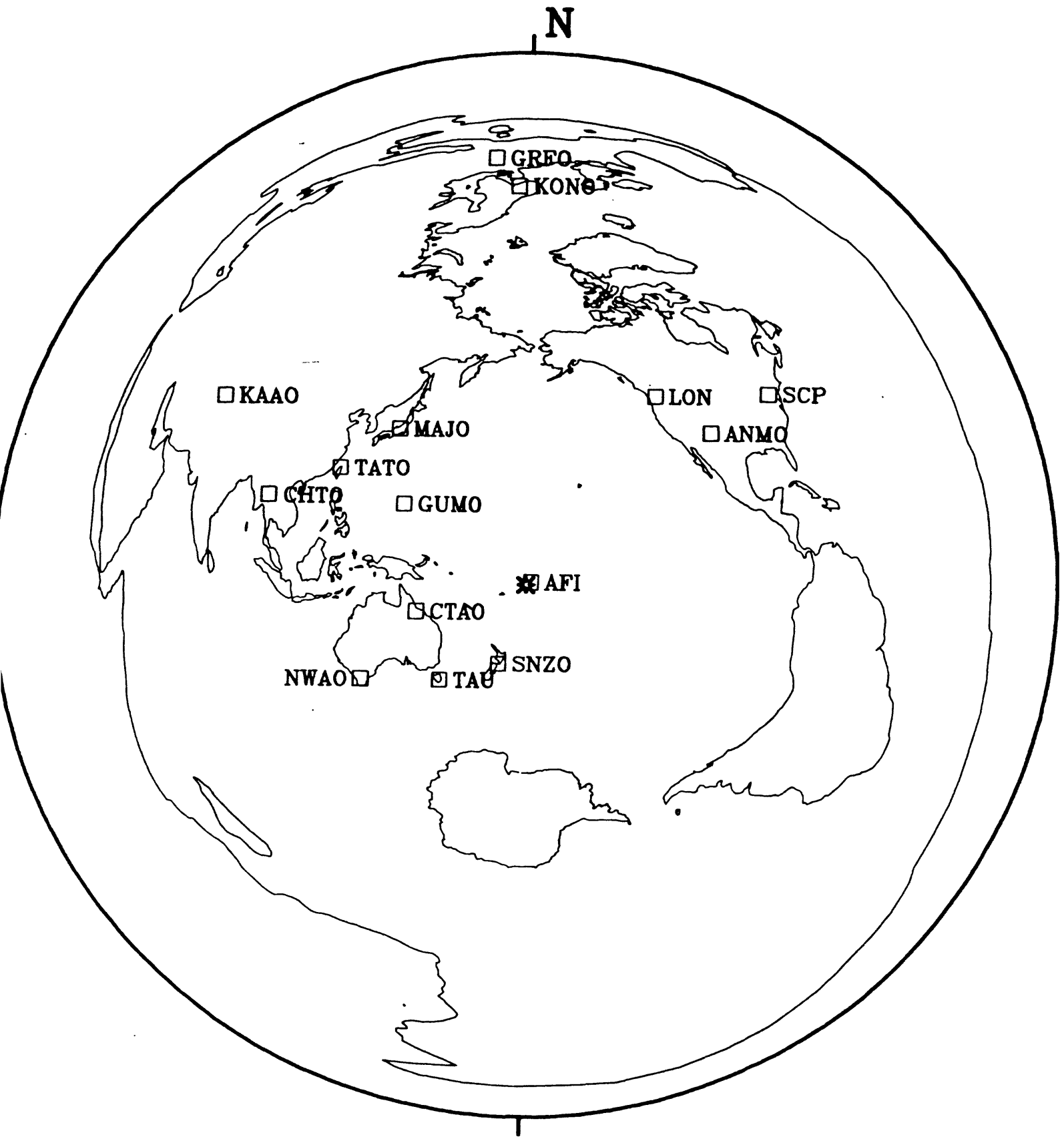

Figure 3. Equidistant azimuthal projection, showing GDSN stations available for this report, centered on the Samoa Islands Region epicenter.

Relocation of Epicenters - Dewey

Prior seismicity and early aftershocks of the Samoa earthquake of September 1, 1981 have been determined using station delays estimated by the Joint Epicenter Determination (JED) (Dewey, 1972). We relocated epicenters of shallow earthquakes that occurred from 7 months prior (February 1, 1981) to the mainshock to one week after (September 8, 1981) the mainshock and that had initially been assigned by the NEIS to the region bounded by 14.5° S, 16.0° S, 172.0° W and 174.0° W.

Our location process required two stages. In the first stage, we used JED to estimate variances of the arrival-time observations and to estimate station delays for 15 well-recorded earthquakes. In the second stage, we computed the epicenters of all shocks with a single event location program, using the JED-computed variances to weight observations and construct confidence ellipses on the epicentral coordinates, and using the JED-computed station delays to adjust the theoretical travel-times for systematic early or late arrivals.

The calibration event for the JED was the foreshock of September 1, 1981, 0723 GMT, which was restrained to the epicenter that had been determined by the NEIS using unadjusted travel-times. It is very likely that the assumed epicenter of the calibration event is biased. This appears likely on principle because the ray paths to some stations are likely to sample anomalous velocity structure associated with the Tonga subduction zone. Also, the station delays computed for the nearest station, AFI (Δ 2.0°, Az 50°), are so large that they cannot be attributed solely to anomalous velocity between the hypocenter and station, but must imply that the calibration event, and therefore the entire group of epicenters, are biased. The P-wave station delay at AFI (-8.0 s) and the S-wave delay (-13.1 s), both imply that our assumed epicenter for the calibration event is biased about 60 km further from AFI (i.e. to the SW) than the true location. The precise extent and direction of this bias must await further research. To facilitate comparison of our location with other single event epicenters determined by the NEIS, we have kept the calibration event fixed to its biased location. All the events computed by the JED with respect to the calibration event are therefore also biased by about the same amount as the calibration event.

We have not computed focal depths corresponding to the redetermined epicenters. This is because there were few depth phases recorded for these earthquakes, and because of our suspicion that the severe bias in the epicentral locations would minimize the value of readings of P- and S- waves at AFI for determining focal depth. Most earthquakes were assigned the same focal depths as had been assigned by the NEIS (generally 33 km). The focal depths of the mainshock and the foreshock of September 1, 1981, 0723 GMT, were fixed to the values estimated from modeling of body wave seismograms.

Listed in Table 5, together with the redetermined epicenters, are 90% confidence ellipses (Evernden, 1969) on the epicentral coordinates. These ellipses do not account for mislocation of epicenters due to bias in the assumed position of the calibration event. The ellipses only show the estimated precision of the epicenters relative to each other.

Figure 4 shows those epicenters whose confidence ellipses have semi-major axes less than 30 km long.

We make the following observations on the relocated epicenters.

(1) The trend of the group of epicenters and particularly of the early aftershocks (X's) is about S35°E, contrasting to the strike of S12°E estimated by the focal mechanism study.

(2) The foreshock of 0723 GMT, September 1, 1981, occurred at virtually the same location as the mainshock. Prior teleseismically recorded seismicity also occurred near the mainshock hypocenter on April 6, 1981.

(3) The length of the aftershock zone is about 125 km. However, most of the aftershocks are concentrated in a group near the mainshock epicenter, and the figure of 125 km is based on the sparse teleseismically recorded activity to the NW and SE of the principal group of aftershocks near the mainshock epicenter.

TABLE 5

DATE	JED O.TIME	JED SOUTH LAT.	JED WEST LON.	JED DEPTH	M		JED CONFIDENCE ELLIPSE SEMI-MAJOR AXIS ORIENTATION IN DEGREES COUNTER-CLOCKWISE FROM EAST	LENGTH OF SEMI-MAJOR AXIS (km)	LENGTH OF SEMI-MINOR AXIS (km)	EVENTS USED TO ESTIMATE JED STATION DELAYS
					mb	Ms				
02/06/81	05:43:00.81	15.277	173.510	33	5.3	5.1	123.1	18.8	8.6	
02/15/81	19:03:42.94	15.222	173.634	33	4.8		134.6	31.0	11.4	
02/26/81	06:11:00.93	15.375	173.399	33	5.4	5.2	122.9	16.7	7.2	
04/06/81	00:16:14.30	15.132	173.217	33	4.9		119.0	21.6	9.2	X
04/06/81	00:46:44.96	15.151	173.103	33	4.9		128.9	28.3	10.6	X
04/06/81	01:03:13.75	15.101	173.216	33	4.9		43.8	39.5	19.4	
06/25/81	03:08:49.42	15.268	173.536	50	5.1		128.2	15.7	7.2	
06/25/81	04:40:53.85	16.059	173.137	33			42.1	40.3	14.3	
07/01/81	16:24:47.20	15.608	173.011	33	4.9		127.0	36.0	12.6	
07/06/81	01:02:26.22	15.274	173.516	33	5.6	5.4	117.5	10.4	5.9	
07/30/81	21:55:18.46	16.292	171.625	35	4.7		-24.4	29.2	18.7	
08/21/81	01:46:57.05	15.184	173.844	33	4.6		123.2	38.5	15.4	
08/24/81	22:29:15.90	14.912	173.377	10			129.7	31.3	14.9	
09/01/81	07:23:02.19	15.139	173.288	29	5.8	5.7	*	*	*	X
09/01/81	09:29:31.14	15.088	173.261	25	7.0	7.7	114.5	8.6	5.2	X
09/01/81	09:59:32.84	14.985	173.391	33	5.6		131.6	30.6	10.9	X
09/01/81	10:59:04.52	15.161	173.122	33	5.2		133.9	29.8	12.9	
09/01/81	11:54:40.05	15.296	173.056	33	4.5		127.4	30.0	11.2	X
09/01/81	12:39:15.02	15.161	173.377	33	4.8		125.8	42.3	16.0	
09/01/81	15:24:36.87	15.217	173.217	33	4.8	5.1	128.6	28.3	9.0	X
09/01/81	18:08:08.52	15.195	173.507	33	4.6		118.5	74.0	13.5	
09/01/81	18:38:48.34	15.165	173.455	33	5.7	5.3	121.8	11.3	5.9	X
09/01/81	23:55:45.80	15.174	173.294	33	5.6	5.4	130.7	12.0	6.1	X
09/02/81	00:34:27.38	15.219	173.429	33	4.8	4.9	109.6	21.6	12.3	X
09/02/81	01:46:59.31	15.438	173.147	33	4.4		-35.9	37.2	15.0	X
09/02/81	02:10:26.21	15.607	172.799	33	4.8	4.6	120.0	15.6	9.0	X
09/02/81	06:25:47.20	15.194	173.266	33	4.8	4.8	128.4	14.6	9.6	X
09/02/81	08:44:21.92	15.418	173.061	33	5.3	5.5	118.2	9.4	5.7	X
09/02/81	10:30:53.73	14.899	173.681	33	5.3	5.1	118.0	16.6	8.6	X
09/03/81	00:46:21.91	15.322	173.093	33	4.7	4.7	124.8	38.7	12.3	
09/04/81	03:31:15.82	14.977	173.441	33	4.5	4.7	117.3	111.3	14.3	

* CALIBRATION EVENT

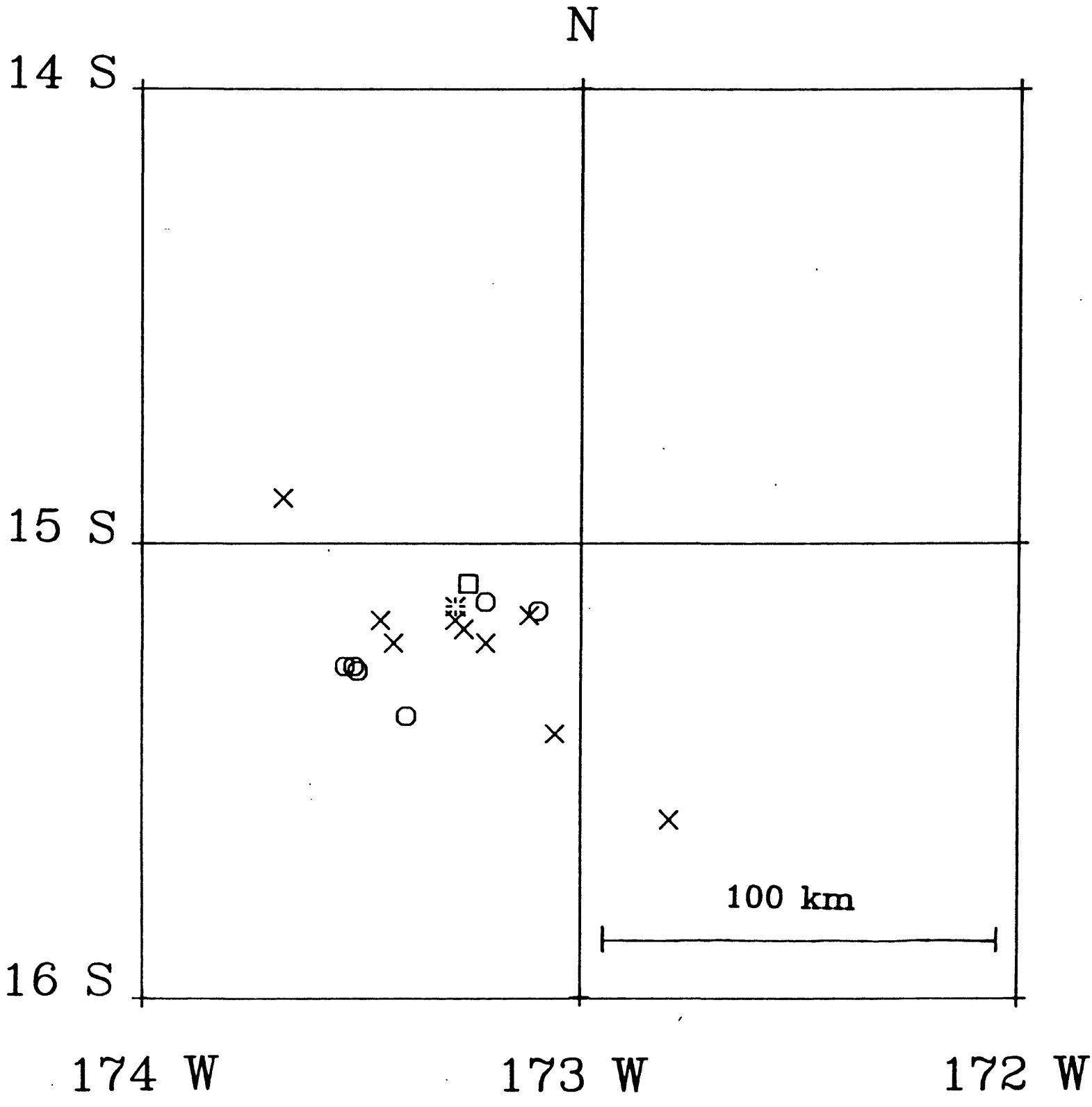

Figure 4. Epicenters of mainshock (square) of 0929 GMT, September 1, 1981, prior seismicity (octagons), and early aftershocks (X's) as located by JED relative to foreshock of 0723 GMT, September 1, 1981 (•). Only epicenters are plotted for which the corresponding 90% confidence ellipses (Table 5) have semi-major axes less than 30 km in length.

Source Parameters

The seismic source parameter solutions for this report were obtained from five techniques utilizing WWSSN analog and GDSN digital data. The techniques used are the P-wave first motion fault plane solution, the waveform inversion solution, the centroid-moment tensor solution, the mantle wave moment solution, and the broadband waveform analysis solution.

Fault Plane Solution - Needham and Zirbes

The fault plane solution was computed using a total of 120 P-wave (P, pP and PKP) first motion observations, 74 read from LPZ components and 46 from SPZ components. Most of the LP earth motions were read by the USGS from the processed digital waveforms or from WWSSN seismograms. All other earth motions used in this solution were reported to NEIS by the station analysts. A list of these 120 stations along with the station-epicenter distance, epicenter-station azimuth, dt/Δ in sec./deg., focal angle computed using the J-B velocity model, and the polarity, direction and type of earth motion, is presented in Appendix III.

The preferred fault plane solution from P-wave first motions corresponds to a normal fault-type mechanism. The fairly well controlled fault plane strikes N78°W and dips 70°SSW. The poorly controlled auxiliary plane strikes N78°W and dips 20°NNE. The P-axis plunges 65.0° toward azimuth 12.0° and the T-axis plunges 25.0° toward azimuth 192.0°. The focal sphere solution is shown in Figure 5a.

A focal mechanism reported by Johnson and Molnar (1972) for the Samoa Islands Region earthquake of April 20, 1968 is shown in Figure 5b. The PDE location of this earthquake is approximately 90 km SE of the September 1, 1981 earthquake. This fault plane solution, with the P-axis plunging 8.0° toward azimuth 64.0° and the T-axis plunging 26.0° toward azimuth 188.0°, is remarkably similar to the solution for the September 1 earthquake.

An alternate fault plane solution for this earthquake that is consistent with the first motion data is shown in Figure 6. This solution would imply a moderate right lateral strike-slip component on the SSW dipping plane. The moment tensor solutions of Sipkin (this report) are not consistent with the strike-slip component of this mechanism.

The long-period P-wave motions from the GDSN stations available for this study are presented in Figure 7. The first motion from station KAAO was not used in the fault plane solution due to the questionable direction of the first motion. The waveform for station AFI is not presented as it was clipped immediately after the long period P onset. The direction of earth motion for stations CTAO and NWAO, both positioned very near a nodal plane of the fault plane solution, could be misread with normal analog seismogram resolution. With the high resolution of these two stations and the digital capability to artificially amplify the onset amplitude, a definite direction of earth motion can be reported as is shown on Figures 8 and 9.

Waveform Inversion and Centroid Moment Tensor Solutions - Sipkin

One of the waveform inversion techniques described by Sipkin (1982) has been applied to a subset of the digitally recorded GDSN long-period body-wave data. Long- and short-period composite P-waveforms (P, pP, sP) in the distance range 28° to 94° were examined for clipping or other types of contamination and were then subdivided into groups depending upon the degree of contamination. Far field Green's functions for these composite P waves were computed using the WKBJ method (Chapman, 1978) and the long-period waveforms were inverted using a semi-automated multichannel signal enhancement algorithm. The

Figure 5a. Lower hemisphere projection of Samoa Islands Region fault plane solution computed from P-wave first motions. Large symbols are LPZ P-wave first motions and small symbols are SPZ P-wave first motions.

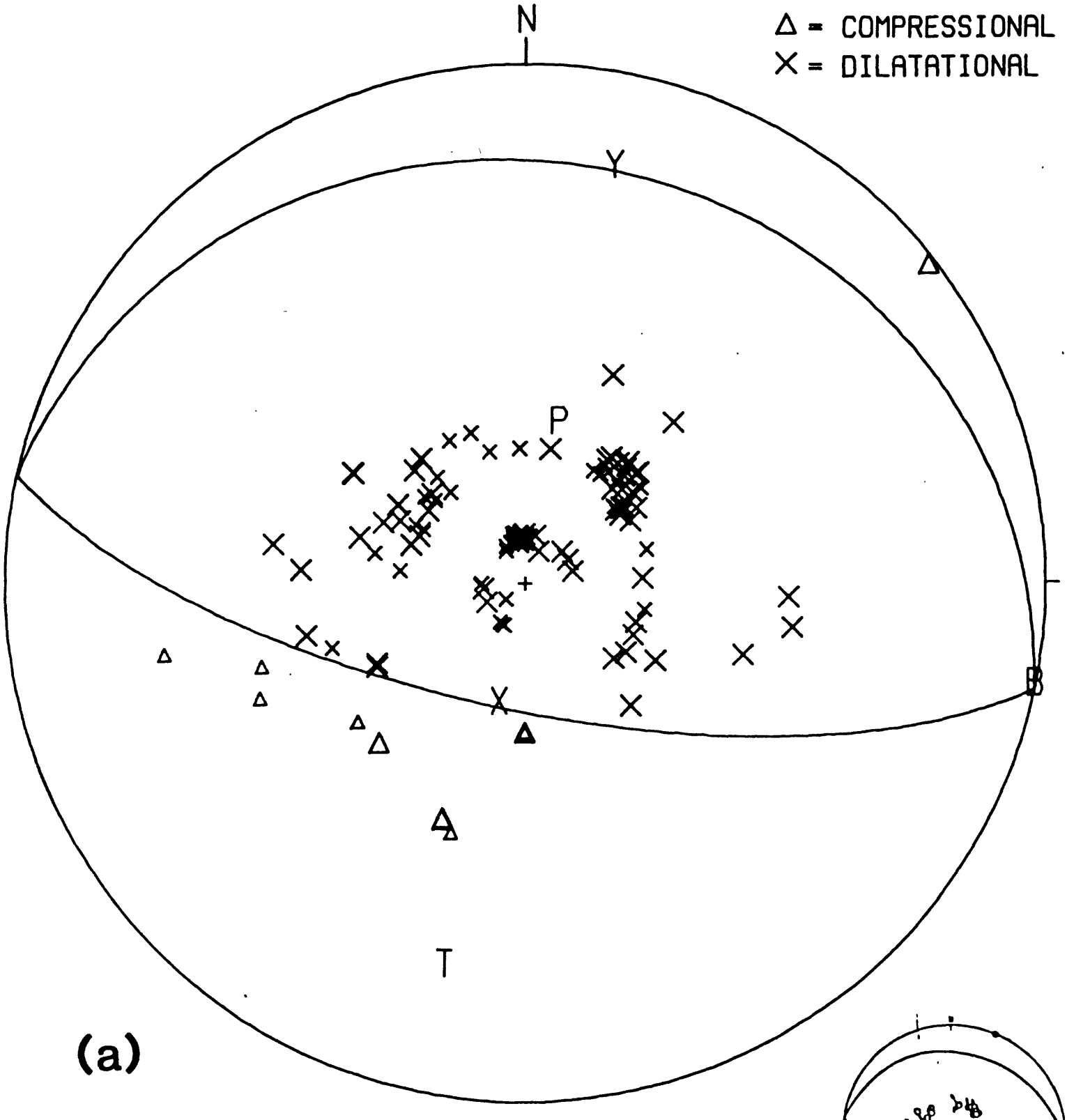

Figure 5b. Fault plane solution from Johnson Molnar (1972) with ● being dilation and O being compressional first motions.

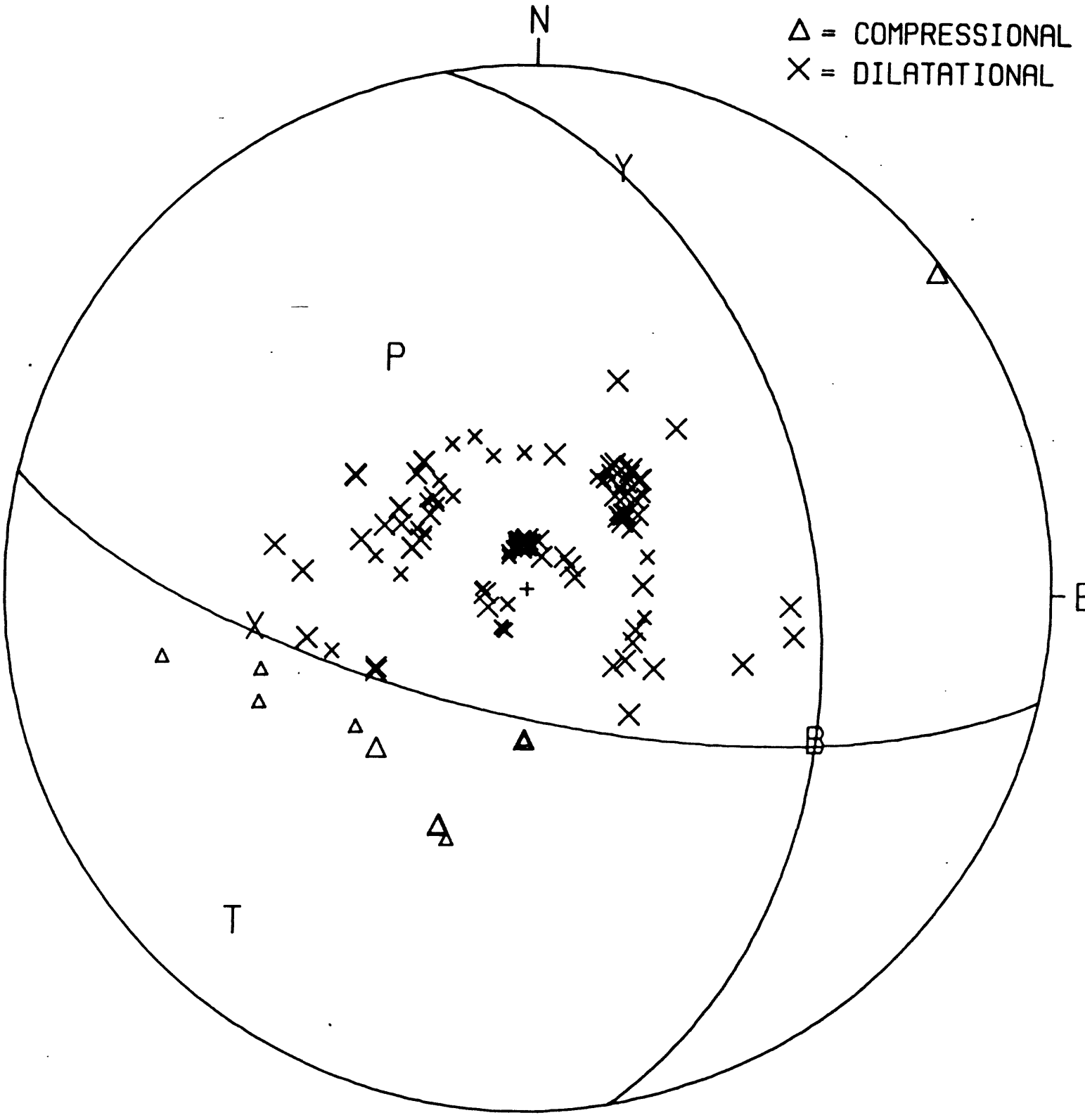

Figure 6. Lower hemisphere projection of alternate Samoa Islands Region fault plane solution.

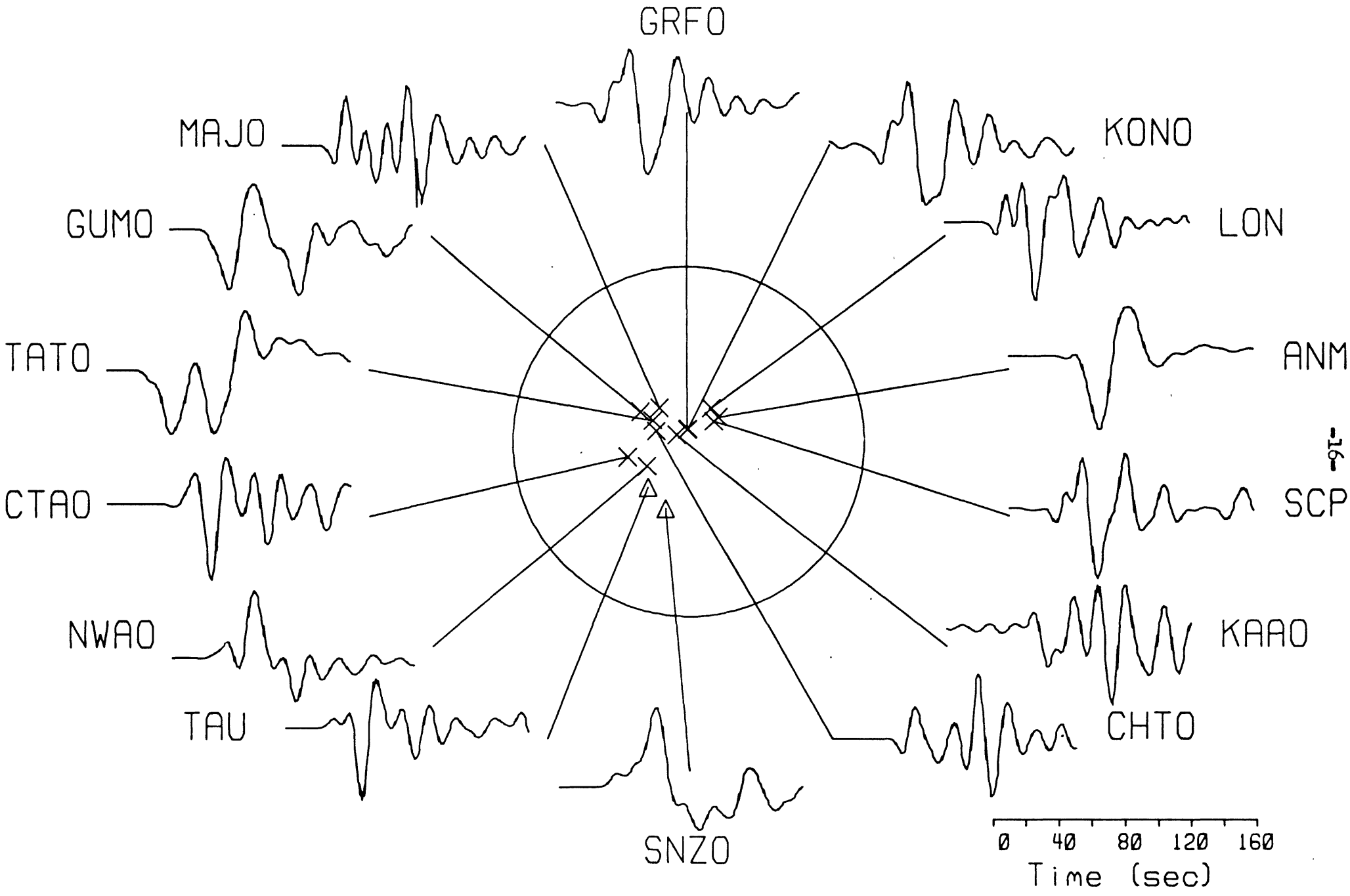

Figure 7. LPZ P-waveforms from GDSN stations. Amplitudes normalized to give a uniform display.

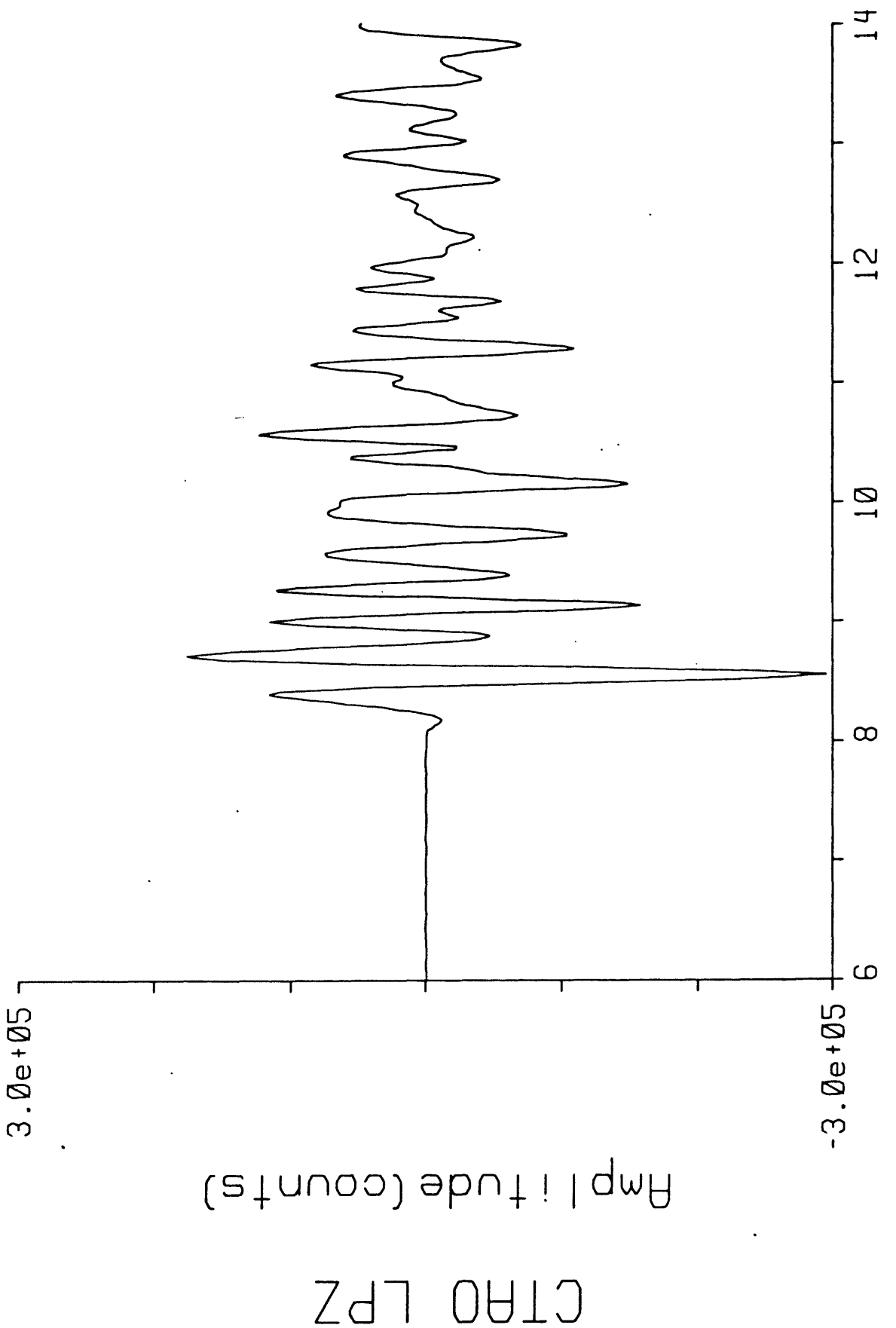

Figure 8. LPZ P-waveforms from GDSN station CTAO.

Figure 9. LPZ P-waveforms from GDSN station NWAO.

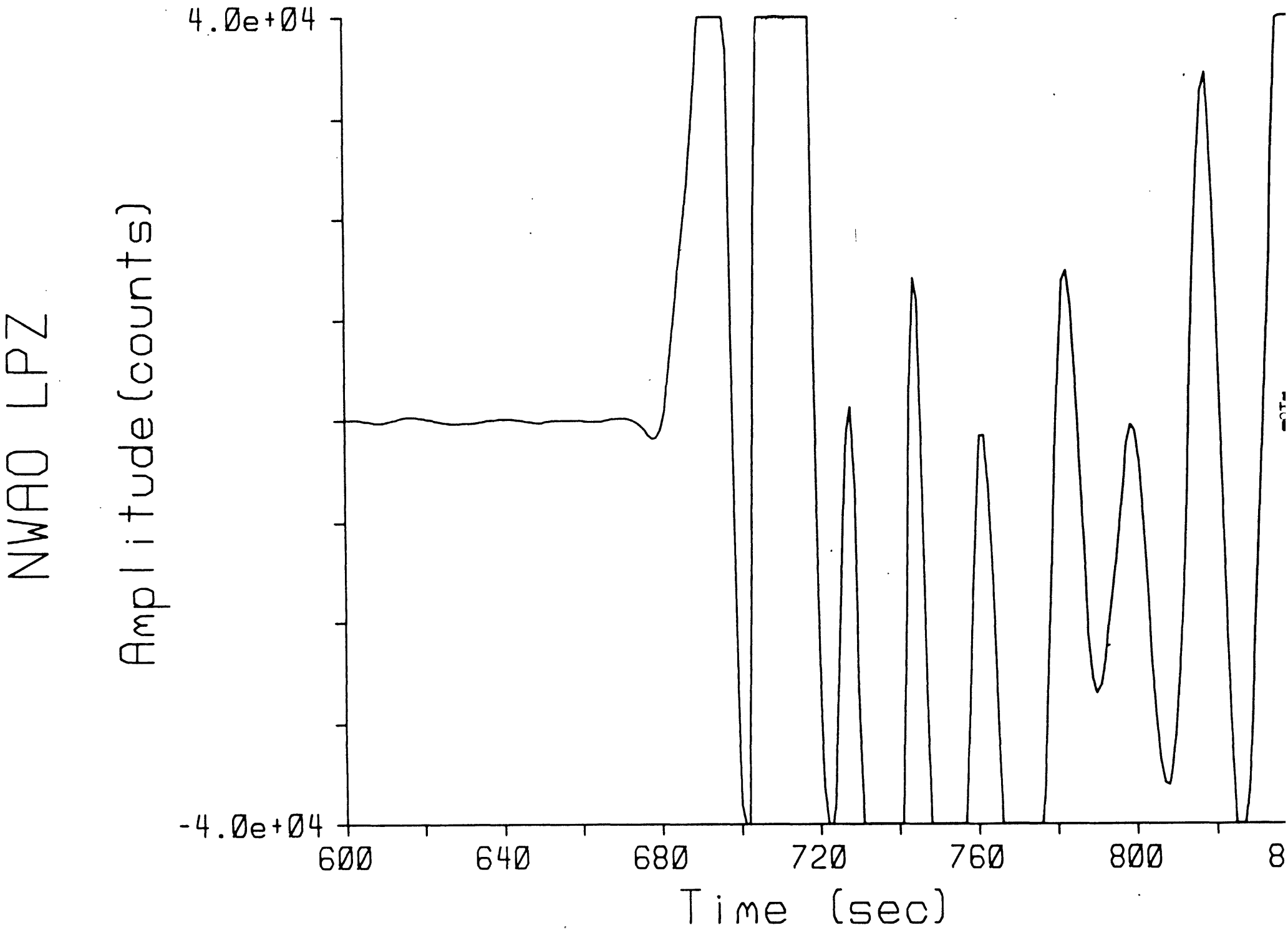

source depth was refined by finding the depth for which the misfit to the data (in a least squares sense) is minimized.

The long-period P-waves examined are shown in Figure 10. Those at NWAO and ANMO are possibly clipped and those at GUMO and TATO are questionable. Three separate sets of inversions were carried out, first using all eight waveforms, then excluding NWAO and ANMO, and finally also excluding GUMO and TATO. 50 to 58 seconds of each waveform were used and all inversions were performed with the moment rate tensor constrained to be purely deviatoric. Since estimates of source depth ranges from 20 km (centroid solution, this report) to 33 km (PDE), the inversions were carried out using Green's functions computed for a variety of source depths between 18 and 33 km. The best double couple solutions for source depths of 20, 22, and 33 km are shown in Figure 11. The smallest misfit to the data occurred for a depth of 22 km using the six station subset which excluded the waveforms from NWAO and ANMO. The similarity of the solutions obtained from all three data subsets is an indication of the robustness of the method used. The source parameters obtained when the moment tensor is decomposed into its eigenvalues and principal axes are given in Table 6 along with the centroid moment tensor solution. This representation is equivalent to and contains the same amount of information as the moment tensor representation. A comparison between the real and synthetic data is shown in Figure 12. One should be aware, however, before accepting 22 km as the best source depth, that this estimate may be biased by the earth model used to compute the Green's functions, in this case model 1066B (Gilbert and Dziewonski, 1975). This model has a discontinuity at 21 km with crustal velocities above and mantle velocities below.

Since the source was not constrained to be a double couple the intermediate eigenvalue, although small (less than 9% of the other two eigenvalues), is not zero. In order to interpret such solutions in ways that will be familiar, one can either plot the nodal planes of the best double couple, or, more accurately, can plot the nodal lines of the principal axes representation on the lower half of the focal sphere. Both of these representations are shown in Figure 13.

In all of the inversions the source was assumed to be a point in both time and space and the solutions represent the 'average' source. This source will not necessarily correspond to the solution obtained by fitting first motion data, especially if there is a change in the source geometry during faulting. The inversion procedure can, however, in many cases be carried out without imposing the constraint that the source time function be a delta function (in the far field). A preliminary analysis for this event indicates that the amount and quality of the data are not sufficient to determine each element of the moment rate tensor as a function of time, and thus determine the source geometry as a function of time. It is possible, however, to determine a source time function for this event, which is shown in Figure 14. The data inverted is the six station subset which excludes the waveforms from NWAO and ANMO; the Green's functions are those for a source depth of 22 km. The duration is approximately 28 seconds with two peaks in activity, one at 7 sec with a width of approximately 7.5 sec and a sharper peak at 21 sec with a width of approximately 3.5 sec. Choy (this report) has found this event to be composed of two subevents separated in time by about 25 sec, with durations of approximately 25 sec each. Due to the time window used in the inversion, the second subevent reported by Choy was not included in the portion of the time series analyzed; the two subevents resolved in the inversion correspond to the first subevent reported by Choy.

Now that many new and useful ways of determining seismic source

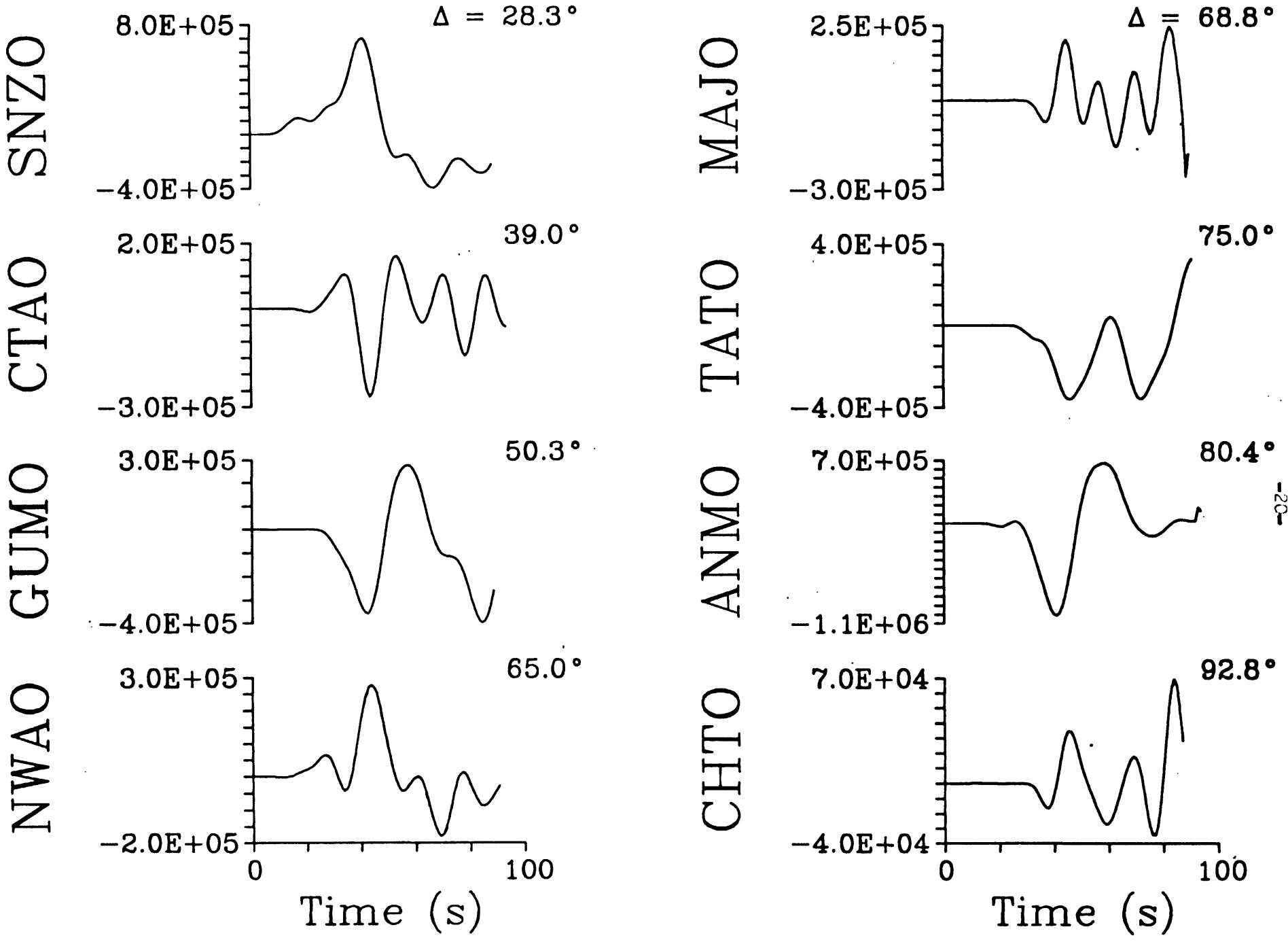

Figure 10. Long-period P waves recorded by the GDSN in the distance range 28° to 94°.

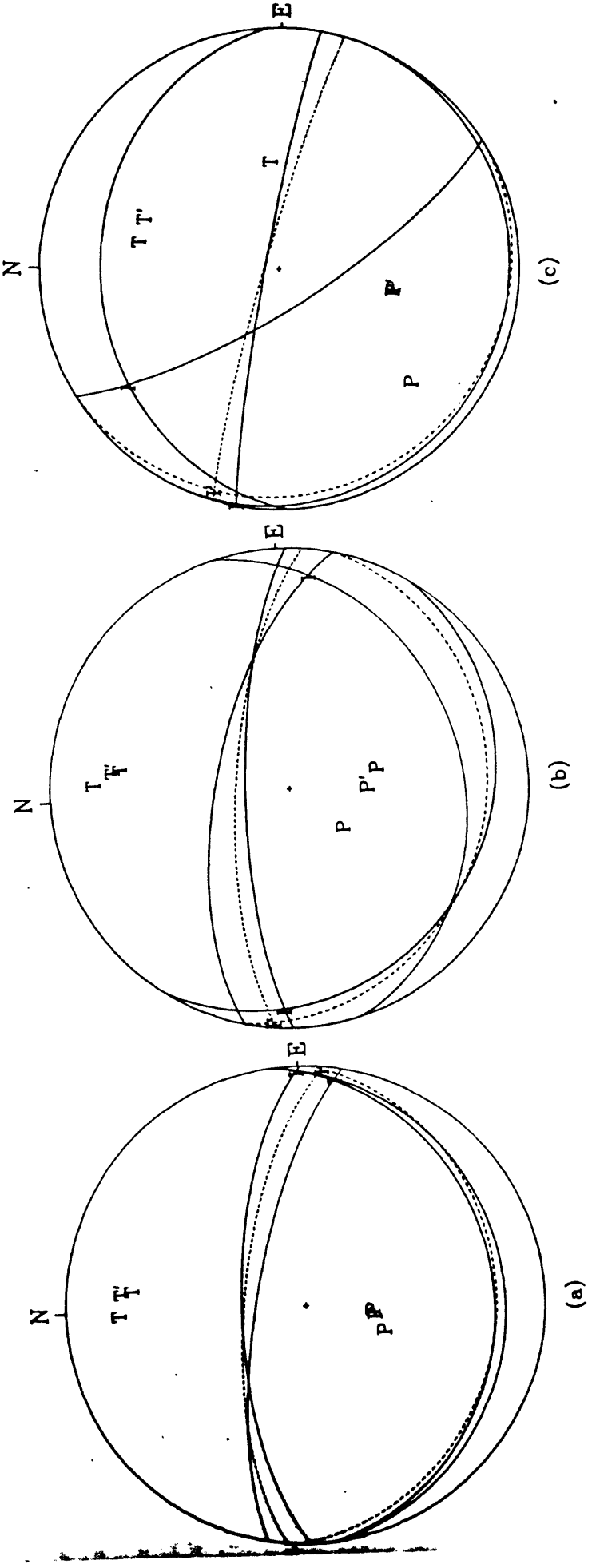

Figure 11. Nodal plane solutions for the three data subsets. Dashed curves correspond to solutions for the six station subset. Green's functions computed for source depths of (a) 20 km, (b) 22 km, (c) 33 km.

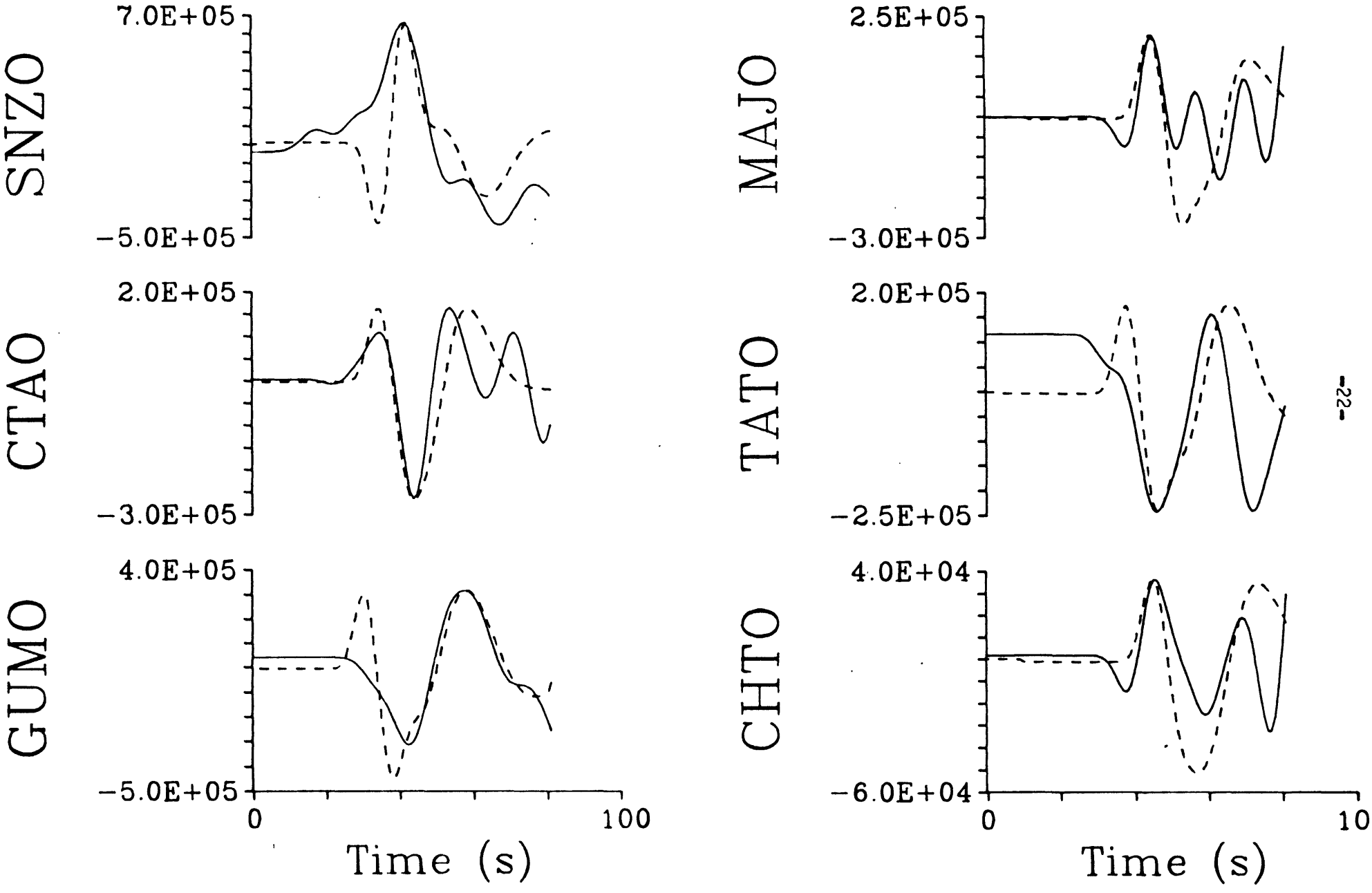

Figure 12. Comparison between the real data (solid curves) and synthetic data (dashed curves) for a source depth of 22 km.

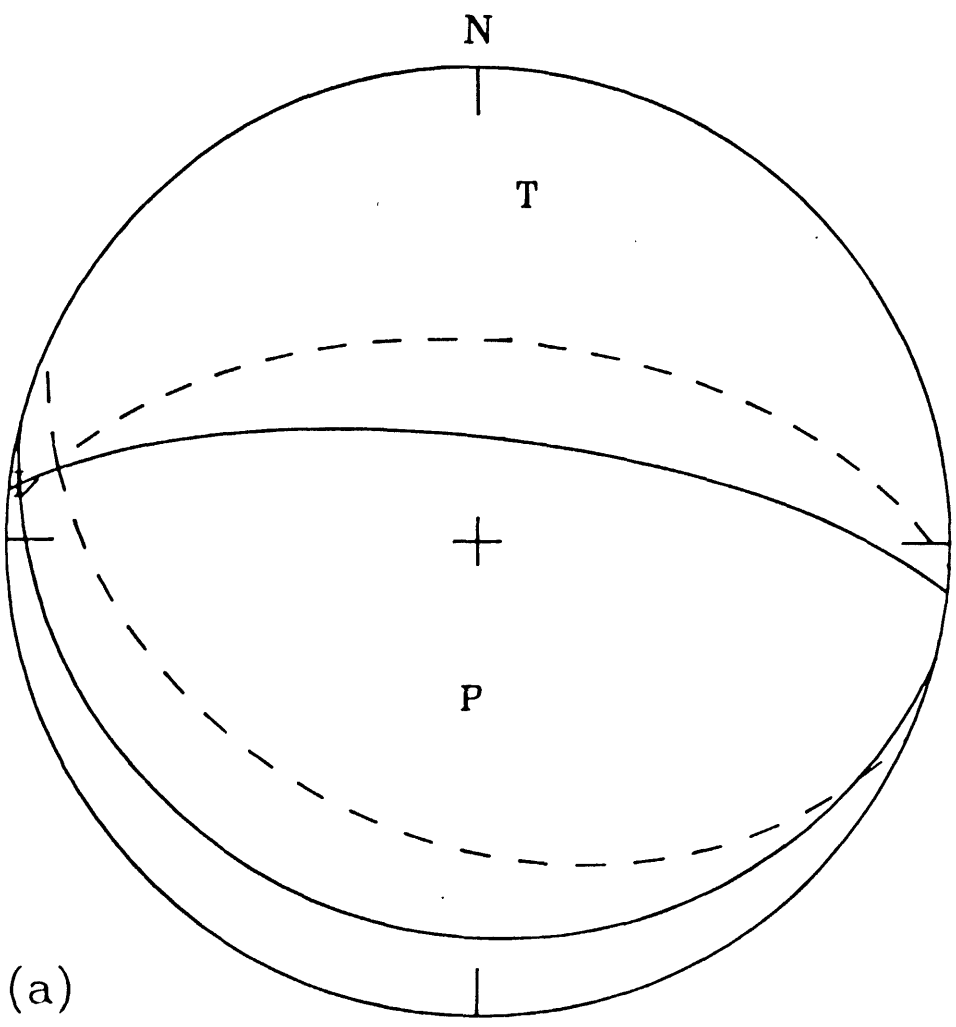

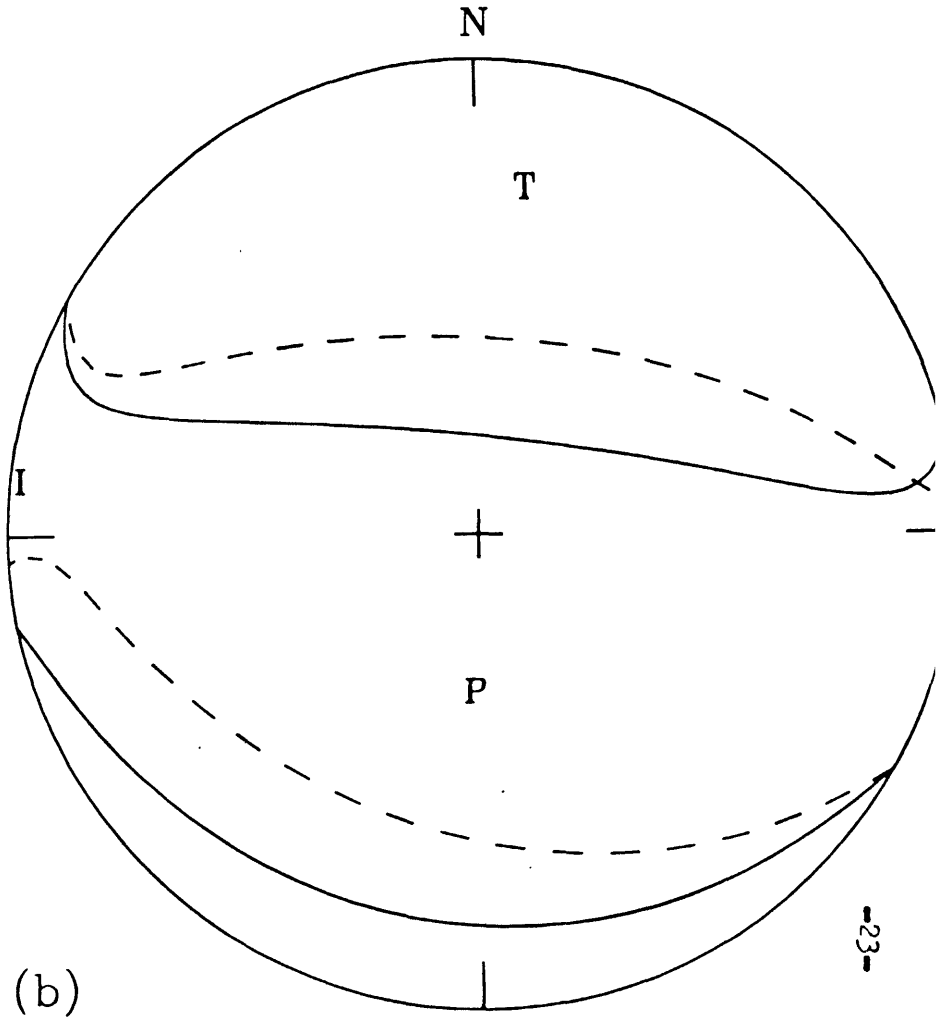

Figure 13a. Nodal plane solution for the six station data subset and a source depth of 22 km (solid curve) and the best double couple from the centroid moment tensor solution (this report) (dashed curve);

Figure 13b. Nodal lines of the moment tensor solutions.

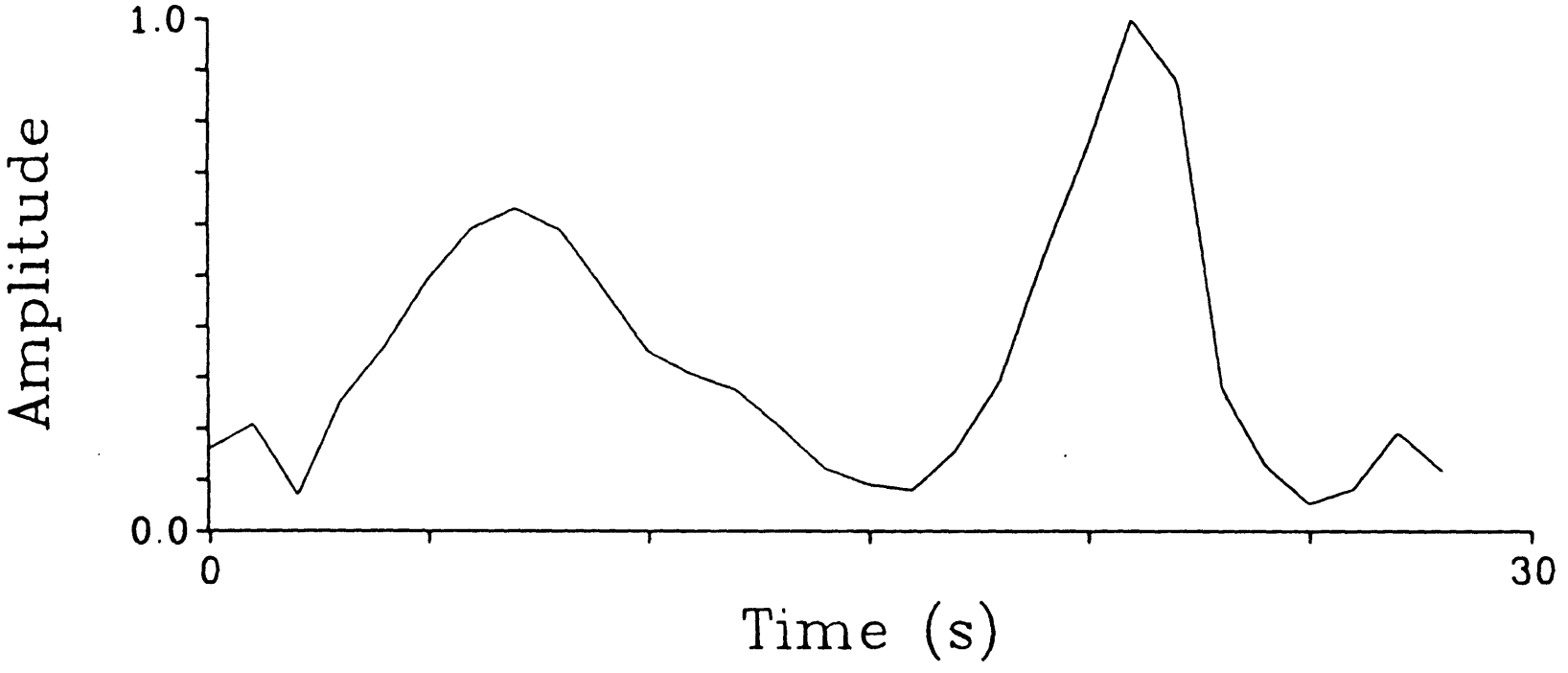

Figure 14. Source time function determined from the six station data subset and a source depth of 22 km.

parameters are becoming available a caveat is in order. When comparing different source solutions the portion of the seismogram analyzed and the frequency band utilized must be considered explicitly. However, the differences between such solutions may possibly be used to understand more completely the spacio-temporal history of the rupture process. Hopefully, at some time in the near future such syntheses will become standard procedure.

The waveform inversion technique described in Dziewonski, and others (1981) and the July 1981 Monthly Summary, now expanded to include mantle waves, has been applied to the long period body wave and mantle wave data from the GDSN. The body wave data consists of the three rotated components from twelve stations with a time window starting at the cessation of clipping or other nonlinearities (if any) and ending at the arrival of the fundamental mode surface waves. These records are low-pass filtered by a tapered filter with a cut-off period of 45 sec before being inverted. Mantle waves from 14 stations (40 records) were also used in the inversion after being low-pass filtered by a filter with a cut-off period of 135 seconds.

The non-linear least-squares inversion resulted in very small perturbations to the Preliminary Determination of Epicenters (PDE) epicentral location (0.03° in latitude and 0.01° in longitude). The depth was held fixed at 20 km. The only sizable perturbation to the PDE estimate of the source parameters was in the origin time, a change amounting to 15 sec. This perturbation can be interpreted either in terms of the duration of a constant amplitude source time function or in terms of source multiplicity. If the length of a constant amplitude source time function is established by requiring that the scalar moment determined in different bands of frequency be as constant as possible, a half-duration of the source of 20 sec is arrived at.

The moment tensor, in order to be more easily interpreted, has been rotated into the principal axes system (Table 6). Since the source was not constrained to be a double couple the intermediate eigenvalue (length of the null axis) is not identically equal to zero. However, since the intermediate eigenvalue is relatively small (less than 6% of the other two eigenvalues) the solution is very close to being a double couple. The nodal planes of the best double couple solution and the nodal lines of the moment tensor are shown projected onto the lower half of the focal sphere in Figure 13. Total moment is $M_0 = 1.9 \times 10^{27}$ dyne-cm.

TABLE 6

USGS moment tensor solution
Data: unfiltered L.P. GDSN body waves
Constraints: zero trace
No. of stations: 6
Depth: 22 km
Principal axes:

	Value ($\times 10^{27}$ dyne·cm)	Azimuth	Plunge.
P	-1.69	182	63
T	1.83	8	27
I	-0.15	277	2

Best double couple:

$M_0 = 1.8 \times 10^{27}$ dyne·cm

	Strike	Dip	Slip
NP1	104	18	277
NP2	276	72	268

****

Centroid moment tensor solution
Data: GDSN
L.P. body waves: 12 Stations, 36 Components, Corner Period at 45 sec
Mantle waves: 14 Stations, 40 Components, Corner Period at 135 sec
Origin time: 9:29:47.4±0.2
Latitude: 15.02S±0.01
Longitude: 173.16W±0.02
Depth: 20.0 Fixed
Half-duration 20.0
Principal axes:

	Value ($\times 10^{27}$ dyne·cm)	Azimuth	Plunge.
P	-1.88	143	76
T	1.99	12	9
I	-0.11	282	10

Best double couple:

$M_0 = 1.9 \times 10^{27}$ dyne·cm

	Strike	Dip	Slip
NP1	115	37	287
NP2	273	55	257

Mantle Wave Moment - Buland

Visual examination of GDSN recordings of the September 1, 1981 Samoa event reveals significant mantle wave activity as late as R4 and G4 (Figure 15). Vertical and transverse records 20,000 sec in length from 14 stations were processed as described by Buland and Taggart (1981). Mantle waves were not observed at CHTO due to instrumental problems. AFI was not actually used either as its proximity to the source resulted in clipping during R1 and G1 and interference between later even and odd mantle wave passes (eg. R2 and R3). Spectral estimates from various mantle wave passes over the period range of 100 to 250 sec were corrected to constant distance and averaged to yield the radiation pattern shown in Figure 16. The solid and dashed lines represent average spectral amplitude of Rayleigh waves and Love waves respectively in cm-sec plotted at the same scale. The general features of the observed radiation pattern agree quite closely with those predicted by sources as calculated by Sipkin (this report). The radiation pattern predicted by the P-wave first motion fault plane solution done by Needham is rotated about 5° counterclockwise from the observed results. The radiation pattern shows no obvious asymmetry diagnostic of a complex extended rupture process. Note that the lack of clear nodes in the Love wave radiation pattern is typical of this method. Theoretically the nodes are very sharp for this type of source. They are not observed because the station coverage is not good enough, because mantle waves with low signal to noise are not processed, and because they are obscured by multi-pathing.

In order to estimate moment, our empirical results were compared with theoretical spectra generated from the moment tensor and source depth derived by Sipkin (this report). The centroid moment tensor solution was chosen as the most likely to represent properly the long period energy. This comparison yields moment estimates of 2.49×10^{27} dyne·cm from Rayleigh waves and 4.06×10^{27} dyne·cm from Love waves. Averaging all data yields an estimate of 3.28×10^{27} dyne·cm or a moment magnitude, M_w, of 7.61. The disparity between estimates from Rayleigh and Love waves indicates that (1) the source is deficient in some component which is a relatively efficient Love wave generator or (2) the source is deeper than the 20 km assumed. The additional evidence of a significant, systematic trend in Rayleigh moment estimate as a function of period tends to support the latter hypothesis. However, the complete rationalization of all data would require a source depth in excess of 35 km, which violates other evidence. We presume, therefore, that the real problem is a deficiency in the spherically averaged Earth model used to generate the theoretical results.

Preliminary Analysis of Broadband GDSN Data - Choy and Zirbes

The band-limited spectral content of standard long- and short-period seismograms make depth determination and the inference of source characteristics difficult. Long-period records are sufficiently smoothed that only average properties of the source can be obtained. The peak of the standard short-period seismographs, on the other hand, is usually near 1 Hz. This is inappropriate for studying the rupture process of moderate-sized and larger earthquakes because their corner frequencies are generally at a much lower frequency than 1 Hz. In this section, a determination of the depth of the Samoa earthquake and qualitative comments about the extent of its rupture complexity are made by a simultaneous analysis of the short-period records, the broadband ground displacements and the broadband ground velocities.

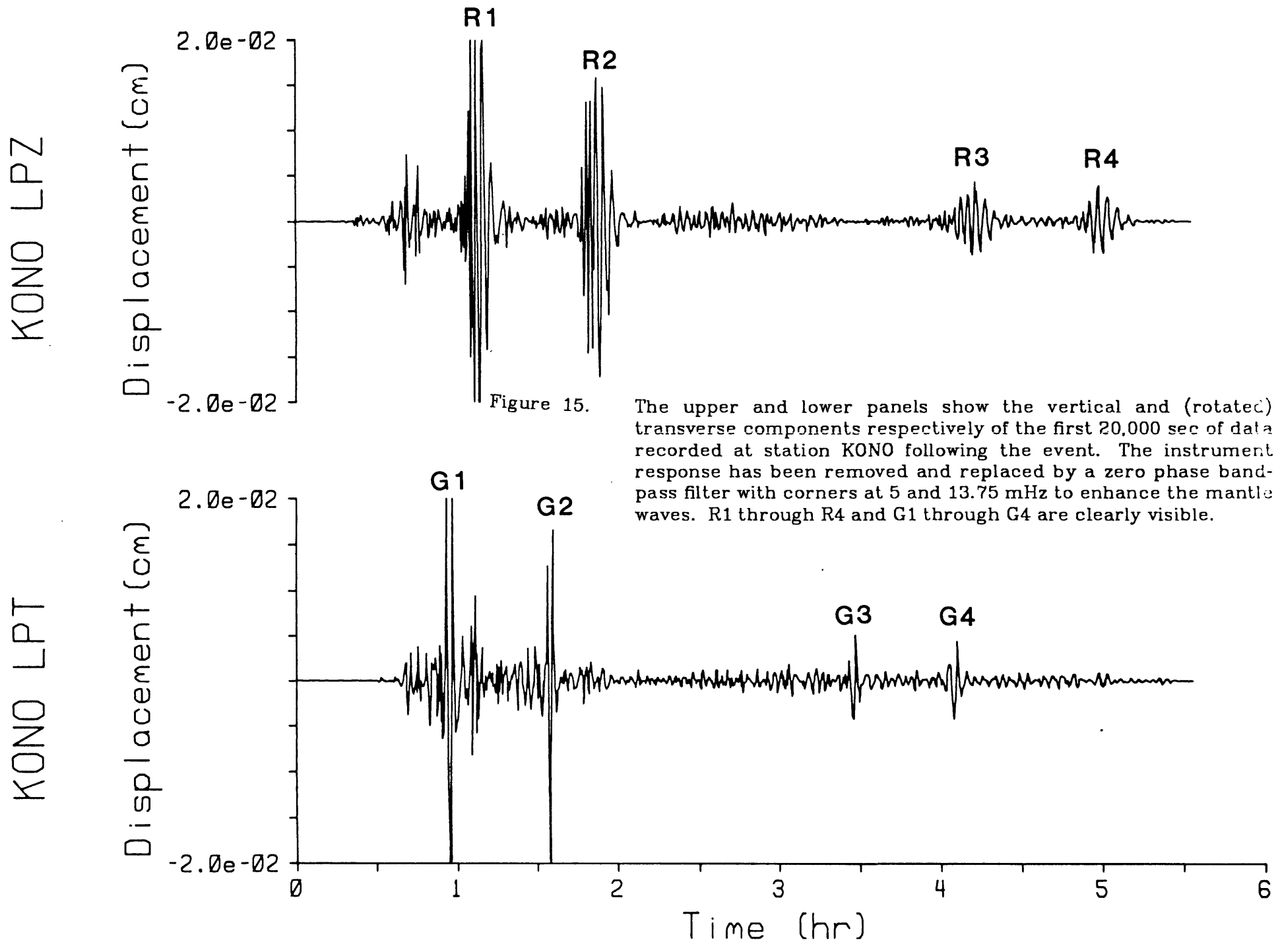

Figure 15. The upper and lower panels show the vertical and (rotated) transverse components respectively of the first 20,000 sec of data recorded at station KONO following the event. The instrument response has been removed and replaced by a zero phase band-pass filter with corners at 5 and 13.75 mHz to enhance the mantle waves. R1 through R4 and G1 through G4 are clearly visible.

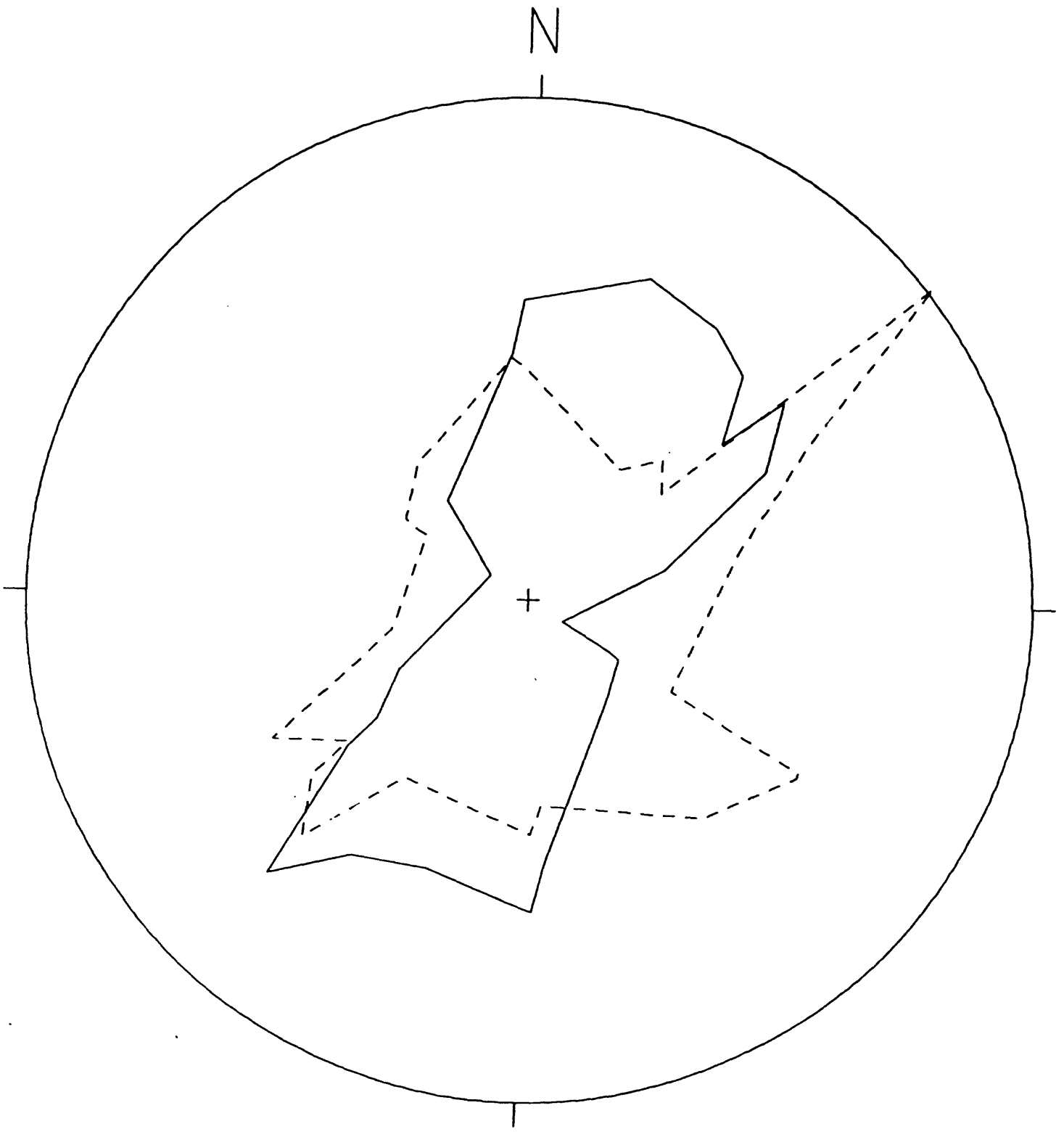

Figure 16. Average spectral amplitude, normalized to a distance of 90°, in cm-sec for Rayleigh waves (solid line) and Love waves (dashed line) are shown as a function of azimuth. Each station has the potential for yielding information on azimuth and 180° off azimuth. The circle corresponds to a spectral amplitude of 6.0 cm-sec.

Depth of the initial rupture

The digitally recorded GDSN records that are available for this event are shown in Figures 17-23. (Stations which may have had clipped waveforms were not used in this analysis.) With the exception of stations SCP and LON, the original short-period records for each station are shown in part (a) (Figures 19-23). The corresponding broadband records of ground displacement and velocity are shown in parts (b) and (c), respectively. The broadband records are obtained by the simultaneous deconvolution of the long- and short-period records as described by Harvey and Choy (1982) and Choy and Boatwright (1981). This processing was not needed for SCP and LON (Figures 17 and 18, respectively) because they are DWWSSN stations that record velocity data directly on an intermediate-frequency channel. This channel has a response that is already flat to velocity from 1-15 sec.

In cases where the displacement was not impulsive, the short-period or velocity records were used to pick the P-wave onset. Because of the shallowness of the earthquake, the free-surface operator (consisting of P, pP, and sP) overlaps the duration of the source-time function. The resulting convolution of the free surface operator and the source-time function makes it very difficult to distinguish the body-phase arrivals in resulting displacement waveforms at four of the stations (LON, KONO, MAJO, SNZO). In the other three displacement records, depth phases can be seen. For the SCP displacement, there are two phases with negative polarity at the beginning of the record (Figure 17b). As the focal mechanism predicts a positive polarity for pP, the second phase, indicated by the vertical line, cannot be pP. The absence of pP can be explained by the proximity of its takeoff angle to a nodal plane. This second phase could represent either a complexity of the rupture or sP. The latter interpretation is examined as the polarity and amplitudes of phases identified at other stations appear to satisfy the focal mechanism derived from P-wave first motions. For instance, a sharp change in slope in the second trough of the TATO displacement (marked by a vertical line in Figure 21b) occurs sufficiently late to be sP. The inflection after the P-wave arrival in the TAU displacement (indicated by a vertical line in Figure 22b) is likely to be pP on the basis of its polarity and an arrival time which is earlier than the sP picks at the other stations. The velocity records can supplement this analysis. Because velocity-squared is related to energy radiated through the focal sphere, the velocity waveforms are considerably more complex than the displacement (e.g., Boatwright, 1981). Guided by the few distinct arrivals that appeared well in the displacement records, arrivals in the velocity records can be associated with the pP and sP arrivals at the other stations, indicated by the vertical lines in the bottom record of Figures 17-23. With hindsight, these picks can be correlated with minor inflections in the original displacement records. No attempt was made to pick arrivals at SNZO, which, at a distance of 28.3°, could be significantly affected by upper mantle structure. The T_{pP-P} time that was obtained was 8.2±0.5 sec and T_{sP-P} 11.5±0.5 sec, for an average depth of 25±3 km using the JB earth model.

There appears to be significant energy arriving in the 8 sec that precede PKP in the short-period record of KONO, which is at a distance of 135° (Figure 19). The broadband records, however, put this energy in perspective. The precursor is almost insignificant in the velocity record. It probably represents high-frequency energy scattered from the internal caustic surface of PKP (Haddon and Cleary, 1973). While the peaked response of the short-period instrument can occasionally over-emphasize the importance of this high-frequency scatter, it is usually not representative of the dominant energy of the

source.

Complexity

Body phases such as PP do not arrive within the time window shown in Figures 17-23. Other theoretical phases such as PcP are generally negligible even though they might arrive within the first minute of the record. Consequently, the large amplitudes that persist late in the wavetrain (up to about 50 seconds after the initial P-arrival) indicate a complexity in the rupture. The rupture appears to have occurred in at least two distinguishable stages which we call events. The bold vertical line in Figure 24 approximately partitions the end of the first event (i.e., the total duration of the convolution of the free-surface operator and the source-time function) and the beginning of the next event. The first major event has a duration of about 25 sec. Its signature at SCP, KONO, TATO, and MAJO are the first two troughs and the next peak which correlate from record to record. The correlation extends to the TAU and SNZO records as well if polarity and amplitude changes due to focal mechanism are considered.

If the depth of the second event is assumed to be the same as the initial one, then the relative delays between P and the surface reflections are the same for the two events. However, their amplitudes and polarities can vary if the fault plane has rotated. There is also a possibility that the duration of the source function could change. The character of the second event is clearest in the MAJO record (Figure 25a). The horizontal bracket indicates what is interpreted as the temporal extent of the first event. The waveform from this first event is superimposed as a dashed line on top of the suspected second event to demonstrate the correlation in waveforms. At SCP (Figure 25b), the second event can also be recognized, but its signature is slightly different in amplitude from the first event (the dashed line which overlays the second event). This must be because the mechanism of the second event has rotated with respect to the first one. Consequently, the ease with which such a correlation can be made for each record varies. For example, although there is certainly a second event in the TAU record (Figure 24), its amplitude is much smaller than that of the first event. This rotation in mechanism is consistent with the different mechanisms that were obtained by using the first motion of P-waves (first part of this report) and by using moment tensor analyses (as discussed in other portions of this report). The mechanism obtained from moment tensor analysis probably represents an average of the entire rupture process. In contrast, the mechanism obtained by the P-wave motions is accurate only for the first event. The surface-wave analysis, which uses long periods that are sensitive to the average mechanism of the entire rupture, also agrees better with the moment tensor solution relative to the first-motion solution.

The displacements of Figure 24 are lined up according to the arrival of the first P-wave. Thus, if there is a systematic phase delay in the arrival of the peaks of the second event among the records, the azimuth of the second nucleation relative to the first one could be inferred. However, within an uncertainty of ±3 sec there does not appear to be a systematic shift. All that can be concluded is that about 25 sec after the first nucleation there occurred another event. On the basis of displacement waveforms the second event had a similar depth and occurred near the same hypocenter as the first event. The moments and source-time functions of the two events are not significantly different from each other, although there must be some difference between their fault planes.

Because of the overlap of the pP and P waveforms, it is difficult to single out a distinct phase from which a source duration could be obtained for the first

subevent. The clearest phase is P(diff) at SCP. After compensating for propagation effects, the source function is found to have a duration of about 9 sec. The initial rise time in displacement corresponds to the first cycle in velocity which Boatwright (1981) calls the rupture phase. This rupture phase has an average duration of about 5 sec. More detailed analyses of the complexity and time functions can be obtained using methods described by, for example, Kanamori and Stewart (1978), Langston and Helmberger (1975) or Choy and Boatwright (1982).

Depth of the foreshock

As the JED analysis in another portion of this report required a depth to be determined for a master event, we also analyzed the foreshock for depth phases. This was done, as previously described, by a simultaneous analysis of short-period, broadband displacement and broadband velocity records. Only the GDSN records at ANMO and LON were usable for this smaller event (Figure 26). The duration of the source function is sufficiently short (about 6 sec) that the pP+sP arrival is well-separated from the P pulse. Its signature is clearly seen in displacement and the velocity record provides good time resolution. On the basis of these two records, the T_{pP-P} time is 9.5±0.5 sec. which gives a depth of 29.5±3 km for the the JB earth model.

Figure 17. (a) The broadband displacement record at SCP (Δ 103.6°) obtained by integrating the velocity record beneath it.

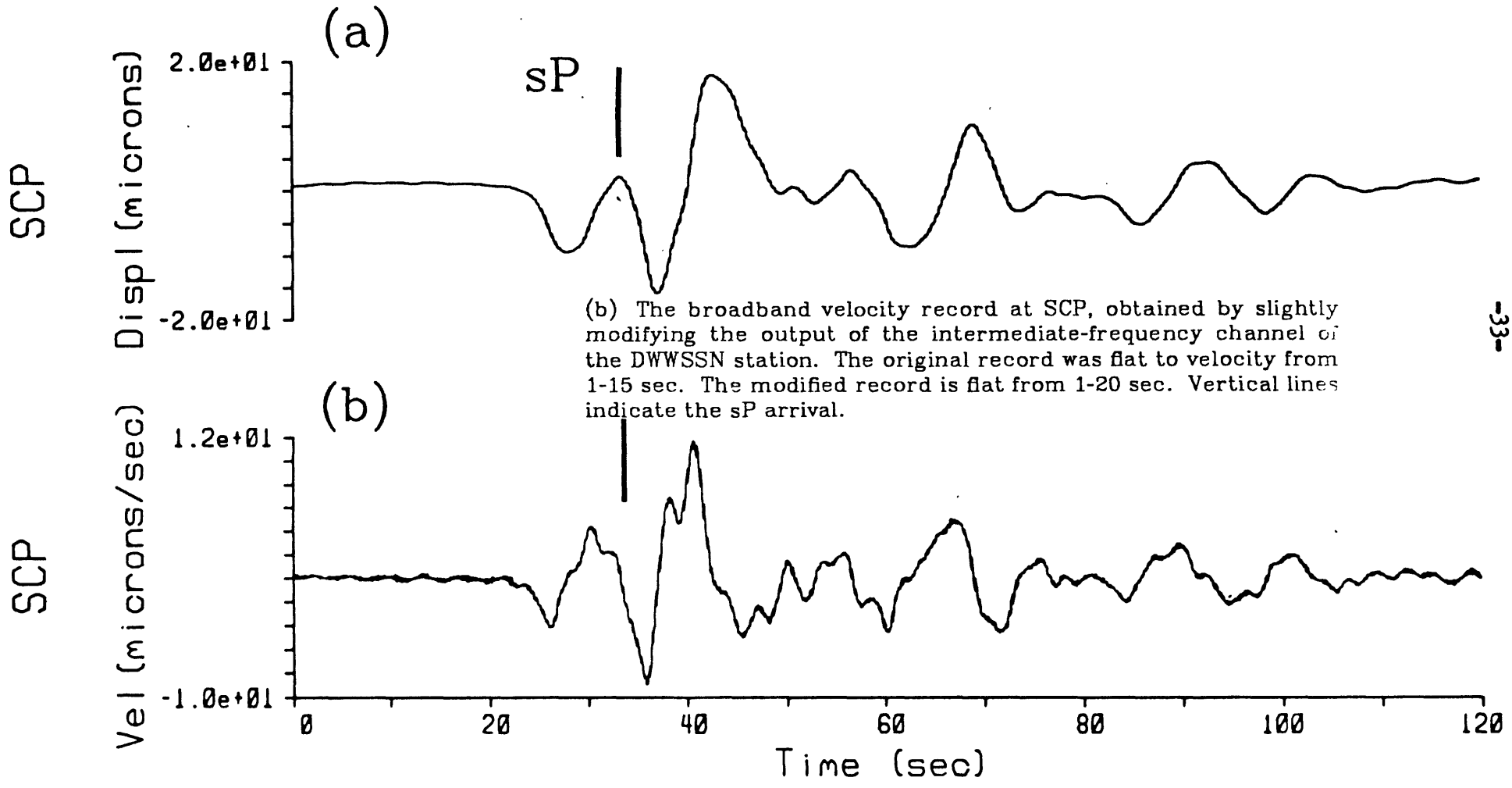

(b) The broadband velocity record at SCP, obtained by slightly modifying the output of the intermediate-frequency channel of the DWWSSN station. The original record was flat to velocity from 1-15 sec. The modified record is flat from 1-20 sec. Vertical lines indicate the sP arrival.

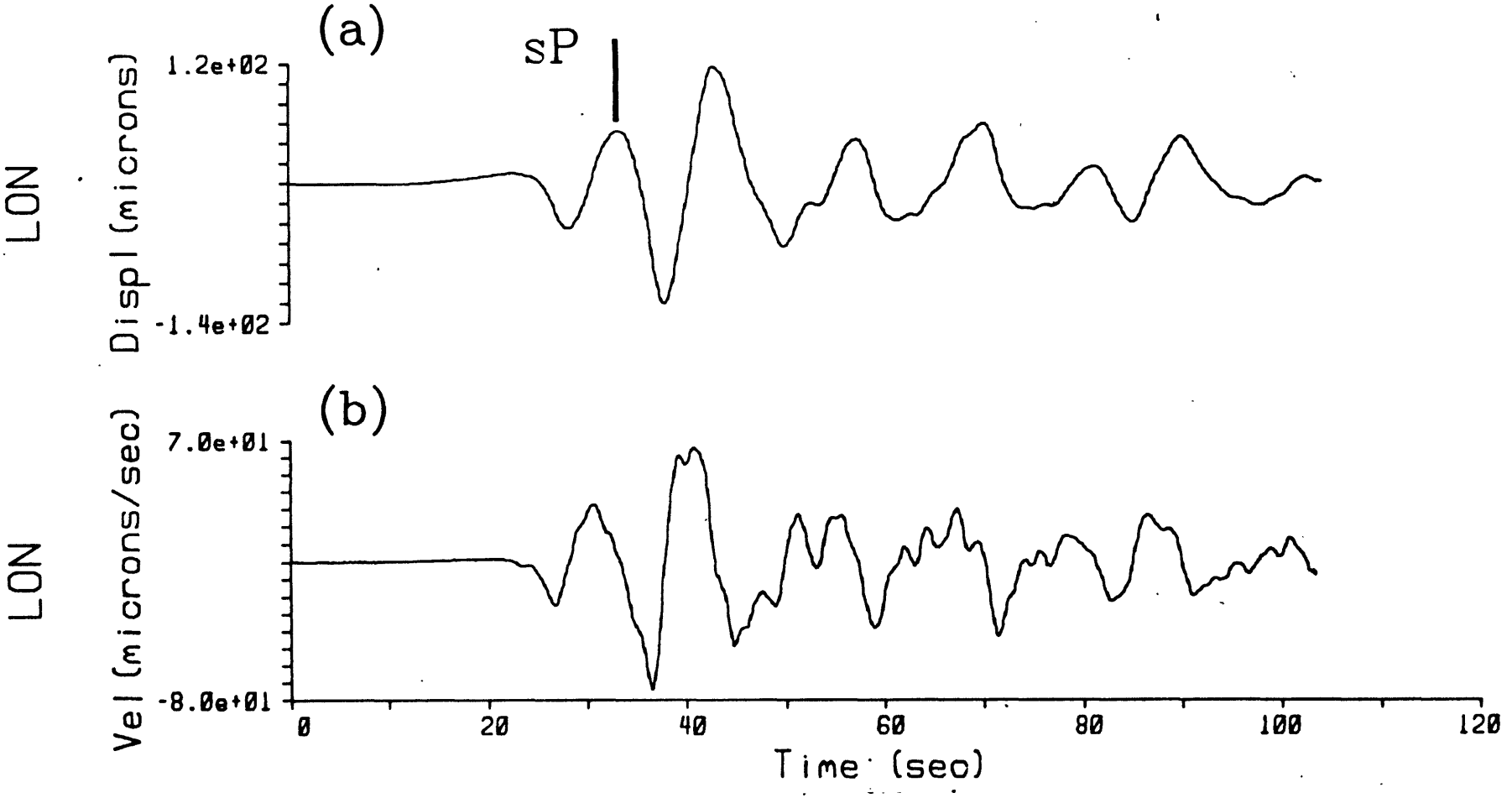

Figure 18. (a) The broadband displacement record at LON (Δ 78.6°), which is a DWWSSN station, obtained by integrating the velocity record beneath it.
(b) The broadband velocity record for LON, obtained by slightly modifying the output of the intermediate-frequency channel of the DWWSSN station. The original record was flat to velocity from 1-15 sec. The modified record is flat from 1-20 sec. Vertical lines indicate sP arrival.

Figure 19. (a) The original digitally recorded short-period record for KONO (Δ 135.4°). Note the precursory energy that arrives before the PKP arrival (indicated by the vertical line in the short-period and displacement records). (The long-period data are shown in Fig. 7).

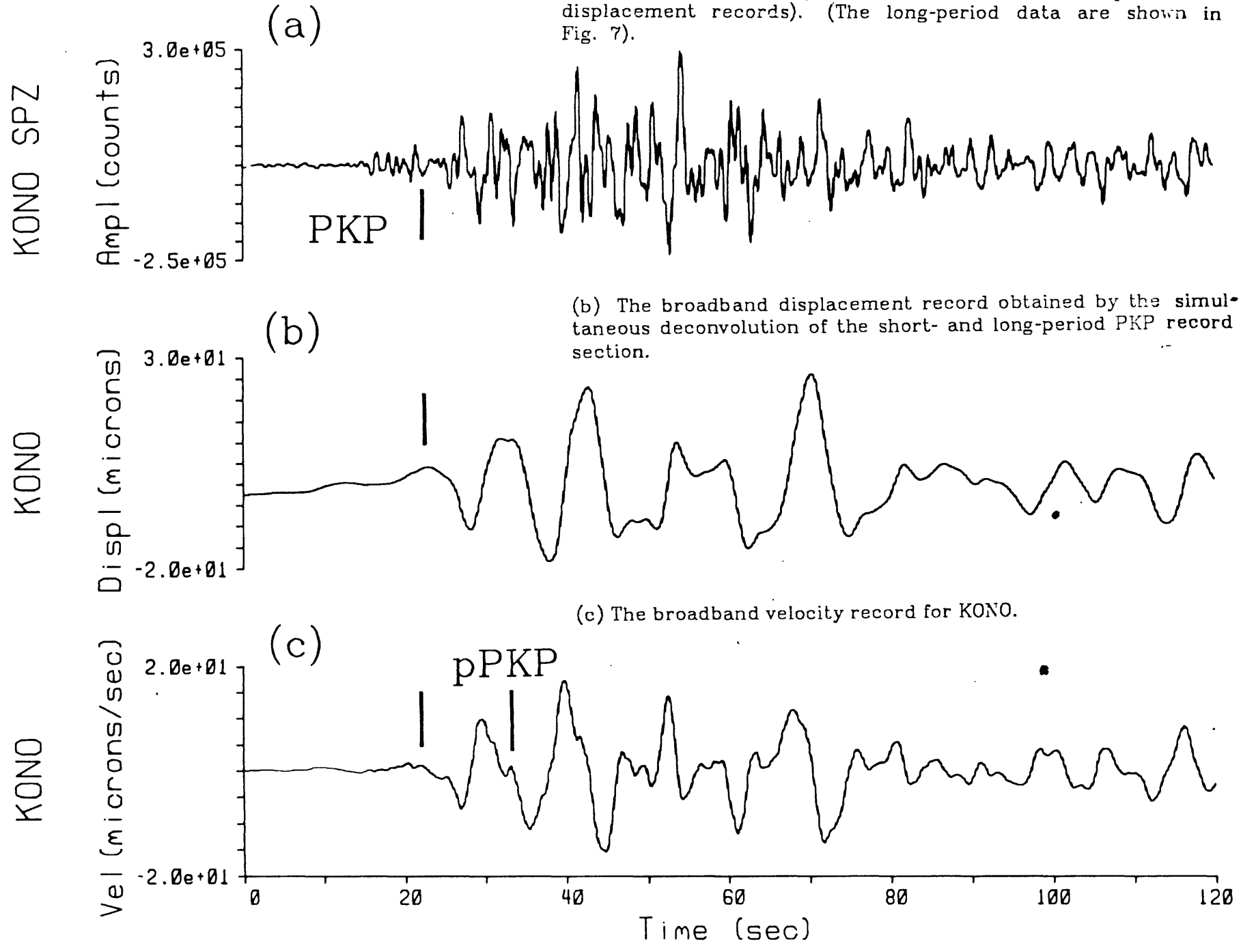

(b) The broadband displacement record obtained by the simultaneous deconvolution of the short- and long-period PKP record section.

(c) The broadband velocity record for KONO.

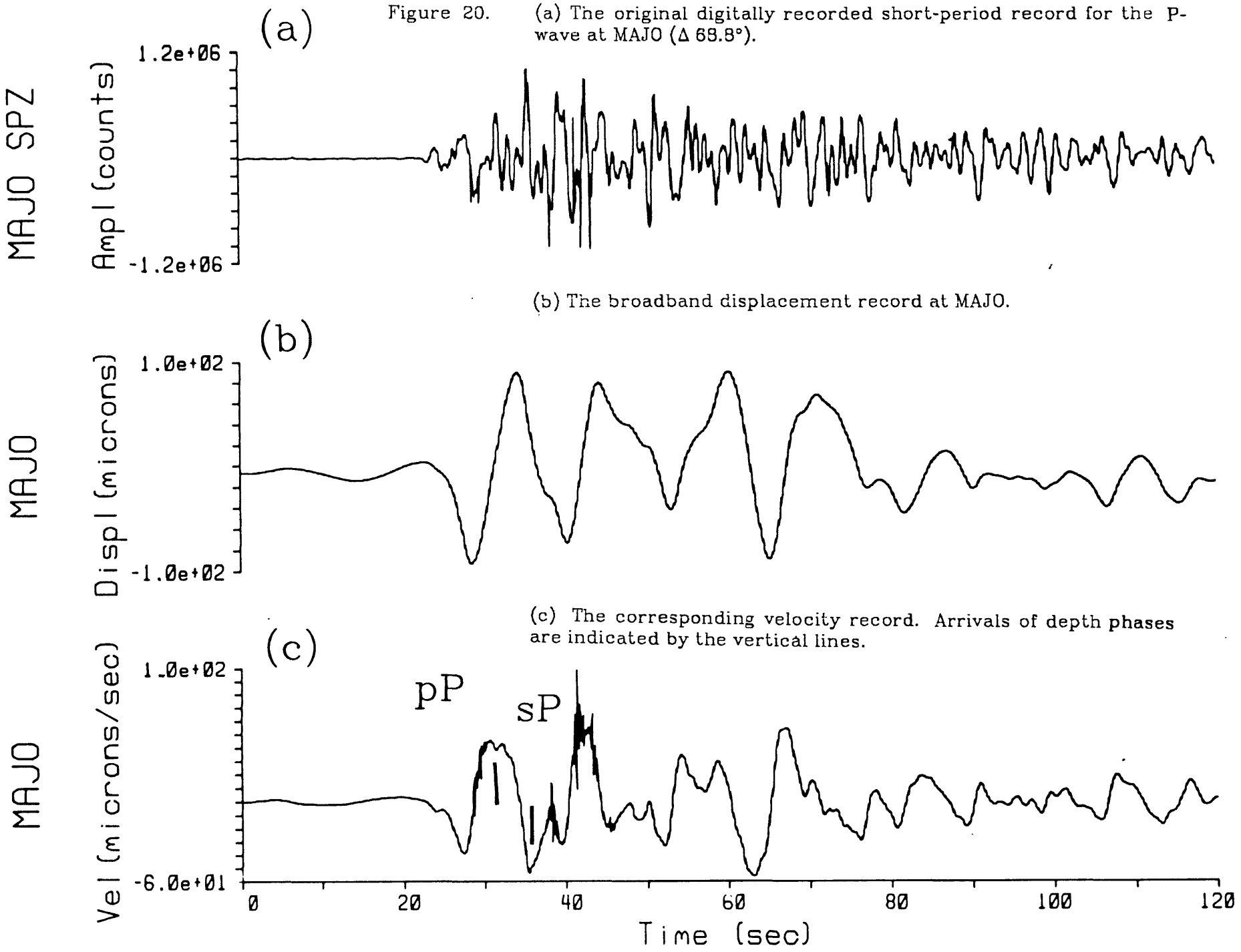

Figure 20. (a) The original digitally recorded short-period record for the P-wave at MAJO (Δ 68.8°).

(b) The broadband displacement record at MAJO.

(c) The corresponding velocity record. Arrivals of depth phases are indicated by the vertical lines.

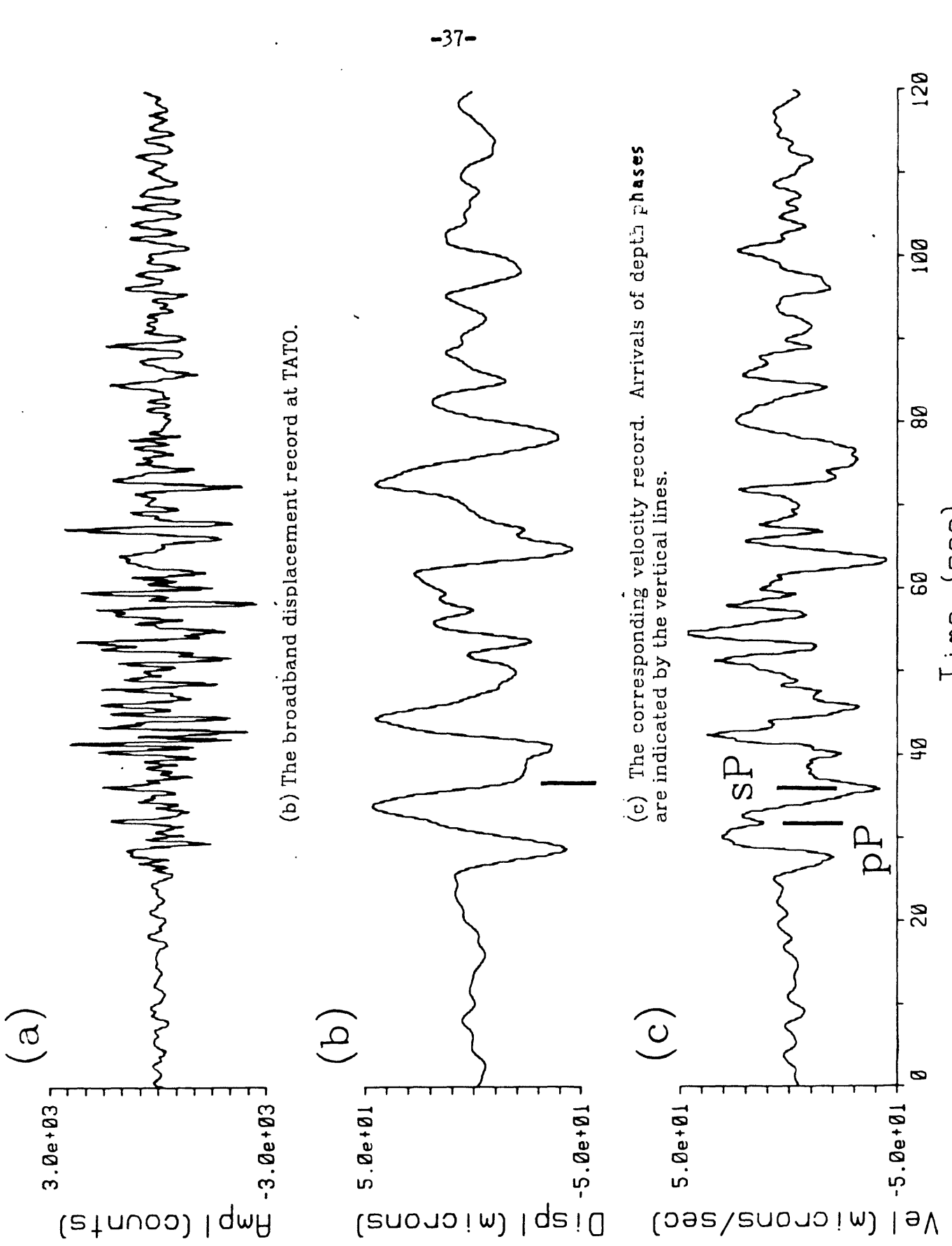

(a) The original digitally recorded short period record for the wave at TATO (Δ 75.0°).

(b) The broadband displacement record at TATO.

(c) The corresponding velocity record. Arrivals of depth phases are indicated by the vertical lines.

wave at TAU (Δ 43.8°).

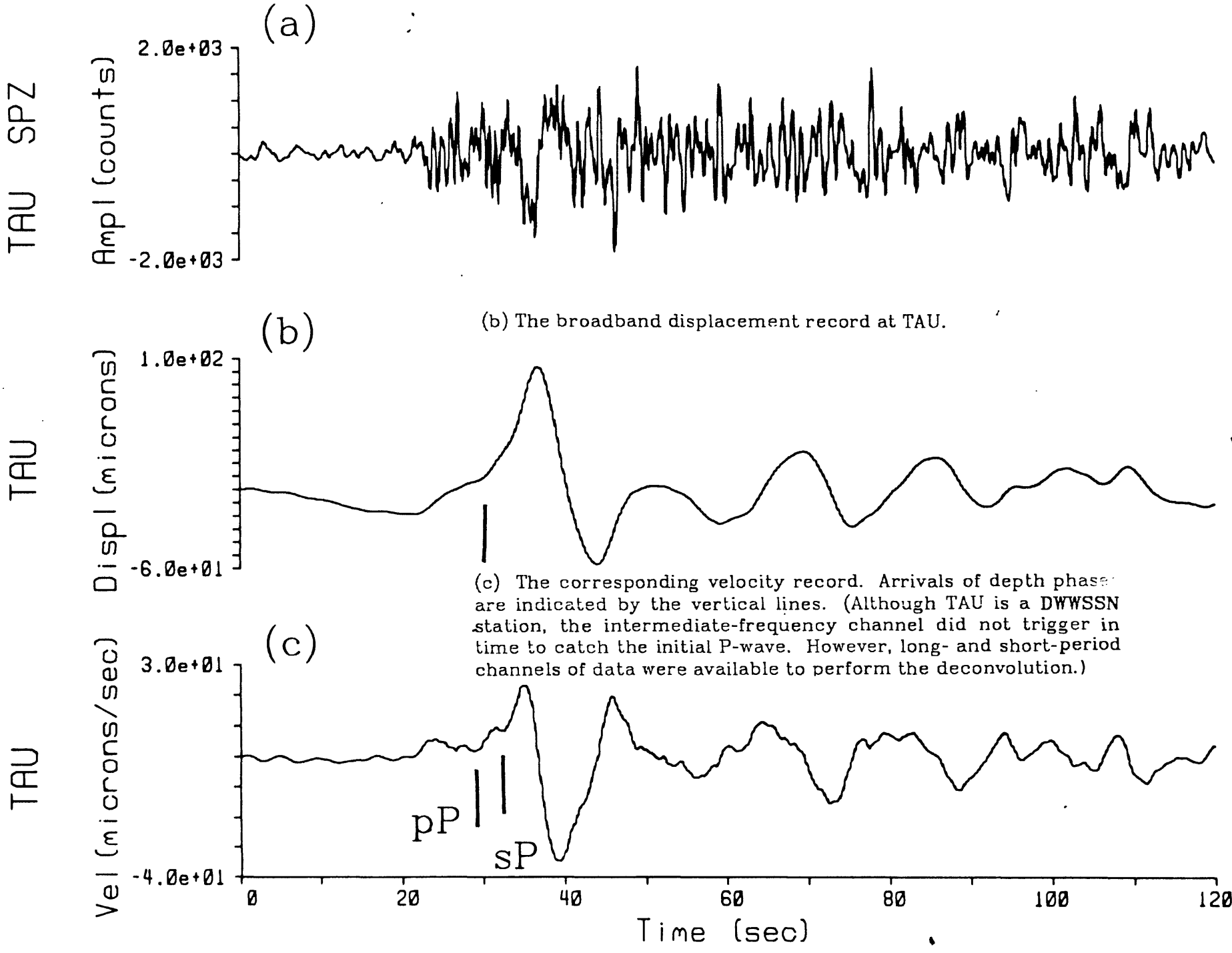

(b) The broadband displacement record at TAU.

(c) The corresponding velocity record. Arrivals of depth phase are indicated by the vertical lines. (Although TAU is a DWWSSN station, the intermediate-frequency channel did not trigger in time to catch the initial P-wave. However, long- and short-period channels of data were available to perform the deconvolution.)

Figure 23. (a) The original digitally recorded short-period record for the P-wave at SNZO (Δ 28.6°).

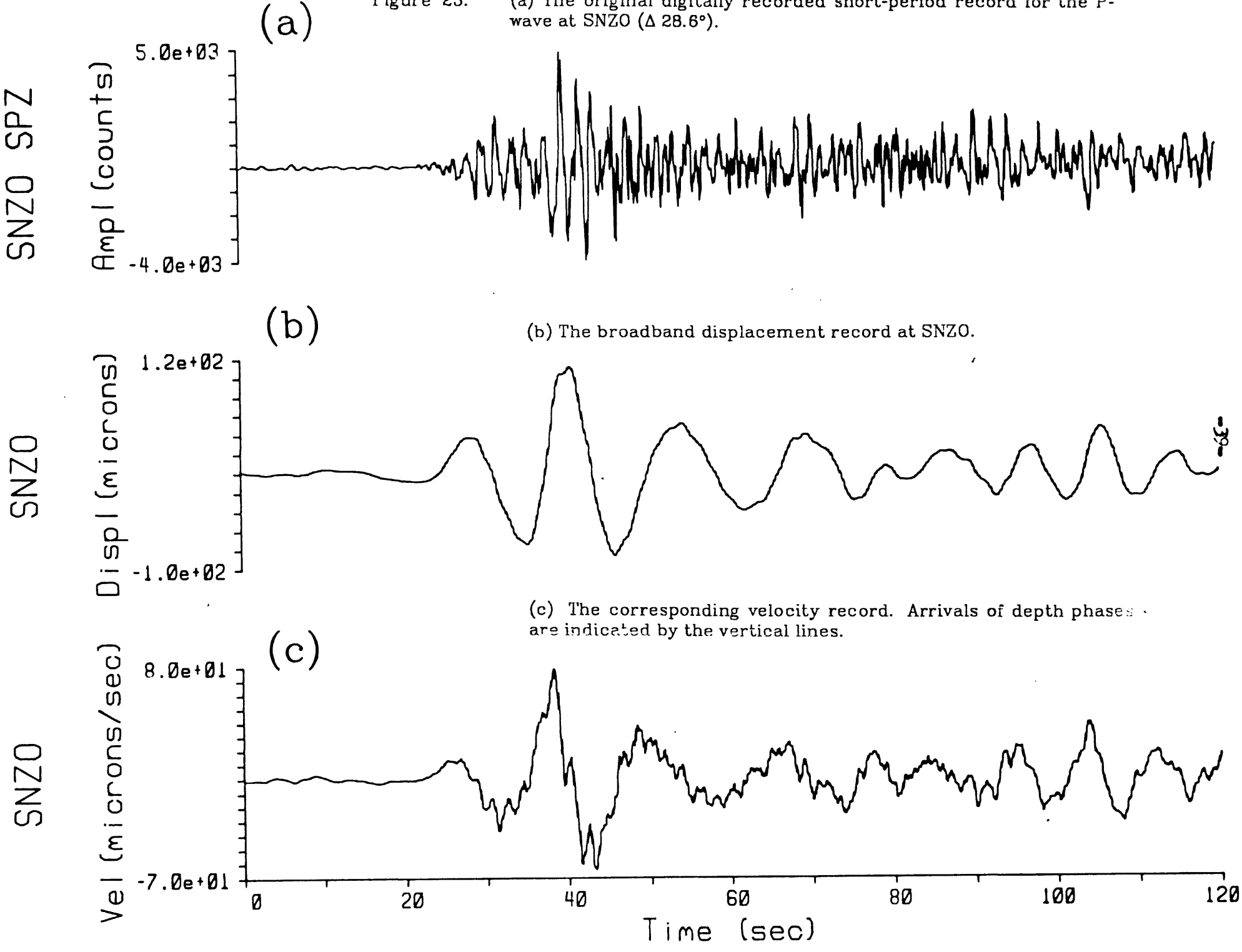

(b) The broadband displacement record at SNZO.

(c) The corresponding velocity record. Arrivals of depth phases are indicated by the vertical lines.

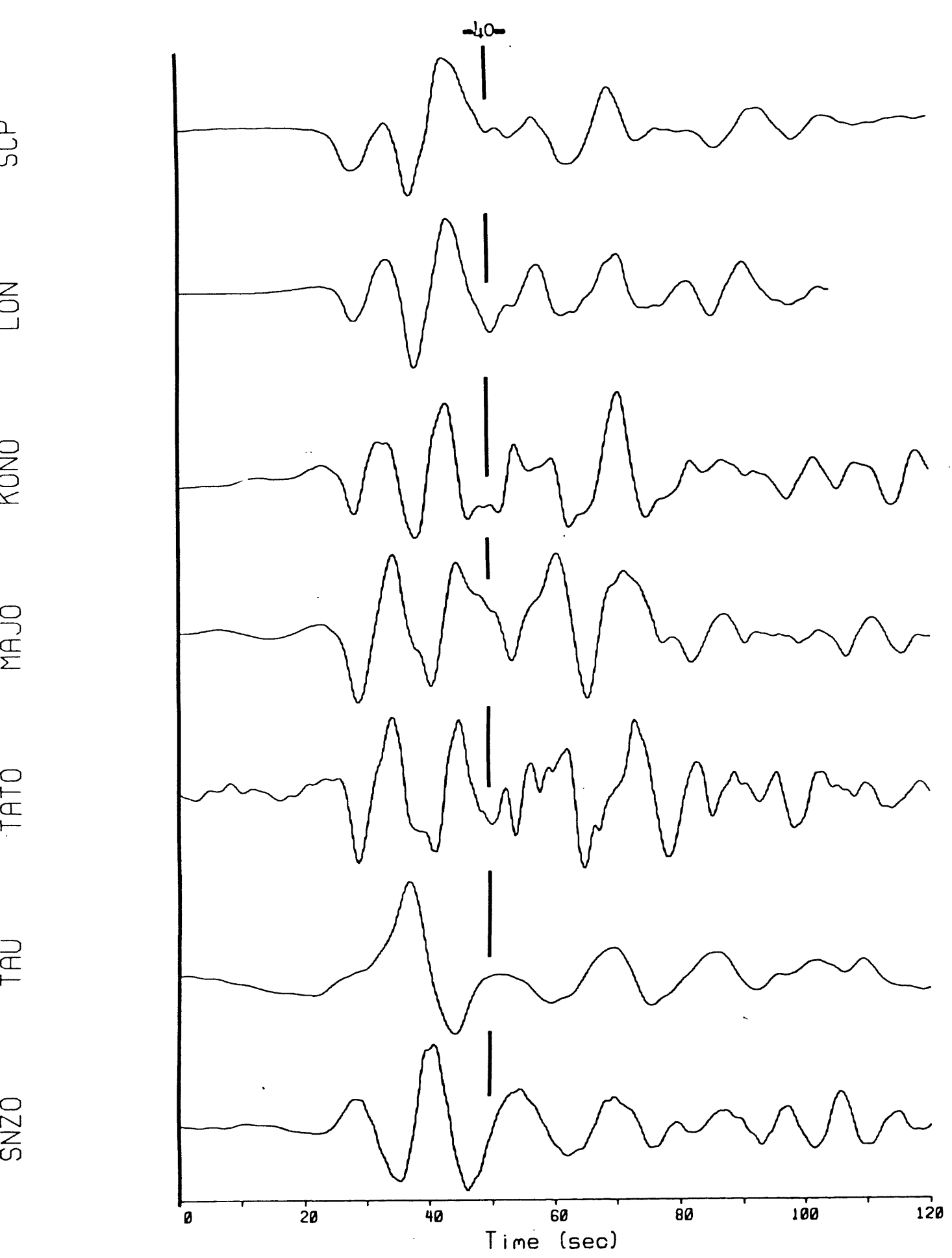

Figure 24. The suite of broadband displacement records are stacked up with the P-waves aligned. The vertical line indicates the approximate end of the first event of this complex rupture and the beginning of the second event.

the horizontal bracket. That waveform is superimposed (dashed line) on the suspected second event to illustrate the correlation between the two.

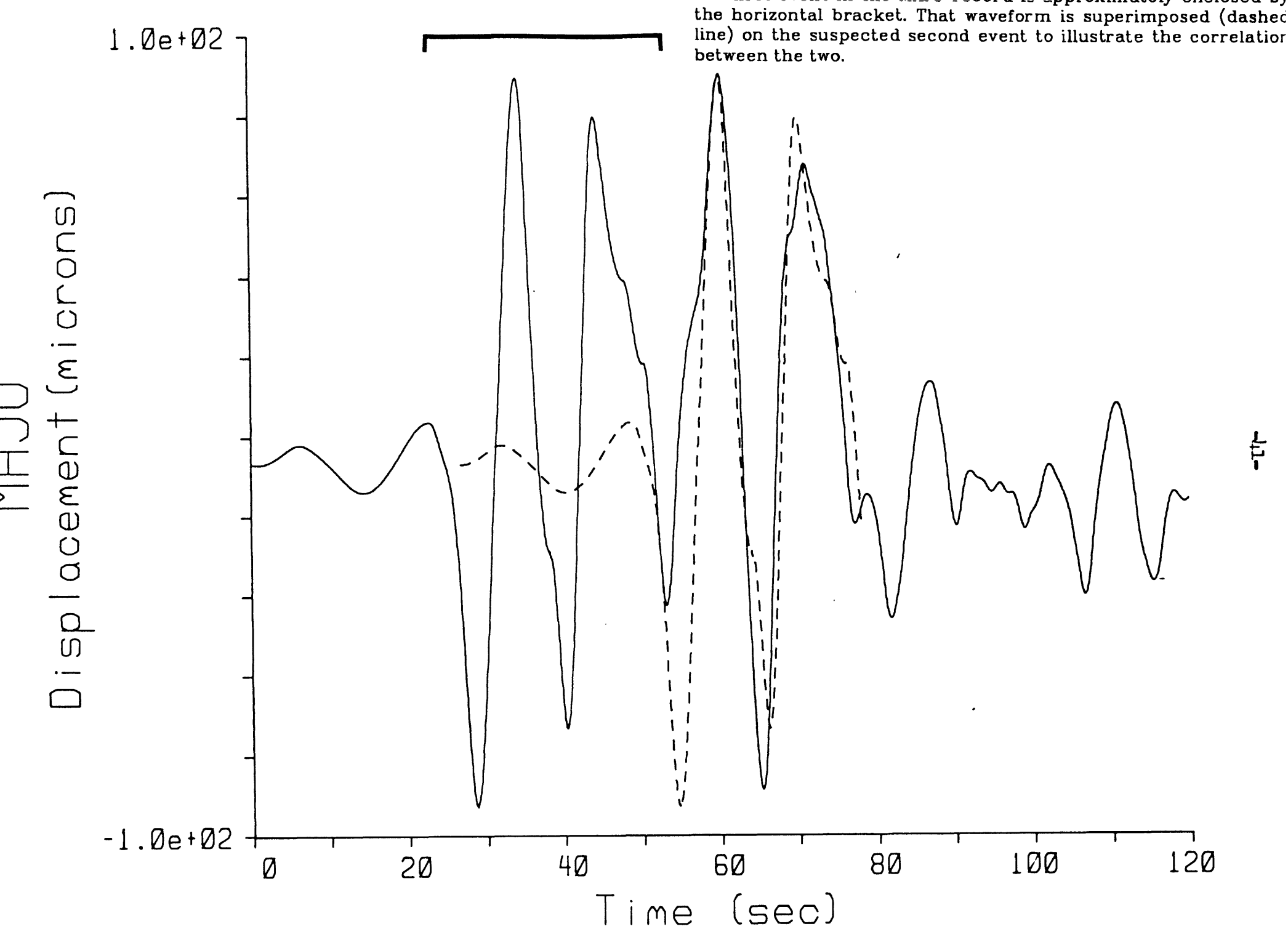

Figure 25b. The first event on the SCP displacement (within the horizontal bracket) is superimposed (dashed line) on top of the suspected second event. The amplitude of the P-wave (first negative pulse) is apparently much smaller for the second event. It is likely the result of a relative rotation in focal mechanism.

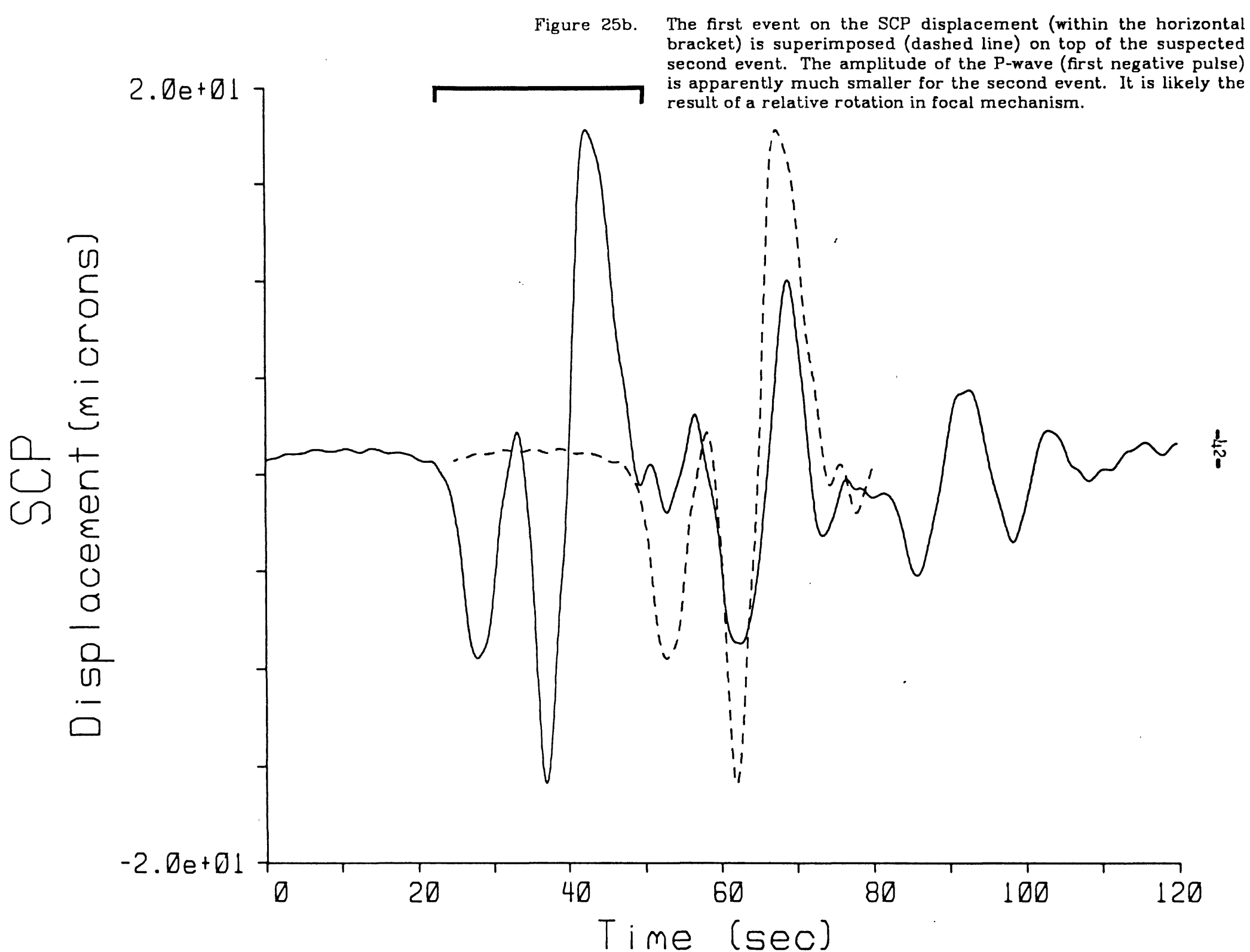

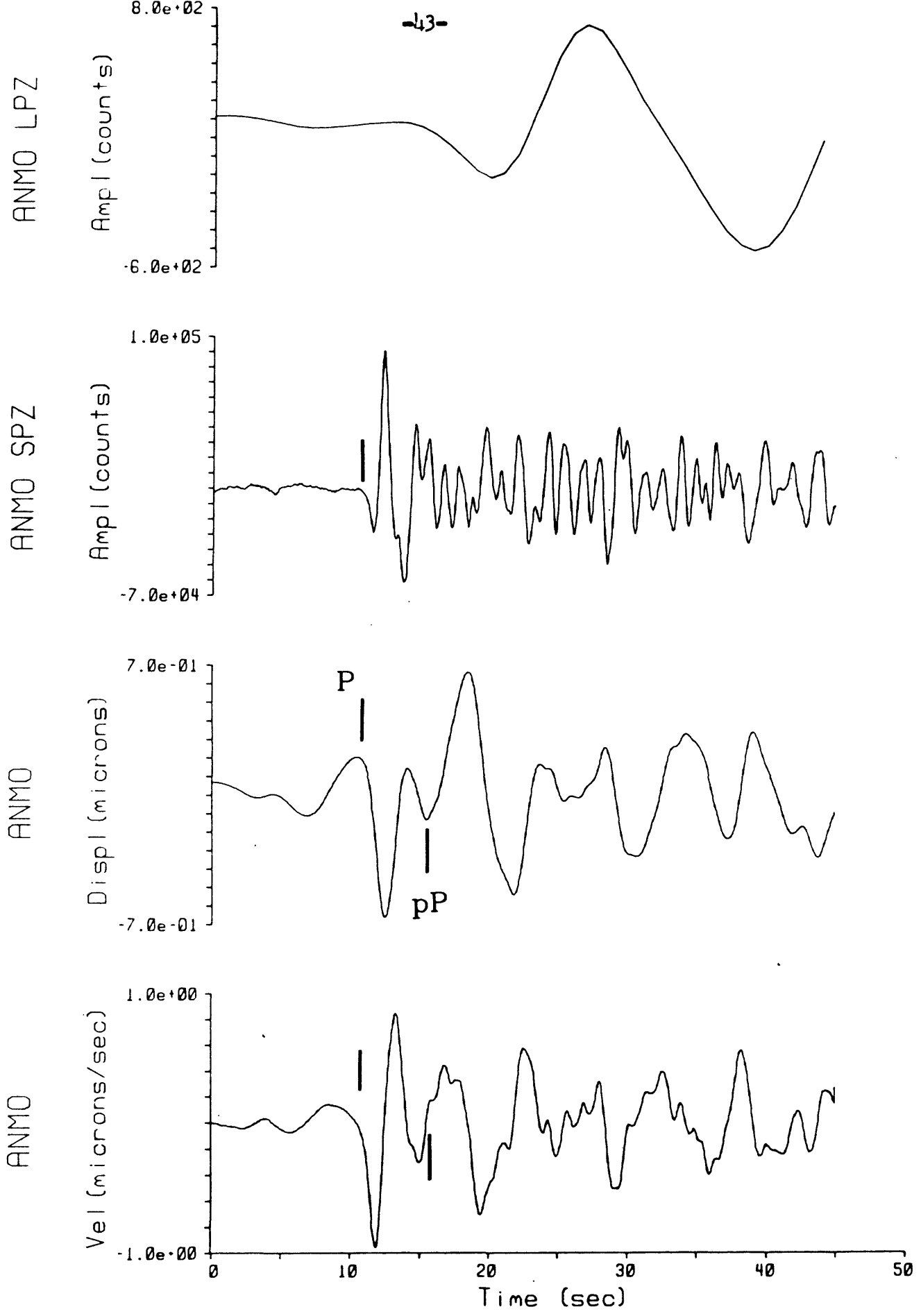

Figure 26a. The long- and short-period records for ANMO for the foreshock (top). It is followed by the displacement and velocity records. The pP arrival is indicated by the vertical line.

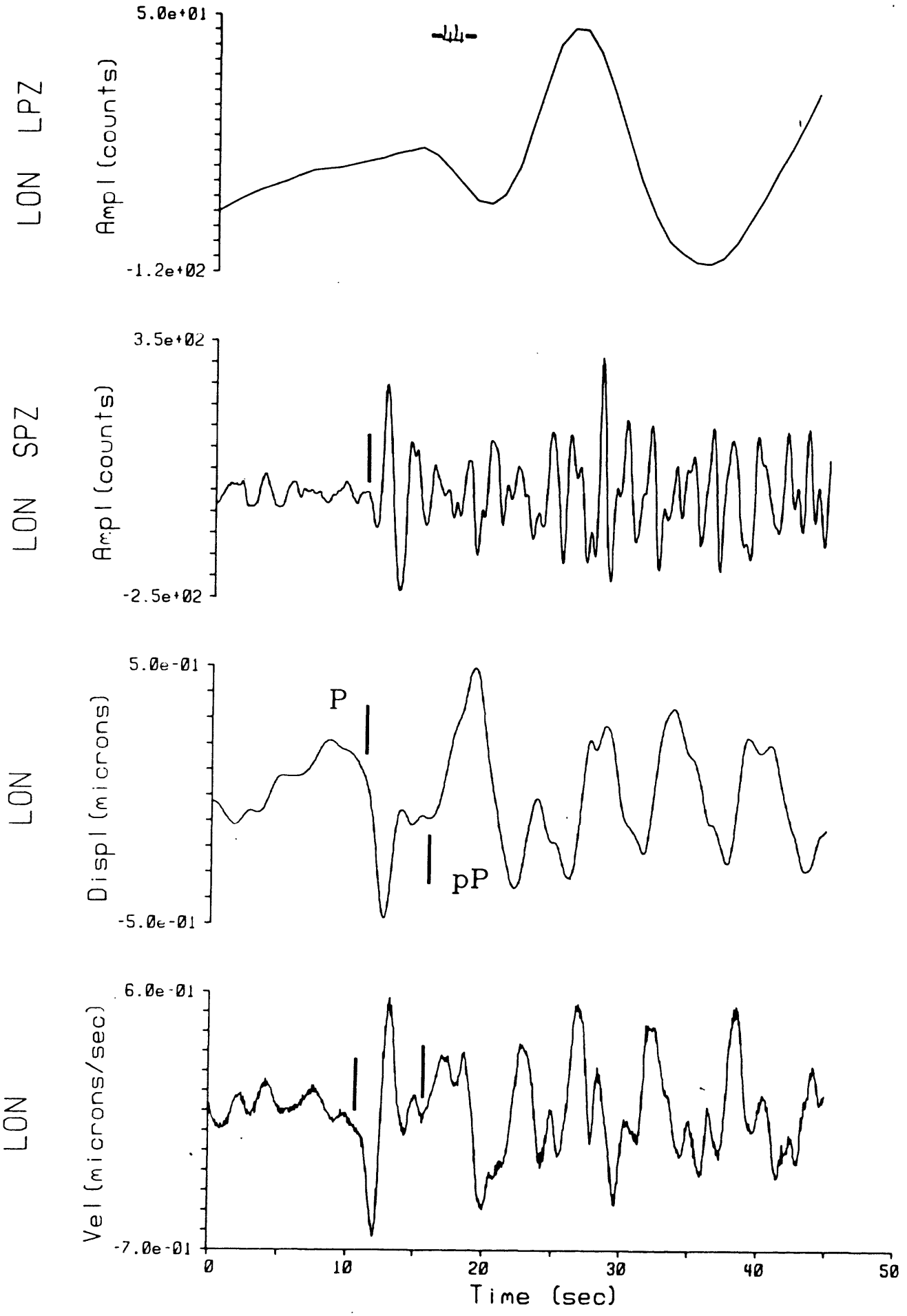

Figure 26b. The long-period, short-period, displacement and velocity records for LON. (The intermediate channel at LON did not trigger for the foreshock. The broadband records were obtained by the simultaneous deconvolution of the long- and short-period records.) The pP arrival is indicated by the vertical line.

References

Boatwright, J., 1981. Quasidynamic models of simple earthquakes: an application to an aftershock of the 1975 Oroville, California earthquake, *Bull. Seism. Soc. Am.*, **71**, 69-74.

Buland, R. and J. Taggart, 1981. A mantle wave magnitude for the St. Elias, Alaska, earthquake of 28 February 1979. *Bull. Seism. Soc. Am.*, **71**, 1143-1159.

Chapman, C.H., 1978. A new method for computing synthetic seismograms. *Geophys. J. R. Astr. Soc.*, **54**, 481-518.

Choy, G.L. and J. Boatwright, 1982. Broadband analysis of the extended foreshock sequence of the Miyagi-Oki earthquake of June 12, 1978, submitted *Bull. Seism. Soc. Am.*

Choy, G.L. and J. Boatwright, 1981. The rupture characteristics of two deep earthquakes inferred from broadband GDSN data, *Bull. Seism. Soc. Am.*, **71**, 691-711.

Dewey, J. W., 1972. Seismicity and tectonics of western Venezuela, *Bull. Seism. Soc. Am.*, **62**,

Dziewonski, A.M., T.-A. Chou and J.H. Woodhouse, 1981. Determination of earthquake source parameters from waveform data for studies of global and regional seismicity. *J. Geophys. Res.*, *86*, 2825-2852.

Evernden, J.F., 1969. Precision of epicenters obtained by small numbers of world-wide stations. *Bull. Seism. Soc. Am.*, **59**, 1365-1398.

Gilbert, F. and A.M. Dziewonski, 1975. An application of normal mode theory to the retrieval of structural parameters and source mechanisms from seismic spectra. *Phil. Trans. R. Soc. London, Ser. A*, **278**, 187-269.

Haddon, R.A.W. and J.R. Cleary, 1973. A note on the interpretation of precursors to PKP, *Phys. Earth and Planet. Interiors*, **7**, 495-497.

Harvey, D. and G.L. Choy, 1982. Broadband deconvolution of GDSN data, *Geophys. J. R. Astr. Soc.*, in press.

Isacks, B., L.R. Sykes, and J. Oliver, 1969. Focal mechanisms of deep and shallow earthquakes in the Tonga-Kermadec region and the tectonics of island arcs, *Geol. Soc. Am. Bull.*, **80**, 1443-1470.

Johnson, T. and P. Molnar, 1972. Focal mechanisms and plate tectonics of the Southeast Pacific, *J. Geophys. Res.*, **77**, 5000-5032.

Langston, C.A. and D.V. Helmberger, 1975. A procedure for modeling shallow dislocation sources, *Geophy. J.*, **42**, 117-130.

Leeds, A.R., 1975. Lithospheric thickness in the western Pacific, *Phys. Earth Planet. Int.*, **11**, 61-64.

Kanamori, H. and G. Stewart, 1976. Seismological aspects of the Guatemala earthquake of February 4, 1976, *J. Geophys. Res.*, **83**, 3427-3424.

Minster, J.B and T. Jordan, 1978. Present-day plate motions, *J. Geophys. Res*, 83, 5331-5354.

Mitronovas, W., B. Isacks and L. Seeber, 1969. Earthquake locations and seismic wave propagation in the upper 250 km of the Tonga Island Arc, *Bull. Seism. Soc. Am.*, **59**, 1115-1135.

Schlater, J.G., B. Parsons, and C. Jaupart, 1981. Oceans and continents: similarities and differences in the mechanism of heat loss, *J. Geophys. Res.*, **86**, 11,535-11,552.

Sipkin, S.A., 1982. Estimation of earthquake source parameters from the inversion of waveform data: Synthetic waveforms. *Phys. Earth Planet. Inter.*, in press.

APPENDIX I

SAMOA ISLANDS REGION

DATE:	SEP 01,1981	
TIME:	09 29 30.59	+/-0.09 sec
LAT:	15.203 S	+/-2.90 km
LON:	173.101 W	+/-2.50 km
DEPTH:	25.0 km	GEOPHYSICIST
STNS USED	239 of 374	STAND DEV: 1.2 sec
mb MAG	6.9	(21 station(s))
Ms MAG	7.7	(13 station(s))

FELT VI AT APIA. LOCAL TSUNAMI (24 cm PEAK TO PEAK) RECORDED AT PAGO PAGO.

STA	PH	TIME	SEC PH	TIME	mb	Ms	DIST	AZ	RES
AFI	IPC	09 29 54.0					1.8	45.1	-6.8X
VUN	IPD	09 31 40.9	ES	09 32 20.9	7.6X		8.6	249.8	-5.0X
SVA	EP	09 31 39.0			7.8X		8.6	249.1	2.6X
NDF	IP	09 32 02.0					9.4	253.1	14.3X
RAR	IP	09 32 43.0					14.0	117.2	-6.6X
PVC	IPC	09 33 43.1					18.1	259.4	2.2X
NOU	IPC	09 34 12.2	IS	09 38 12.0			20.6	246.9	1.6
KOU	IPC	09 34 25.4					22.2	252.8	-1.0
AFR	IP	09 34 32.2					22.5	99.1	2.5X
PAE	IP	09 34 34.2					22.7	99.4	2.6X
PPT	IP	09 34 34.3					22.7	99.2	2.7X
PPN	IP	09 34 35.6					22.8	99.1	2.6X
TVO	IP	09 34 37.6					23.0	99.7	2.8X
CRZ	P	09 34 37.0					23.0	211.3	2.1
GBZ	P	09 34 39.5					23.3	203.9	2.3X
ONE	EP	09 34 43.0					23.4	206.4	5.0X
PMO	IP	09 34 48.0					24.3	92.9	0.4
WTZ	P	09 34 48.3					24.3	199.3	0.9
TPT	IP	09 34 50.9					24.6	93.9	0.7
VAH	IP	09 34 50.4					24.6	93.5	0.5
GNZ	EP	09 34 51.2	S	09 39 28.0			24.6	196.9	0.9
RUV	IP	09 34 52.6					24.8	93.4	0.3
KRP	P	09 34 53.0					24.8	201.8	1.4
HNR	EPR	09 35 10.0	ES	09 40 20.0			26.9	279.1	-2.0
MNG	P	09 35 13.5	(S)	09 40 14.0			27.2	199.2	-0.8
WEL	P	09 35 20.1	S	09 40 19.9			28.0	199.7	-1.7
			SCS	09 46 15.2					
SNZO	EP	09 35 21.0					28.1	199.8	-1.2
KKZ	EP	09 35 34.0					30.3	199.3	-8.1X
PAA	EP	09 36 01.0					32.1	282.6	3.0X
RHP	P	09 35 56.3	(pP)	09 36 11.3			32.2	203.1	-2.3
			I	09 36 15.3					
MSZ	P	09 36 07.3	E	09 36 12.2			33.5	204.9	-2.7
COO	IPD	09 36 26.1					35.5	238.4	-1.6

SAMOA ISLANDS REGION

DATE:	SEP 01,1981	
TIME:	09 29 30.59	+/-0.09 sec
LAT:	15.203 S	+/-2.90 km
LON:	173.101 W	+/-2.50 km
DEPTH:	25.0 km	GEOPHYSICIST
STNS USED	239 of 374	STAND DEV: 1.2 sec
mb MAG	6.9	(21 station(s))
Ms MAG	7.7	(13 station(s))

FELT VI AT APIA. LOCAL TSUNAMI (24 cm PEAK TO PEAK) RECORDED AT PAGO PAGO.

STA	PH	TIME	SEC PH	TIME	mb	Ms	DIST	AZ	RES
RKT	IP	09 36 40.7					36.8	108.3	2.4X
RIV	EP	09 36 43.0					37.2	233.6	1.4
KVG	EP	09 36 49.0					37.7	285.9	2.6X
LMG	EP	09 36 54.0					38.4	274.8	2.1
CTA	IPD	09 36 56.6	IS	09 42 42.0			39.0	256.8	-0.2
PMG	IPDR	09 37 00.0				6.4X	39.2	273.7	1.2
KIP	IP	09 37 00.0					39.3	22.5	0.7
CAN	IPD	09 36 58.4					39.4	232.4	-1.7
YOU	IPD	09 37 02.1					39.5	234.2	1.0
WAM	EP	09 37 02.0					39.8	231.1	-1.3
MOM	EP	09 37 15.5					41.1	284.7	1.3
TOO	IPC	09 37 27.1			5.9X		42.8	230.7	-1.1
WAB	EP	09 37 37.0					43.5	278.1	2.9X
TAU	EP	09 37 34.0	I	09 37 37.1			43.7	222.7	-0.9
			ES	09 44 16.0					
STK	EP	09 37 40.0					44.4	239.8	-1.0
MCQ	EP	09 37 49.0					44.8	202.8	4.7X
BFD	EP	09 37 48.0					44.9	232.3	2.8X
ISQ	EP	09 37 48.0					45.2	255.8	-0.1
JAY	EPC	09 38 05.0			6.3X		47.3	280.8	0.8
ADE	EPC	09 38 03.2			6.4X		47.4	236.3	-1.5
WB2	EP	09 38 23.8					50.2	256.6	-2.6
WRA	P	09 38 25.0			5.6X		50.2	256.6	-1.4
GUA	EPR	09 38 28.0	I	09 38 33.5	7.1	7.0X	50.4	302.4	-0.3
			ES	09 45 41.0					
GUMO	EPR	09 38 29.2	I	09 39 03.1	7.1		50.5	302.4	0.4
PJG	EP	09 38 28.8					50.5	302.4	0.0
ASP	IPD	09 38 26.5					50.5	251.7	-2.2
KNA	EP	09 39 07.0					55.9	261.1	-1.9
WBN	IPC	09 39 15.3					57.1	248.5	-2.0
DRV	EP	09 39 37.4					59.9	199.6	1.1
KLG	EP	09 39 45.0					61.4	243.0	-2.6
SBA	EP	09 40 03.0					63.5	184.7	2.7X
MBL	IPC	09 40 04.0					63.6	253.7	2.0

SAMOA ISLANDS REGION

DATE:	SEP 01,1981	
TIME:	09 29 30.59	+/-0.09 sec
LAT:	15.203 S	+/-2.90 km
LON:	173.101 W	+/-2.50 km
DEPTH:	25.0 km	GEOPHYSICIST
STNS USED	239 of 374	STAND DEV: 1.2 sec
mb MAG	6.9	(21 station(s))
Ms MAG	7.7	(13 station(s))

FELT VI AT APIA. LOCAL TSUNAMI (24 cm PEAK TO PEAK) RECORDED AT PAGO PAGO.

STA	PH	TIME	SEC PH	TIME	mb	Ms	DIST	AZ	RES
MEK	EP	09 40 05.0					64.2	247.5	-1.1
PPH	EPC	09 40 08.5			7.2		64.4	286.6	1.4
DAV	IPR	09 40 08.0					64.7	285.6	-1.1
NWAO	EP	09 40 10.0					65.0	240.5	-0.8
MUN	EP	09 40 15.0					65.9	241.5	-1.7
PLP	EPD	09 40 23.0					66.7	289.6	-1.0
MKS	IPC	09 40 32.2					66.8	271.0	9.6X
ADK	EP	09 40 20.1					66.9	357.6	-2.4
KYS	EP	09 40 24.5					66.9	319.6	1.5
NAU	EP	09 40 26.0					67.4	251.7	-0.6
CNP	EPD	09 40 32.0			7.8		67.5	290.7	4.8X
OYM	EP	09 40 27.3					67.6	319.2	-0.3
TSK	EP	09 40 27.0					67.6	320.4	-0.3
DDR	EP	09 40 29.9					68.0	319.7	-0.2
LGP	EPD	09 40 36.0			7.1		68.5	290.9	2.3X
SMY	EP	09 40 30.5				7.6	68.6	351.7	-2.5
MAT	IPD	09 40 35.7	ES	09 49 40.0	6.7		68.9	319.6	-0.3
KUR	IPD	09 40 42.0	IS	09 50 16.0			69.8	331.7	1.3
SKR	IPD	09 40 47.0					70.9	339.8	-0.6
SAO	EP	09 40 47.7					71.0	41.8	-0.6
PRI	EP	09 40 49.2	EP'P'	10 08 55.5			71.1	42.7	-0.1
BKS	EPD	09 40 49.0	ES	09 50 22.5	6.7	7.9	71.2	40.4	-0.3
			ESCS	09 51 01.0					
			EP'P'	10 08 48.5					
			E	10 40 03.2					
MHC	EP	09 40 49.5					71.2	41.2	-0.3
PGP	EP	09 40 56.0					71.2	290.2	6.2X
ARN	EP	09 40 47.7	E	09 40 53.6			71.3	41.2	-2.4
			E	09 41 03.9					
SHK	EPDR	09 40 50.8	E	09 50 15.2			71.4	315.0	0.0
SAP	EP	09 40 52.0	ES	09 50 08.0			71.5	326.5	1.1
MAN	EP	09 40 55.5					71.5	291.4	3.8X
QCP	EP	09 40 48.0					71.5	291.4	-3.7X
PAS	IP	09 40 51.0	E	09 42 16.0			71.7	45.6	-1.4

SAMOA ISLANDS REGION

DATE:	SEP 01,1981	
TIME:	09 29 30.59	+/-0.09 sec
LAT:	15.203 S	+/-2.90 km
LON:	173.101 W	+/-2.50 km
DEPTH:	25.0 km	GEOPHYSICIST
STNS USED	239 of 374	STAND DEV: 1.2 sec
mb MAG	6.9	(21 station(s))
Ms MAG	7.7	(13 station(s))

FELT VI AT APIA. LOCAL TSUNAMI (24 cm PEAK TO PEAK) RECORDED AT PAGO PAGO.

STA	PH	TIME	SEC PH	TIME	mb	Ms	DIST	AZ	RES
			EPP	09 43 40.0					
			EPPP	09 45 26.0					
			ES	09 50 16.0					
			ESS	09 54 20.0					
PPR	EP	09 40 57.5					72.0	285.8	2.9X
PET	EPD	09 40 54.0					72.2	342.5	1.0
FRI	EP	09 40 55.0					72.3	42.4	-0.8
JAS	EP	09 40 55.5	EPKKP	10 01 47.2			72.3	41.3	-0.9
			EP'P'	10 08 56.1					
ORV	EP	09 40 57.2	E	09 41 01.2			72.6	39.4	-0.9
WDC	IPD	09 40 57.5	EPKKP	10 01 47.4			72.6	38.0	-0.6
			EP'P'	10 08 46.0					
BAG	IPR	09 40 58.0					72.6	292.9	-0.5
TRT	EPC	09 41 03.2			6.6		72.9	266.5	3.2X
MIN	EP	09 40 59.5					73.1	38.7	-1.2
KKM	IPD	09 41 05.4			6.2X		73.1	281.3	3.9X
SZP	EPD	09 41 08.0			6.0X		73.2	293.9	6.5X
PIP	EP	09 41 04.4					73.3	294.8	2.1
GLA	IP	09 41 03.0					73.4	48.2	0.0
MNV	EP	09 41 06.0					74.1	42.0	-0.7
KDC	EP	09 41 08.0					74.7	11.3	-1.4
COR	IPD	09 41 09.0					74.8	34.4	-1.2
SPA	IPC	09 41 12.3			6.5	7.0X	74.9	180.0	1.3
TATO	E(P)	09 41 15.0					75.2	301.4	1.7
ANP	IPR	09 41 16.5	IS	09 51 02.0			75.3	301.6	2.7X
BMN	IPD	09 41 16.0					75.8	40.7	-0.6
TUC	IPD	09 41 17.9	E	09 41 21.4			76.0	50.6	-0.1
EUR	IP	09 41 17.1					76.1	42.0	-1.2
SHW	(P)	09 41 19.7					76.4	33.7	0.2
PHC	EPD	09 41 21.3			5.8X		76.8	27.8	-0.5
PGC	EP	09 41 25.0					77.3	31.2	0.4
QZH	PD	09 41 28.0	IS	09 51 15.0			77.6	300.3	1.3
			ISKS	09 51 37.0					
SSE	EP	09 41 32.0	S	09 51 32.0			78.1	306.9	2.9X

SAMOA ISLANDS REGION

DATE:	SEP 01,1981	
TIME:	09 29 30.59	+/-0.09 sec
LAT:	15.203 S	+/-2.90 km
LON:	173.101 W	+/-2.50 km
DEPTH:	25.0 km	GEOPHYSICIST
STNS USED	239 of 374	STAND DEV: 1.2 sec
mb MAG	6.9	(21 station(s))
Ms MAG	7.7	(13 station(s))

FELT VI AT APIA. LOCAL TSUNAMI (24 cm PEAK TO PEAK) RECORDED AT PAGO PAGO.

STA	PH	TIME	SEC PH	TIME	mb	Ms	DIST	AZ	RES
			SKS	09 51 38.0					
SIT	EP	09 41 29.8					78.5	20.0	-1.3
PMR	EP	09 41 31.4			7.0	7.4	78.9	11.4	-1.5
PCA	EP	09 41 36.0					79.6	16.0	-0.9
PNT	EPD	09 41 36.9			6.7		79.7	32.3	-0.7
CRX	EP	09 41 40.3					80.0	66.7	0.1
NJ2	IPD	09 41 43.5	SKS	09 51 55.0			80.3	307.0	2.4X
NEW	IPD	09 41 40.2					80.4	34.2	-1.2
HKC	IP	09 41 42.0	IS	09 51 38.0			80.4	296.2	0.2
ALQ	IPDR	09 41 42.0				8.0	80.5	49.9	-0.3
ANMO	PD	09 41 42.4					80.5	49.9	0.1
MCD	EP	09 41 40.0					80.5	342.6	-1.6
IIC	EP	09 41 42.4					80.5	66.5	-0.4
IIP	EP	09 41 43.5					80.6	67.0	-0.2
REX	IP	09 41 49.0					81.0	40.0	3.9X
CN2	PD	09 41 45.6	PP	09 44 53.0			81.1	319.9	0.3
			S	09 51 49.0					
IIT	EP	09 41 45.7	E	09 42 00.5			81.1	67.5	-0.2
TLX	EP	09 41 46.2	E	09 41 51.3			81.3	66.5	-0.8
MSO	IPD	09 41 45.0			6.9		81.4	36.6	-1.6
GZH	EP	09 41 49.8	ES	09 51 59.0			81.4	296.7	2.8X
YKM	IP	09 41 47.0					81.5	34.2	-0.3
BCM	EPD	09 41 49.6					81.7	38.0	1.3
BUT	EPD	09 41 48.1					81.7	37.8	-0.5
BDW	IPD	09 41 49.3					81.9	41.7	-0.5
VHO	IP	09 41 56.0					81.9	69.7	5.8X
COL	IPD	09 41 49.4					82.1	10.6	-0.8
FBA	EP	09 41 48.6					82.1	10.6	-1.6
IMA	EP	09 41 51.2					82.3	7.9	-0.1
SEY	PD	09 41 52.0	ES	09 51 58.4			82.4	344.8	0.6
ILT	IPD	09 41 54.0	IS	09 52 24.0			83.0	357.9	-0.3
WHN	EP	09 41 58.0	S	09 52 18.0			83.2	304.0	1.5
GOL	IPD	09 41 57.0					83.3	46.0	-0.1
TIA	PD	09 41 58.3	SKS	09 52 13.0		83.3	310.2	1.5	

SAMOA ISLANDS REGION

DATE:	SEP 01,1981	
TIME:	09 29 30.59	+/-0.09 sec
LAT:	15.203 S	+/-2.90 km
LON:	173.101 W	+/-2.50 km
DEPTH:	25.0 km	GEOPHYSICIST
STNS USED	239 of 374	STAND DEV: 1.2 sec
mb MAG	6.9	(21 station(s))
Ms MAG	7.7	(13 station(s))

FELT VI AT APIA. LOCAL TSUNAMI (24 cm PEAK TO PEAK) RECORDED AT PAGO PAGO.

STA	PH	TIME	SEC PH	TIME	mb	Ms	DIST	AZ	RES
LUB	EP	09 41 56.5					83.4	52.7	-0.7
GLD	EP	09 41 58.0	E	09 42 02.6		8.0	83.4	46.0	0.3
			E	09 43 13.0					
JCT	EP	09 41 58.2				7.2	83.8	56.3	-1.3
AIA	E(P)	09 42 08.0	E(S)	09 52 34.0			84.0	156.4	8.4X
KGM	EPC	09 42 05.0	E	09 42 07.4			84.3	273.6	2.5X
SES	IPD	09 42 04.0			7.0		84.9	34.6	-0.5
EDM	IPD	09 42 04.9			6.7		85.2	31.4	-0.9
BJI	PD	09 42 09.0	ES	09 52 35.0			85.5	313.4	1.1
PPI	EP	09 42 16.6			5.5X		86.5	270.5	3.2X
IPM	EPC	09 42 18.1	E	09 42 58.0	6.1X		87.2	275.5	1.4
			E	09 43 03.1					
LPS	IPD	09 42 21.5			6.6		88.0	74.7	1.0
MAW	EP	09 42 21.0					88.1	198.5	1.2
GYA	PD	09 42 23.0	S	09 52 59.0			88.2	297.9	1.6
SNG	EP	09 42 23.0	ES	09 53 10.0	5.4X	7.6	88.3	277.9	1.2
PSI	EPC	09 42 23.7			5.5X		88.7	273.1	-0.4
TUL	IPDR	09 42 23.6	E	09 42 37.6	6.8	8.0	88.9	52.4	-0.5
YAK	IPC	09 42 43.0					89.0	336.6	18.7X
TSI	EPD	09 42 32.4					89.3	273.8	5.7X
RLO	EPD	09 42 25.4					89.5	52.3	-1.9
PCT	EP	09 42 29.0					89.5	285.3	1.3
YKA	EP	09 42 45.9					89.8	23.3	17.9X
YKC	EP	09 42 28.0					89.8	23.4	-0.2
BTO	IPD	09 42 31.7	S	09 53 16.0			90.1	312.1	1.6
			I	09 53 33.0					
KMI	P	09 42 38.0	S	09 53 31.0			91.2	295.6	2.5X
SJS	IPC	09 42 40.8					91.7	80.2	3.1X
FFC	EP	09 42 36.0			6.6		91.8	33.3	-1.3
SAN	IP	09 42 40.5					91.8	125.2	2.6X
PEL	IPDR	09 42 40.2					91.9	124.9	1.9
BDT	EP	09 42 43.6	E	09 42 56.8			92.4	287.1	2.7X
LM2	EP	09 42 46.2					92.6	103.2	4.4X
TLL	EP	09 42 45.5					92.7	122.1	2.8X

SAMOA ISLANDS REGION

DATE:	SEP 01,1981	
TIME:	09 29 30.59	+/-0.09 sec
LAT:	15.203 S	+/-2.90 km
LON:	173.101 W	+/-2.50 km
DEPTH:	25.0 km	GEOPHYSICIST
STNS USED	239 of 374	STAND DEV: 1.2 sec
mb MAG	6.9	(21 station(s))
Ms MAG	7.7	(13 station(s))

FELT VI AT APIA. LOCAL TSUNAMI (24 cm PEAK TO PEAK) RECORDED AT PAGO PAGO.

STA	PH	TIME	SEC PH	TIME	mb	Ms	DIST	AZ	RES
NNA	IPD	09 42 43.9			6.6		92.8	103.1	0.9
PT06	EP	09 42 45.6					92.8	105.0	2.0X
CHG	IPC	09 42 45.6	I	09 43 00.0	6.1X		92.9	288.6	2.5X
			E	09 47 08.0					
CHTO	IPC	09 42 45.5					92.9	288.6	2.4X
BSI	EPC	09 42 46.5					92.9	274.9	3.0X
PT02	EP	09 42 48.0					92.9	104.2	4.5X
PT04	EP	09 42 51.3					93.2	106.0	6.5X
LZH	IPD	09 42 46.5	IPP	09 46 36.0			93.3	306.3	1.4
			SKS	09 53 11.0					
			S	09 53 53.0					
			PS	09 55 21.5					
			SS	10 00 22.0					
MDZ	E(P)	09 42 49.3					93.4	125.2	3.9X
FVM	IPD	09 42 45.5	E	09 42 49.6			93.6	51.7	-0.4
			E	09 42 56.1					
CEN	EP	09 42 51.0					93.9	124.0	3.1X
HUA	E(P)	09 42 54.8					94.2	103.6	4.8X
CFA	EPD	09 42 50.5	PP	09 46 35.0			94.3	124.2	0.8
			S	09 53 40.0					
TIK	EPD	09 42 50.7					94.9	344.3	-0.5
ANT	EP	09 42 59.0	E	09 43 04.5			95.2	116.1	5.4X
PSO	EP	09 43 00.5					95.9	90.4	2.9X
ARE	EP	09 43 04.0					96.5	108.9	3.9X
MBC	EP	09 42 59.0			6.6		96.7	11.2	-0.4
CHI	P	09 42 58.5					96.7	48.5	-1.5
LHC	IP	09 43 02.0			7.4		97.2	41.9	-0.2
FCC	EP	09 43 05.0					97.3	31.0	2.8X
TCA	EPD	09 43 07.0					97.3	125.1	3.8X
IRK	EP	09 43 03.0					97.4	322.1	-0.1
CYA	EPD	09 43 05.1					97.4	122.0	1.2
ZAK	IPD	09 43 04.3	ES	09 53 46.0			97.6	320.1	0.6
ORT	EP	09 43 03.9					97.8	55.0	-1.3
CHN	EP	09 43 12.0					98.5	87.1	3.0X

SAMOA ISLANDS REGION

DATE:	SEP 01,1981	
TIME:	09 29 30.59	+/-0.09 sec
LAT:	15.203 S	+/-2.90 km
LON:	173.101 W	+/-2.50 km
DEPTH:	25.0 km	GEOPHYSICIST
STNS USED	239 of 374	STAND DEV: 1.2 sec
mb MAG	6.9	(21 station(s))
Ms MAG	7.7	(13 station(s))

FELT VI AT APIA. LOCAL TSUNAMI (24 cm PEAK TO PEAK) RECORDED AT PAGO PAGO.

STA	PH	TIME	SEC PH	TIME	mb	Ms	DIST	AZ	RES
PRM	EP	09 43 11.5	E	09 46 14.3			89.0	57.2	1.0
			E	09 59 44.8					
SLA	EP	09 43 14.4					99.0	118.6	3.3X
UTO	IPD	09 43 10.0					99.6	49.5	-3.2X
LPB	P	09 43 17.0	SKS	09 50 16.0			99.6	110.0	2.9X
BOG	IP	09 43 17.0					99.9	87.8	1.3
GAI.	IPdiff	09 43 24.5					100.2	81.6	7.7X
FUQ	IPdiff	09 43 21.0					100.4	87.1	2.9X
LPA	IPdiff	09 43 24.4	ISKS	09 54 01.2		7.6	100.9	130.8	5.1X
CLE	EPdiff	09 43 22.0					101.1	49.9	2.1
RES	EPdiff	09 43 24.0			7.0		101.5	15.4	3.1X
LSA	PdiffD	09 43 29.4					102.3	297.6	3.2X
OTT	EPdiff	09 43 42.0					105.8	46.6	1.1
WMQ	Pdiff	09 43 47.0	PP	09 47 33.0			107.0	311.7	0.8
MNT	EPdiff	09 43 49.0					107.3	46.6	1.6
ALE	EPdiff	09 43 51.0			6.1X		107.7	7.4	2.6X
QUA	EPdiff	09 43 53.0			6.4X		108.0	49.8	2.5X
JKM	EPdiff	09 43 59.2					109.7	46.6	1.1
FDA5	EPKP	09 48 08.5					109.9	125.5	6.2X
SJG	EPdiff	09 44 03.0	E	09 48 40.0			110.4	76.0	1.1
MIM	EPdiff	09 44 05.2					110.5	47.0	3.4X
HNME	EPdiff	09 44 07.3					111.2	46.1	2.2X
HYB	PdiffD	09 44 10.0	E	09 48 06.5			111.6	283.0	2.8X
SCH	EPdiff	09 44 09.0					111.7	36.7	2.1
GBA	PKPC	09 48 12.1					111.9	278.8	6.0X
TRN	EPdiff	09 44 18.0					113.5	84.8	2.2X
NDI	EPdiff	09 44 22.0	EPP	09 49 00.0			114.2	294.4	3.3X
			EPKS	09 52 20.0					
			ESKS	09 55 02.0					
NDI	EPKP	09 48 11.5					114.2	294.9	1.2
KSH	Pdiff	09 44 29.0	PKKP	09 48 16.0			115.6	306.7	4.2X
			IPP	09 49 12.0					
KBS	IPKP	09 48 15.7					116.2	358.9	3.1X
BAO	EPKP	09 48 18.0					117.7	117.1	0.6

SAMOA ISLANDS REGION

DATE:	SEP 01,1981	
TIME:	09 29 30.59	+/-0.09 sec
LAT:	15.203 S	+/-2.90 km
LON:	173.101 W	+/-2.50 km
DEPTH:	25.0 km	GEOPHYSICIST
STNS USED	239 of 374	STAND DEV: 1.2 sec
mb MAG	6.9	(21 station(s))
Ms MAG	7.7	(13 station(s))

FELT VI AT APIA. LOCAL TSUNAMI (24 cm PEAK TO PEAK) RECORDED AT PAGO PAGO.

STA	PH	TIME	SEC PH	TIME	mb	Ms	DIST	AZ	RES
KAAO	EPKP	09 48 24.0					121.3	301.3	0.2
QUE	PKP	09 48 29.0					123.2	296.3	1.4
KEV	IPKP	09 48 29.0	I	09 48 33.2			124.0	351.7	1.3
			EPP	09 50 12.0					
TRO	EPKP	09 48 28.6					125.1	354.9	-1.1
SOB3	E(PKP)	09 48 37.0					126.2	114.5	3.3X
SOD	EPKP	09 48 31.0	I	09 48 34.0			126.3	350.7	-1.2
			I	09 48 44.5					
			EPP	09 50 31.0					
KIR	EPKP	09 48 30.0					126.7	353.7	-2.9X
AKU	IPKP	09 48 36.1	E	09 48 45.7			126.8	12.6	2.9X
REY	EPKP	09 48 41.7	I	09 48 52.2			127.2	15.4	7.6X
			E	09 50 43.7					
AVY	IPKPC	09 48 36.7					127.4	231.2	0.7
KJF	EPKP	09 48 29.0	I	09 48 38.1			129.0	348.5	-8.4X
			EPP	09 50 37.0					
			EPKS	09 52 00.0					
			E	10 01 27.0					
TGI	EPKP	09 48 28.0					129.6	300.3	-11.8X
KHI	E(PKP)	09 48 29.0					129.9	301.9	-11.3X
SUF	EPKP	09 48 32.0	I	09 48 43.8			130.6	348.5	-8.6X
CNG	EPKP	09 48 51.0	E	09 49 10.0			132.0	211.1	6.8X
			E	09 49 54.0					
			E	09 51 18.0					
			E	09 52 15.0					
			E	09 53 10.0					
NUR	IPKP	09 48 38.3	I	09 48 51.9			133.0	348.1	-6.7X
			EPP	09 51 10.0					
			EPKS	09 52 12.0					
			E	10 01 21.0					
SUR	IPKPD	09 48 46.3			7.5	8.1	134.3	207.3	-2.6
UPP	IPKP	09 48 51.2	IPP	09 51 19.8			134.7	352.4	2.8X
KSR	IPKPD	09 48 54.2					134.8	205.7	4.3X
BER	IPKP	09 48 40.6					134.9	1.1	-8.0X

SAMOA ISLANDS REGION

DATE:	SEP 01,1981	
TIME:	09 29 30.59	+/-0.09 sec
LAT:	15.203 S	+/-2.90 km
LON:	173.101 W	+/-2.50 km
DEPTH:	25.0 km	GEOPHYSICIST
STNS USED	239 of 374	STAND DEV: 1.2 sec
mb MAG	6.9	(21 station(s))
Ms MAG	7.7	(13 station(s))

FELT VI AT APIA. LOCAL TSUNAMI (24 cm PEAK TO PEAK) RECORDED AT PAGO PAGO.

STA	PH	TIME	SEC PH	TIME	mb	Ms	DIST	AZ	RES
HFS	IPKP	09 48 35.2				7.4	134.9	355.2	-13.5X
TEH	EPKP	09 48 51.0					135.4	305.7	0.3
KON	EPKP	09 48 39.9					135.6	358.0	-10.1X
KONO	E(PKP)	09 48 43.0					135.6	358.0	-7.0X
NPA	EPKP	09 48 56.0	E	09 49 11.0			136.1	228.2	3.7X
			E	09 49 38.0					
			E	09 52 32.0					
CIR	EPKP	09 48 48.0	IPP	09 51 45.0			136.6	214.6	-5.2X
CLK	EPKP	09 48 53.0					138.6	223.3	-4.2X
BUL	IPKPD	09 48 51.0	IPP	09 51 55.0			138.9	211.9	-6.7X
KER	EPKP	09 48 53.0					139.1	305.3	-4.7X
EKA	PKPC	09 48 56.1					130.2	8.8	-0.9
TET	EPKP	09 48 58.0					139.2	221.3	-0.1
DMU	EPKP	09 48 54.1					139.9	12.7	-4.2
MTD	EPKP	09 48 54.0					140.0	218.5	-5.6
DCN	EPKP	09 48 55.4					140.3	13.3	-3.6X
DDK	EPKP	09 48 54.2					140.5	12.5	-5.1X
DLE	EPKP	09 48 54.4					140.5	12.7	-5.0X
DKM	EPKP	09 48 54.6					140.6	12.5	-5.0X
KRI	EPKP	09 48 54.0					141.1	216.1	-7.6X
WIN	EPKP	09 48 59.0				6.6X	141.2	195.1	-2.7
ECB	EPKP	09 48 56.2					141.4	13.4	-4.7X
WAR	EPKPU	09 48 59.0	E	09 49 34.0		7.8	141.4	346.1	-1.9
			E	09 51 59.0					
			E	09 52 39.0					
ECP	EPKP	09 48 57.8					141.6	13.2	-3.6X
WIT	EPKP	09 49 01.0					142.5	0.2	-1.8
BRN	EPKP	09 49 05.0					142.5	353.7	2.0
KRA	EPKPD	09 49 01.3	I	09 49 05.8			143.7	345.8	-3.7X
			I	09 49 15.8					
			I	09 49 28.3					
			I	09 52 14.0					
			I	09 55 30.0					
KSP	IPKPC	09 49 02.3					143.7	349.9	-2.7

SAMOA ISLANDS REGION

DATE:	SEP 01,1981	
TIME:	09 29 30.59	+/-0.09 sec
LAT:	15.203 S	+/-2.90 km
LON:	173.101 W	+/-2.50 km
DEPTH:	25.0 km	GEOPHYSICIST
STNS USED	239 of 374	STAND DEV: 1.2 sec
mb MAG	6.9	(21 station(s))
Ms MAG	7.7	(13 station(s))

FELT VI AT APIA. LOCAL TSUNAMI (24 cm PEAK TO PEAK) RECORDED AT PAGO PAGO.

STA	PH	TIME	SEC PH	TIME	mb	Ms	DIST	AZ	RES
IAS	EPKP	09 49 04.0					143.8	336.0	-1.2
BRG	EPKP	09 49 03.3					144.0	352.4	-2.2
UCC	PKPDF	09 49 04.1	PP	09 52 16.0			144.4	2.8	-2.1
			E	10 02 35.0					
BIR	IPKP	09 49 09.0					144.5	335.0	2.5X
HOF	EPKP	09 49 05.0					144.7	354.5	-1.9
PRU	EPKP	09 49 05.5	E	09 49 09.0		7.9X	144.8	351.4	-1.4
			E	09 49 20.0					
			pPKP	09 49 42.5					
			PP	09 53 47.0					
BMR	EPKP	09 49 07.0					144.8	340.5	0.0
ARO	IPKPD	09 49 08.9					144.9	268.5	0.8
JOS	IPKPD	09 49 07.0					145.0	344.1	-0.2
DOU	PKP	09 49 06.9	E	10 05 18.0			145.1	2.6	-0.6
FOC	EPKP	09 49 14.0					145.1	334.8	6.4X
ODB	EPKP	09 49 09.0					145.1	335.0	1.4
VRI	EPKPD	09 49 05.5					145.2	335.6	-2.2
GRFO	IPKPD	09 49 01.0					145.4	355.1	-7.0X
CJR	EPKP	09 49 09.0					145.6	339.5	0.5
WLF	PKPR	09 49 11.0	E	09 52 34.0			145.6	0.9	2.7X
			E	10 02 49.0					
KHC	IPKPD	09 49 09.0	E	09 50 16.0			145.7	352.2	0.4
			E	09 52 44.9					
MLR	IPKPC	09 49 11.0					145.8	335.9	2.0
WET	IPKPD	09 49 08.3					145.8	353.0	-0.4
ZST	IPKP	09 49 08.7	E	10 03 46.0			146.0	347.8	-0.4
			I	10 19 10.6					
SRO	IPKP	09 49 10.8					146.1	346.1	1.6
VIE	IPKPR	09 49 12.0					146.1	348.6	2.8X
VKA	EPKP	09 49 09.0	ID	09 49 10.9			146.1	348.7	-0.2
NAI	EPKP	09 49 13.0					146.2	243.6	2.4X
STU	IPKP	09 49 11.0				7.6	146.5	357.2	1.2
BUH	EPKP	09 49 10.0					146.6	358.4	0.0
DEV	IPKPD	09 49 12.0					146.6	339.5	2.0

SAMOA ISLANDS REGION

DATE:	SEP 01,1981	
TIME:	09 29 30.59	+/-0.09 sec
LAT:	15.203 S	+/-2.90 km
LON:	173.101 W	+/-2.50 km
DEPTH:	25.0 km	GEOPHYSICIST
STNS USED	239 of 374	STAND DEV: 1.2 sec
mb MAG	6.9	(21 station(s))
Ms MAG	7.7	(13 station(s))

FELT VI AT APIA. LOCAL TSUNAMI (24 cm PEAK TO PEAK) RECORDED AT PAGO PAGO.

STA	PH	TIME	SEC PH	TIME	mb	Ms	DIST	AZ	RES
BUC2	EPKP	09 49 15.0					146.7	334.5	4.9X
KMR	PKPR	09 49 10.4					146.7	351.2	0.2
FUR	EPKP	09 49 11.5					146.9	354.7	0.9
SGR	EPKP	09 49 10.6					146.9	9.7	0.1
ECH	IPKPD	09 49 12.6					147.1	359.7	1.8
GZR	IPKPC	09 49 11.5					147.1	339.2	0.6
BHG	EPKP	09 49 10.5					147.2	252.5	-0.5
TIM	IPKPC	09 49 11.5					147.3	341.3	0.4
BAF	IPKPC	09 49 12.4	I	10 19 13.8			147.5	359.9	1.1
ZUL	EPKP	09 49 11.5					147.8	358.1	-0.5
LOR	EPKP	09 49 13.3					147.9	3.9	1.1
PVL	IPKPC	09 49 13.0					148.1	334.3	0.5
SSF	EPKP	09 49 13.6					148.1	4.4	1.2
LBF	EPKP	09 49 13.6					148.2	3.8	0.9
OGA	IPKPD	09 49 13.5					148.2	354.6	0.6
AAE	EPKP	09 49 18.0					148.3	262.6	4.0X
AVF	EPKP	09 49 13.7					148.4	4.6	0.9
SMF	EPKP	09 49 14.3					148.5	4.0	1.1
LJU	IPKPC	09 49 14.4	I	09 49 16.9			148.6	349.8	1.1
			I	09 49 19.8					
			I	09 50 52.9					
			E(PP)	09 52 53.4					
TCF	EPKP	09 49 14.5					148.8	6.3	0.9
DIM	EPKP	09 49 16.0					148.8	332.6	2.4X
MZF	EPKP	09 49 15.1					148.9	5.8	1.4
TRI	EPKP	09 49 13.6	IPP	09 53 06.0			149.0	350.6	-0.3
			IPPP	09 56 52.0					
			I	10 00 59.0					
			I	10 01 56.0					
			ISKP	10 03 20.0					
			I	10 10 02.0					
			ISS	10 12 48.0					
DIX	EPKP	09 49 14.5					149.2	359.3	-0.1
KDZ	IPKPD	09 49 14.0					149.2	332.4	-0.3

SAMOA ISLANDS REGION

DATE:	SEP 01,1981	
TIME:	09 29 30.59	+/-0.09 sec
LAT:	15.203 S	+/-2.90 km
LON:	173.101 W	+/-2.50 km
DEPTH:	25.0 km	GEOPHYSICIST
STNS USED	239 of 374	STAND DEV: 1.2 sec
mb MAG	6.9	(21 station(s))
Ms MAG	7.7	(13 station(s))

FELT VI AT APIA. LOCAL TSUNAMI (24 cm PEAK TO PEAK) RECORDED AT PAGO PAGO.

STA	PH	TIME	SEC PH	TIME	mb	Ms	DIST	AZ	RES
STS	EPKP	09 49 21.0					149.4	22.6	6.4X
SAL	EPKP	09 49 15.0					149.5	355.0	0.3
RJF	EPKP	09 49 16.1					149.7	7.5	1.2
LFF	EPKP	09 49 16.1					149.9	8.7	0.8
CAF	EPKP	09 49 17.2					150.1	6.9	1.6
LPO	EPKP	09 49 17.6					150.2	8.2	1.8
SKO	EPKP	09 49 22.0	I	09 50 57.0			150.5	337.6	5.7X
VAY	EPKP	09 49 15.8					150.6	335.5	-0.7
PTO	IPKPD	09 49 17.2					150.9	24.5	0.4
THE	EPKP	09 49 16.8					151.1	334.2	-0.3
FIR	EPKP	09 49 18.0					151.3	353.4	0.7
OCE	EPKP	09 49 18.8					151.4	11.3	1.2
EPF	EPKP	09 49 19.6					151.7	10.2	1.5
FRF	EPKP	09 49 19.5					151.7	0.4	1.4
LRG	EPKP	09 49 19.7					151.8	0.8	1.5
MLS	EPKP	09 49 19.5					151.9	9.1	1.1
LMR	EPKP	09 49 20.0					152.0	0.6	1.6
AQU	EPKP	09 49 23.0					152.4	349.6	3.9X
MNS	EPKP	09 49 19.0	IPP	09 53 10.0			152.5	350.7	-0.1
CVF	EPKP	09 49 20.7					152.7	356.8	1.2
DUI	EPKP	09 49 20.0					152.8	347.5	0.3
ATH	IPKPD	09 49 20.0	IPP	09 53 12.0			152.9	329.9	0.1
			ISS	10 13 00.0					
BRT	EPKP	09 49 20.0					152.9	342.7	0.2
RMP	IPKP	09 49 21.0	EPKS	09 53 20.0			153.0	350.4	1.0
			IPS	10 02 20.0					
EBR	EPKP	09 49 22.0	E	09 49 33.0			153.9	11.1	0.9
SFS	IPKP	09 49 28.0	I	09 50 08.0			155.8	26.5	4.1X
			I	09 52 24.0					
			IPP	09 53 40.0					
			ISKS	09 56 20.0					
MBO	IPKP	09 49 31.9	I	09 49 33.9			156.9	88.9	6.0X
			I	09 49 43.1					
			I	09 50 40.0					

SAMOA ISLANDS REGION

DATE:	SEP 01,1981	
TIME:	09 29 30.59	+/-0.09 sec
LAT:	15.203 S	+/-2.90 km
LON:	173.101 W	+/-2.50 km
DEPTH:	25.0 km	GEOPHYSICIST
STNS USED	239 of 374	STAND DEV: 1.2 sec
mb MAG	6.9	(21 station(s))
Ms MAG	7.7	(13 station(s))

FELT VI AT APIA. LOCAL TSUNAMI (24 cm PEAK TO PEAK) RECORDED AT PAGO PAGO.

STA	PH	TIME	SEC PH	TIME	mb	Ms	DIST	AZ	RES
			I	09 50 44.5					
			I	09 51 17.9					
BNG	IPKPD	09 49 38.0					164.3	228.1	4.1X
KIC	EPKP	09 49 35.1	E	09 50 37.0			165.6	126.3	0.2
			PP	09 54 23.4					

APPENDIX II

SAMOA ISLANDS REGION EARTHQUAKE

DATE: 01 SEPTEMBER 1981
TIME: 09:29:30.59 UTC
LOCATION: 15.203° S, 173.101° W
DEPTH: 25 KM
MAGNITUDE: 6.9 m_b, 7.7 M_s, (7.9 M_s BRK), (7.7 M_s PAS)

HISTORICAL EARTHQUAKES WITH MAGNITUDES ≥6.0 WITHIN A TWO DEGREE GRID OF THE SEPTEMBER 1, 1981 HYPOCENTER

DATE	TIME(UTC)	LAT.	LON.	DEPTH	MAG.		SOURCE	COMMENTS
					m_b	M_s		
05/08/13	18:35:24.0	17.00S	174.50W	200	7.00*		G-R	*PAS m_b
06/26/17	05:59:42.0	15.50S	173.00W	25		8.70*	G-R	TSUNAMI *PAS M_s
07/03/27	10:37:49.0	15.00S	172.50W			6.25*	G-R	*PAS M_s
08/03/29	12:49:28.0	17.00S	172.50W			6.50*	G-R	*PAS M_s
06/09/31	13:52:12.0	14.00S	174.00W			6.50*	G-R	*PAS M_s
07/20/31	08:30:30.0	14.00S	173.00W	80	6.50*		G-R	*PAS m_b
01/27/33	22:36:35.0	16.00S	172.00W	50		6.75*	G-R	FELT *PAS M_s
06/18/33	03:53:58.0	15.00S	172.00W			6.00*	G-R	FELT *PAS M_s
06/24/33	18:55:30.0	16.00S	173.50W			6.75*	G-R	FELT *PAS M_s
01/31/34	10:06:30.0	16.00S	173.50W			6.25*	G-R	*PAS M_s
04/24/34	17:36:20.0	14.00S	174.00W			6.25*	G-R	*PAS M_s
08/21/35	13:48:44.0	16.00S	174.00W	100	6.25*		G-R	*PAS m_b
03/20/36	23:53:03.0	14.50S	173.50W			6.25*	G-R	*PAS M_s
06/16/36	00:33:31.0	15.00S	175.00W			6.00*	G-R	*PAS M_s
06/08/39	20:46:53.0	15.50S	174.00W	100	7.20*		G-R	*PAS m_b
10/30/39	13:12:36.0	16.00S	174.00W	150	6.50*		G-R	*PAS m_b
04/14/40	09:33:22.0	16.00S	174.00W	200	6.25*		G-R	*PAS m_b
07/20/40	01:53:53.0	15.50S	173.00W			6.00*	G-R	*PAS M_s
08/11/40	16:46:44.0	15.50S	172.00W			6.00*	G-R	*PAS M_s
08/24/40	13:31:07.0	15.50S	173.00W			6.00*	G-R	*PAS M_s
10/05/41	10:11:12.0	14.50S	173.75W			6.50*	G-R	*PAS M_s
12/22/42	04:14:40.0	16.75S	174.00W	50		6.75*	G-R	*PAS M_s
06/03/43	20:48:03.0	16.00S	173.00W			6.50*	G-R	*PAS M_s
09/11/43	19:34:00.0	15.00S	174.00W			6.90*	G-R	*PAS M_s
10/11/44	09:45:15.0	15.00S	173.00W	80	6.75*		G-R	DAMAGE *PAS m_b
06/29/48	10:28:37.0	15.50S	172.50W	60	7.00*		G-R	*PAS m_b
02/10/49	21:56:39.0	16.00S	173.00W			6.75*	CGS	*PAS M_s
04/18/49	21:34:49.0	15.50S	173.50W	100	7.00*		CGS	FELT *PAS m_b
02/11/50	11:29:56.2	15.34S	175.23W	236	6.50*		SYK	*PAS m_b
11/24/50	13:03:40.0	15.50S	173.00W			6.38*	ISS	*PAS M_s
11/24/50	20:18:46.0	15.50S	173.00W			6.38*	ISS	*PAS M_s

SAMOA ISLANDS REGION EARTHQUAKE

DATE: 01 SEPTEMBER 1981
TIME: 09:29:30.59 UTC
LOCATION: 15.203° S, 173.101° W
DEPTH: 25 KM
MAGNITUDE: 6.9 m_b, 7.7 M_s, (7.9 M_s BRK), (7.7 M_s PAS)

HISTORICAL EARTHQUAKES WITH MAGNITUDES ≥6.0 WITHIN A TWO DEGREE GRID OF THE SEPTEMBER 1, 1981 HYPOCENTER

DATE	TIME(UTC)	LAT.	LON.	DEPTH	MAG.		SOURCE	COMMENTS
					m_b	M_s		
02/13/51	11:55:49.7	15.50S	175.04W	236	6.9*		SYK	*PAS m_b
04/10/51	10:55:38.0	15.50S	173.00W			6.75*	ISS	FELT (IV) *PAS M_s
09/09/51	04:43:57.0	16.20S	173.20W			6.63*	ISS	FELT (II) *PAS M_s
02/25/52	01:17:03.0	16.70S	173.50W			6.90*	ISS	FELT (II) *PAS M_s
10/18/52	20:33:14.0	15.80S	172.80W			6.00*	ISS	*ROM M_s
10/29/52	19:34:21.0	16.90S	173.80W	160	6.50*		ISS	FELT (IV) *WEL m_b
07/29/53	23:18:02.0	15.80S	172.80W			6.50*	ISS	*PAS M_s
09/16/53	01:48:42.4	15.12S	174.56W			6.25*	SYK	*PAS M_s
03/10/55	21:10:11.0	15.00S	174.00W			6.38*	CGS	FELT (IV) *BRK M_s
11/10/55	01:44:04.0	15.00S	174.00W	100	6.75*		CGS	FELT (IV) *PAS m_b
03/03/56	00:05:25.0	15.00S	173.50W			6.75*	CGS	FELT *PAS M_s
05/05/56	03:22:27.0	15.50S	173.00W	100	6.00*		CGS	*PAS m_b
05/22/56	03:01:03.0	15.50S	173.00W			6.50*	CGS	FELT *PAS M_s
08/09/56	23:00:46.8	15.94S	175.02W	272	6.75*		SYK	FELT *PAS m_b
09/24/56	06:04:37.0	15.50S	173.50W			6.00*	CGS	FELT *PAS M_s
01/28/57	08:16:19.0	15.50S	173.00W			6.50*	CGS	*PAS M_s
04/14/57	19:17:57.0	15.50S	173.00W			7.50*	CGS	FELT *PAS M_s
09/02/57	09/46/29.0	14.92S	173.35W			6.13*	ISS	FELT *BRK M_s
01/27/58	07:43:58.0	15.00S	174.00W			6.75*	CGS	*PAS M_s
04/21/58	20:14:50.0	15.07S	175.16W			6.50*	ISS	*PAS M_s
08/06/58	21:09:09.0	17.00S	173.00W			6.75*	CGS	*PAS M_s
11/16/58	17:44:48.0	16.00S	172.00W			6.25*	CGS	FELT *PAS M_s
03/31/59	07:20:46.0	15.25S	173.01W			6.00*	ISS	FELT *PAS M_s

SAMOA ISLANDS REGION EARTHQUAKE

DATE: 01 SEPTEMBER 1981
TIME: 09:29:30.59 UTC
LOCATION: 15.203° S, 173.101° W
DEPTH: 25 KM
MAGNITUDE: 6.9 m_b, 7.7 M_s, (7.9 M_s BRK), (7.7 M_s PAS)

HISTORICAL EARTHQUAKES WITH MAGNITUDES ≧6.0 WITHIN A TWO DEGREE GRID OF THE SEPTEMBER 1, 1981 HYPOCENTER

DATE	TIME(UTC)	LAT.	LON.	DEPTH	MAG.		SOURCE	COMMENTS
					m_b	M_s		
04/12/59	20:54:02.6	15.20S	173.72W			6.13*	SYK	FELT *PAS M_s
03/16/60	17:39:16.9	15.51S	173.21W			6.13*	SYK	*MAT M_s
07/11/60	11:55:14.0	15.81S	171.98W	24		6.00*	SYK	*PAS M_s
04/20/61	21:39:10.3	15.20S	173.50W	33N		6.13*	CGS	FELT *PAS M_s
01/05/62	08:08:06.9	15.10S	172.70W	33		6.25*	CGS	*PAS M_s
12/08/62	18:18:28.7	15.40S	173.40W	33		6.75*	CGS	FELT *PAS M_s
02/21/65	11:14:15.1	15.10S	173.20W	33	5.7	6.00*	CGS	FELT *PAS M_s
03/22/65	02:44:47.5	15.30S	173.40W	51	5.9	6.5*	CGS	FELT *PAS M_s
03/23/65	23:54:14.7	15.20S	173.50W	130	5.7	6.5*	CGS	FELT *PAS m_b
01/01/67	07:05:50.2	15.16S	173.74W	40D	6.0	6.63*	CGS	FELT *PAS M_s
03/11/68	08:26:32.8	16.20S	173.90W	112	6.0		CGS	
05/01/69	19:05:24.7	16.80S	174.67W	205D	6.0 6.40*		CGS	*PAS m_b
10/26/69	06:38:03.4	16.17S	173.95W	127D	5.8	6.70*	CGS	FELT *PAS M_s
02/12/72	18:51:57.0	15.31S	173.37W	5	5.9	5.7 6.30*	ERL	FELT (II) *PAS M_s T-WAVE
04/21/72	13:25:21.3	15.30S	173.66W	125	5.6 6.0*		ERL	*BRK m_b
08/07/72	09:24:14.7	16.65S	172.10W	33D	5.8	6.0 6.10*	ERL	*PAS M_s
09/27/72	09:01:43.8	16.47S	172.17W	33N	5.9	6.0 6.00*	ERL	*BRK M_s
12/22/72	16:22:08.9	15.98S	172.42W	33N	5.7	6.0	ERL	
08/05/73	15:47:32.9	16.23S	173.11W	33N	6.1	5.7	ERL	
12/30/73	16:21:29.3	15.32S	173.08W	33N	5.4	6.2	GS	
03/18/74	10:56:12.4	14.93S	172.83W	27D	5.9	6.0 6.00*	GS	FELT (V) *PAS M_s
06/04/74	04:14:15.9	15.85S	175.10W	276D	6.0		GS	*PAS m_b

SAMOA ISLANDS REGION EARTHQUAKE

DATE: 01 SEPTEMBER 1981
TIME: 09:29:30.59 UTC
LOCATION: 15.203° S, 173.101° W
DEPTH: 25 KM
MAGNITUDE: 6.9 m_b, 7.7 M_s, (7.9 M_s BRK), (7.7 M_s PAS)

HISTORICAL EARTHQUAKES WITH MAGNITUDES ≥6.0 WITHIN A TWO DEGREE GRID OF THE SEPTEMBER 1, 1981 HYPOCENTER

DATE	TIME(UTC)	LAT.	LON.	DEPTH	MAG.		SOURCE	COMMENTS
					m_b	M_s		
						6.70*		
12/09/75	09:14:40.6	14.79S	173.00W	33N	6.0	6.2	GS	FELT (VI)
						6.40*		*PAS M_s
12/26/75	15:56:38.7	14.79S	173.00W	33N	6.4	7.8	GS	TSUNAMI
						7.30*		FELT (V)
								*PAS M_s
02/11/76	21:43:55.4	15.26S	172.27W	33N	5.6	5.9	GS	FELT (III)
						6.00*		*BRK M_s
04/02/77	07:15:22.7	16.70S	172.10W	33N	6.8	7.6	GS	TSUNAMI
						7.50*		DAMAGE (VI)
								*PAS M_s
07/24/77	06:22:51.3	15.34S	173.15W	33N	6.0	6.2	GS	FELT (IV)
						6.30*		*PAS M_s
09/13/77	00:21:52.6	15.45S	173.29W	33N	5.7	6.0	GS	FELT (III)
						6.20*		*PAS M_s
03/03/78	10:48:11.1	15.29S	173.52W	33N	5.6	6.2	GS	*PAS M_s
						6.00*		
06/11/78	14:27:55.3	15.26S	173.56W	33N	5.6	6.2	GS	FELT (III)
						6.10*		*PAS M_s
06/17/78	15:11:33.5	17.10S	172.26W	33N	6.6	7.0	GS	*BRK M_s
						7.20*		
06/18/80	10:49:10.0	15.27S	173.57W	43	5.9	6.5	GS	FELT (V)
						6.80*		*PAS M_s
08/24/80	20:10:04.2	15.22S	173.67W	39D	6.0	6.2	GS	FELT (IV)
						6.20*		*BRK M_s
10/09/80	16:19:38.2	15.38S	173.42W	33N	5.7	6.0	GS	*BRK M_s
						6.20*		

SAMOA ISLANDS REGION EARTHQUAKE

DATE: 01 SEPTEMBER 1981
TIME: 09:29:30.59 UTC
LOCATION: 15.203° S, 173.101° W
DEPTH: 25 KM
MAGNITUDE: 6.9 m_b, 7.7 M_s, (7.9 M_s BRK), (7.7 M_s PAS)

HISTORICAL EARTHQUAKES WITH MAGNITUDES ≥6.0 WITHIN A TWO DEGREE GRID OF THE SEPTEMBER 1, 1981 HYPOCENTER

* THESE MAGNITUDES ARE REPORTED FROM SOURCES OTHER THAN CGS, ERL, OR GS. MAGNITUDES ARE ASSUMED TO BE M_s IF DEPTH IS ≤50 KM AND m_b IF DEPTH IS >50 KM.

ABBREVIATIONS USED

G-R GUTTENBERG AND RICHTER "SEISMICITY OF THE EARTH"
ISS INTERNATIONAL SEISMOLOGICAL SUMMARY
SYK L.SYKES
CGS U.S. COAST AND GEODETIC SURVEY
ERL ENVIROMENTAL RESEARCH LABORATORY
GS U.S. GEOLOGICAL SURVEY
PAS CALIFORNIA INSTITUTE OF TECHNOLOGY, PASADENA
BRK UNIVERSITY OF CALIFORNIA, BERKELEY
WEL DEPT. OF SCIENTIFIC AND INDUSTRIAL RESEARCH, WELLINGTON, NZ
MAT JAPANESE METEOROLOGICAL AGENCY, MATSUSHIRO OBSERVATORY, JAPAN
ROM ROME, ITALY OBSERVATORY

APPENDIX III

SAMOA ISLANDS REGION 09/01/1981 Ms 7.7 h=25 km.								
FIRST MOTION PARAMETERS								
STATION	Δ (DEG.)	AZ (DEG.)	dt/dΔ (SEC/DEG.)	FOCAL ANGLE (JB) (DEG.)	QUALITY, DIRECTION AND SOURCE OF EARTH MOTION			
					E or I	C or D	SP-LP	PHASE
AFI	1.724	51.63	14.26	88.44	I	C	LP	P
PVC	17.979	258.72	12.37	60.13	I	C	SP	P
NOU	20.623	246.29	10.30	46.22	I	C	SP	P
KOU	22.166	252.26	9.94	44.17	I	C	SP	P
PPT	22.789	99.70	9.76	43.17	I	D	LP	P
TPT	24.677	93.32	9.53	41.92	I	D	LP	P
GNZ	24.810	196.61	9.47	41.59	I	C	SP	P
HNR	26.836	278.77	9.28	40.58	E	D	LP	P
WEL	28.216	199.46	9.18	40.05	I	C	LP	P
SNZO	28.258	199.53	9.11	39.69	I	C	LP	P
RKT	36.911	108.58	8.44	36.27	I	D	LP	P
CTA	38.952	256.53	8.32	35.68	I	D	LP	P
CTAO	38.952	256.53	8.32	35.68	I	D	LP	P
KIP	39.123	22.71	8.32	35.68	I	D	LP	P
PMG	39.134	273.47	8.32	35.68	I	D	LP	P
TOO	42.897	230.45	8.10	34.60	I	C	SP	P
TAU	43.767	222.51	8.05	34.35	I	C	LP	P
TAU	43.767	222.51	8.05	145.65	E	D	LP	pP
GUA	50.240	302.30	7.66	32.48	E	D	LP	P
GUMO	50.303	302.32	7.62	32.29	I	D	LP	P
ASP	50.457	251.56	7.62	32.29	I	D	SP	P
DAV	64.550	285.49	6.51	27.15	I	D	LP	P
NWAO	65.014	240.42	6.47	26.97	I	D	LP	P
MUN	65.923	241.41	6.39	26.61	I	D	LP	P
MAJO	68.771	319.59	6.14	25.49	I	D	LP	P
MAJO	68.771	319.59	6.14	154.51	E	D	LP	pP
MAT	68.771	319.59	6.14	25.49	I	D	LP	P
MAT	68.771	319.59	6.14	25.49	I	D	SP	P
KUR	69.569	331.69	6.10	25.32	I	D	SP	P
SKR	70.708	339.85	6.03	25.01	I	D	SP	P
BKS	71.046	40.51	5.99	24.83	I	D	LP	P
SHK	71.204	315.02	5.99	24.83	I	D	LP	P
PAS	71.571	45.73	5.96	24.70	I	D	LP	P
JAS	72.225	41.35	5.92	24.52	I	D	SP	P
BAG	72.460	292.88	5.89	24.39	I	D	LP	P
WDC	72.520	38.12	5.89	24.39	I	D	SP	P
KKM	73.021	281.21	5.85	24.21	I	D	SP	P
GSC	73.143	45.36	5.85	24.21	I	D	LP	P
COR	74.615	34.51	5.75	23.77	I	D	LP	P
TATO	75.050	301.38	5.71	23.60	I	D	LP	P
TATO	75.050	301.38	5.71	156.40	E	D	LP	pP
SPA	75.106	180.00	5.71	23.60	I	C	LP	P
SPA	75.106	180.00	5.71	23.60	I	C	SP	P
ANP	75.112	301.59	5.71	23.60	I	D	LP	P
BMN	75.698	40.74	5.68	23.46	I	D	SP	P
TUC	75.961	50.66	5.64	23.29	I	D	SP	P

SAMOA ISLANDS REGION 09/01/1981 Ms 7.7 h=25 km.								
FIRST MOTION PARAMETERS								
STATION	Δ (DEG.)	AZ (DEG.)	dt/dΔ (SEC/DEG.)	FOCAL ANGLE (JB) (DEG.)	QUALITY, DIRECTION AND SOURCE OF EARTH MOTION			
					E or I	C or D	SP-LP	PHASE
LON	76.801	33.48	5.58	23.03	I	D	LP	P
DUG	78.410	42.81	5.48	22.59	I	D	LP	P
HKC	80.226	296.23	5.36	22.07	I	D	LP	P
NEW	80.246	34.22	5.36	22.07	I	D	SP	P
ALQ	80.367	49.94	5.31	21.85	I	D	LP	P
ANMO	80.369	49.94	5.31	21.85	I	D	LP	P
CN2	80.917	319.93	5.26	21.64	I	D	SP	P
MSO	81.221	36.65	5.26	21.64	I	D	SP	P
BDW	81.810	41.78	5.17	21.25	I	D	SP	P
COL	81.954	10.64	5.17	21.25	I	D	LP	P
SEY	82.151	344.85	5.17	21.25	I	D	SP	P
ILT	82.757	357.89	5.11	20.99	I	D	SP	P
TIA	83.114	310.18	5.11	20.99	I	D	SP	P
GOL	83.211	46.00	5.11	20.99	I	D	LP	P
GOL	83.211	46.00	5.11	20.99	I	D	SP	P
JCT	83.737	56.32	5.08	20.86	I	D	LP	P
SES	84.740	34.62	5.02	20.60	I	D	SP	P
EDM	85.022	31.45	4.99	20.48	I	D	SP	P
BJI	85.351	313.38	4.96	20.35	I	D	LP	P
RCD	86.530	42.72	4.86	19.92	I	D	LP	P
IPM	87.084	275.53	4.83	19.79	I	D	SP	P
LPS	88.008	74.74	4.77	19.53	I	D	SP	P
GYA	88.049	297.90	4.77	19.53	I	D	SP	P
TUL	88.776	52.41	4.73	19.36	I	D	LP	P
BTO	89.927	312.15	4.71	19.28	I	D	SP	P
PEL	92.029	124.95	4.67	19.11	I	D	LP	P
CHG	92.752	288.60	4.64	18.98	I	D	LP	P
CHTO	92.752	288.60	4.64	18.98	I	D	LP	P
NNA	92.933	103.15	4.64	18.98	I	D	SP	P
LZH	93.161	306.37	4.64	18.98	I	D	LP	P
SHA	93.346	59.28	4.63	18.94	I	D	LP	P
FVM	93.501	51.75	4.63	18.94	I	D	LP	P
ANT	95.325	116.12	4.56	18.64	I	D	LP	P
ZAK	97.350	320.10	4.52	18.47	I	D	SP	P
UTO	99.502	49.44	4.47	18.26	I	D	SP	P
LPB	99.691	110.02	4.47	18.26	I	D	LP	P
ZOBO	99.752	109.76	4.47	18.26	I	D	LP	P
BOG	99.962	87.86	4.47	18.26	I	D	LP	P
SHIO	100.696	293.69	4.45	18.18	I	D	LP	P
BLA	101.056	54.34	4.45	18.18	I	D	LP	P
LPA	101.082	130.75	4.45	18.18	E	D	LP	P
LSA	102.118	297.68	4.45	18.18	I	D	SP	P
SCP	103.598	51.06	4.45	18.18	I	D	LP	P
WES	108.640	49.93	1.89	7.61	I	D	LP	PKP
SJG	110.391	75.98	1.89	7.61	I	D	LP	PKP
BEC	113.346	60.93	1.89	7.60	E	D	LP	PKP

SAMOA ISLANDS REGION 09/01/1981 Ms 7.7 h=25 km.								
FIRST MOTION PARAMETERS								
STATION	Δ (DEG.)	AZ (DEG.)	dt/dΔ (SEC/DEG.)	FOCAL ANGLE (JB) (DEG.)	QUALITY, DIRECTION AND SOURCE OF EARTH MOTION			
					E or I	C or D	SP-LP	PHASE
KBS	116.002	358.91	1.88	7.57	I	D	LP	PKP
KEV	123.828	351.69	1.87	7.52	I	D	LP	PKP
AKU	126.640	12.57	1.86	7.50	E	D	LP	PKP
NUR	132.734	348.10	1.84	7.39	I	D	LP	PKP
SLR	134.449	207.52	1.83	7.37	I	D	SP	PKP
KSR	134.951	205.90	1.82	7.33	I	D	SP	PKP
KON	135.367	358.00	1.82	7.33	E	D	LP	PKP
KONO	135.367	358.00	1.82	7.33	E	D	LP	PKP
BUL	139.042	212.13	1.78	7.17	I	D	SP	PKP
UCC	144.229	2.68	1.70	6.86	I	D	LP	PKP
JOS	144.730	344.16	1.68	6.78	I	D	SP	PKP
ARO	144.801	268.82	1.68	6.78	I	D	SP	PKP
TNS	144.836	358.20	1.68	6.78	I	D	LP	PKP
GRFO	145.207	355.01	1.68	6.78	I	D	LP	PKP
WLF	145.415	.78	1.68	6.78	I	D	LP	PKP
KHC	145.507	352.17	1.66	6.69	I	D	SP	PKP
WET	145.580	352.97	1.66	6.69	I	D	SP	PKP
VIE	145.915	348.61	1.66	6.69	I	D	LP	PKP
NAI	146.231	243.97	1.66	6.69	I	D	LP	PKP
STU	146.257	357.18	1.66	6.69	I	D	LP	PKP
DEV	146.367	339.56	1.66	6.69	I	D	SP	PKP
KMR	146.480	351.12	1.66	6.69	I	D	LP	PKP
ECH	146.869	359.60	1.64	6.60	I	D	SP	PKP
LOR	147.723	3.79	1.62	6.50	I	D	LP	PKP
OGA	148.026	354.56	1.62	6.50	I	D	SP	PKP
AAE	148.232	262.93	1.62	6.50	I	D	LP	PKP
TRI	148.826	350.60	1.59	6.39	I	D	LP	PKP
KDZ	148.981	332.49	1.59	6.39	I	D	SP	PKP
ATH	152.662	330.01	1.46	5.88	I	D	SP	PKP
MAL	156.144	22.79	1.35	5.42	I	D	LP	PKP
BNG	164.412	228.89	.96	3.87	I	D	SP	PKP